Ph.D. Thesis

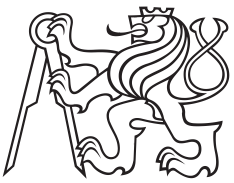

Czech Technical University in Prague

F3

Faculty of Electrical Engineering
Department of Physics

Biocidal Effects of Non-thermal Atmospheric Pressure Plasma

Vladyslava Čeledová

Ph.D. Programme: Electrical Engineering and Information Technology, P2612
Branch of study: Plasma Physics, 1701V011

November 2017

Supervisor: MUDr. Ing. Vítězslav Kříha, Ph.D., Ing. Eva Doležalová, Ph.D.

Acknowledgement / Declaration

I dedicate this Ph.D. thesis to my husband Tomáš, who passed through the long process of doctoral studies with me, who gave me his love, belief and unconditional support at every moment.

My appreciation goes to my supervisor MUDr. Ing. Vítězslav Křiha, Ph.D. for all his support and guidance during the experimental work at the Department of Physics, FEE, CTU in Prague. I want to express my deep gratitude to my co-supervisors Dr. Eva Doležalová and Dr. Peter Lukeš for the opportunity to work in the low-temperature plasma research group of Institute of Plasma Physics of Czech Academy of Sciences; for sharing their valuable knowledge and experience in the field and in the laboratory.

My particular deep thank goes to doc. Jan Píchal for his valuable remarks and engagement during the process of development of this thesis. My warmest gratitude goes to Dr. Miroslav and Barbara Horký, for their support and helpful discussions. I would like to acknowledgment all my co-workers and friends at the Department of Physics (FEE, CTU in Prague) and Institute of Plasma Physics (CAS) for their help, support and remarks.

My great and deep thank goes to my family in Kiev and to Prague for their full time support during the whole time of my studies.

This work was supported by the MEYS CR (project LD14080) and the Czech Technical University in Prague (grant No. SGS13/194/OHK3/3T/13).

I hereby declare that this thesis is the result of my own work and all the sources I used are in the list of references, in accordance with the Methodological Instruction on Ethical Principles in the Preparation of University Theses.

V Praze dne 21. 11. 2017

.....

Abstrakt / Abstract

Náplní této práce je studium biocidních účinků v roztocích vyvolaných působením netermálního plazmatu (NTP), jež jsou v posledních letech předmětem intenzivního výzkumu.

Ke zjištění odezvy baterie E. coli na chemické procesy, vyvolané působením NTP, generovaného v plynné fázi (N_2/O_2) ale působícím pod vodní hladinou, byla použita plazmová tryska napájená zdrojem stejnosměrného napětí. Díky použitému technickému řešení, jež umožnilo přímý kontakt kovového hrotu s ošetřovanou tekutinou, bylo možné sledovat synergické působení iontů přechodných kovů a reaktivních kyslíkových a dusíkových částic na inaktivaci bakterií.

Účinky plazmatu působícího nad hladinou bakteriální suspenze byly zkoumány za použití μAPPJ, generujícího RF plazma v plynné fázi ($He + O_2$). Naměřené výsledky poukazují na dominantní roli reaktivních kyslíkových částic, jež způsobují oxidační stres, vedou k poškození DNA a přechodu bakterie do stavu, v němž je živá ale nekultivovatelná.

Inaktivaci mikroorganizmů lze rovněž docílit rozprášením tekutiny aktivované plazmatem na kontaminovaný povrch. K tomuto účelu byl na listy špenátu pomocí přechodového jiskrového výboje rozprášen 3% roztok silic oregano. Cidní účinky byly pravděpodobně způsobené synergickým působením náboje přenášeného micely na povrch mikroorganizmů a fenoly OEO způsobující fluidaci bakteriální membrány.

Klíčová slova: inaktivace bakterií, plazma, korónový výboj, přechodová jiskra, plazmová tryska.

The subject of this Ph.D. thesis covers bio-chemical pathways in plasma activated liquids (PAW), that are under intensive investigation during last decades. Three possible ways of bacteria inactivation with PAW were studied.

The DC plasma jet generated plasma in gas phase (N_2/O_2) during underwater operation was used to provide postdischarge bacteria treatment. The synergistic effect of transition metal ions and reactive oxygen and reactive nitrogen species was considered to play the dominant role in bacteria inactivation. Moreover, toxicity of the copper ions even in sublethal doses should be taken into account, due to possible DNA damages induced in the cell.

Direct bacteria treatment with PAW was studied using RF operating μAPPJ working in $He + O_2$ gas mixture over the bacterial suspension. Reactive oxygen species were assumed to play a major role in bacteria inactivation process through inducing the oxidative stress, that led to DNA damage and viable but non-cultivable state of bacteria. The evidence of peroxidation of lipids in the bilayer was measured; however, we propose, that it did not play a major role in the bactericidal process.

The contaminated agar and spinach leaves surface was treated by electrospraying of 3% oregano essential oil (OEO) suspended in 5% polysorbate 80 water solution through the transient spark discharge. The synergistic effect of charged and reactive species carried with micelles onto the surface and phenolic component of OEO was assumed to cause membrane fluidisation and resulted to the cell death.

Keywords: plasma inactivation, plasma, corona discharge, plasma jets.

Contents /

Tables / Figures

Chapter 1
Introduction

Non-thermal atmospheric pressure plasma (NTP) as an innovative tool to treat heat sensitive materials, e.g. medical tools, living tissues, food and its packaging is a topic of great interest during the last decades. A significant progress in understanding of plasmachemical reactions and plasma induced bacteria damage was achieved mainly during past ten years [1–3]. Nowadays NTP can be generated by variety of sources, some of them are already used for example in medicine, food preservation, decontamination of heat sensitive materials, etc. [4–6].

Despite intense research plasma induced bacteria decontamination mechanisms are still not well understood. The question is challenging due to diversity of plasma sources, plasma induced processes, their parameters, experimental setups, tissues, etc.

NTP is a source of charged particles, reactive species, UV and visible light, electromagnetic field and heat. Bactericidal actions of these agents depend on the type of treatment, which can be direct or remote. In direct plasma treatment, living tissue, conductive surface with bacterial load or liquid suspension (all mentioned will be further referred as "sample") plays a role of an electrode, thus the current flows through the sample. Although during the remote treatment the sample is not connected to the high voltage directly; the small conduction or displacement current may flow through the sample in some cases [4]. Moreover, the sample itself can be in one of three states of matter (solid, liquid or gaseous), that leads to even higher diversity of induced plasmachemical reactions and physical processes.

Bio-chemical processes directly or indirectly induced by plasma in microorganisms are usually associated with oxidative stress, membrane or DNA damages. Furthermore, oxidative stress itself induces a variety of processes, which can force bacteria into a viable but not cultivable state; evoke apoptosis or nectosis (controlled or uncontrolled cell death).

Dominant pathway(s) of bacteria inactivation highly depends on experimental conditions, which makes cross-study results comparison problematic. Nevertheless, each particular study is considered to assist understanding of the plasma-induced biocidal processes in their whole complexity.

This Ph.D. thesis is focused on antibacterial pathways induced by non-thermal plasma in liquids. Based on the published literature, that will be referred within the thesis, the author hypothesized that:

1 reactive oxygen and reactive nitrogen species (ROS and RNS) play a dominant role in bacteria inactivation, when PAW is generated in atmosphere containing N_2 and O_2;
2 the electrode material should be taken into account, when there is any evidence of its release into the treated liquid from the electrode, as it can induce a non negligible impact to treated microorganisms;
3 reactive oxygen species (ROS) have dominant impact on bacteria in the case when both plasma and the experiment is held in the atmosphere containing oxygen, but free of nitrogen;

4 plasma generated reactive species in gas-liquid interface diffuses into the liquid and induce different chemical reactions. As a result short lived reactive species could occur in the close vicinity of bacteria and induce oxidative processes on the bacterial membrane (e.g. lipid peroxidation) or cause stress to bacteria, that can provoke bacteria to enter viable but not cultivable state.

5 liquid, which contains any biologically active component (e.g. essential oil), can be activated with plasma. Such activation can improve its the biocidal properties.

Three different experiments were performed in order to test the hypotheses mentioned above.

- The DC-operated plasma jet, designed to generate plasma in N_2/O_2 was used to determine effects of reactive nitrogen and oxygen species and their role in bacteria inactivation. Moreover, the jet construction allowed its underwater operation, while the plasma was generated in the gas phase. As a result the jet provoked a non negligible release of metal ions into the treated solution and was used to test the hypotheses 1 and 2.
- Bactericidal pathways of plasma activated water in nitrogen free atmosphere were studied using the micro atmospheric pressure plasma jet (μAPPJ) operated over the water surface. Experimental setup was designed to prevent an access of ambient atmosphere to the treated sample, while the jet operated in $He + O_2$ gas mixture. The role of reactive oxygen species in plasma induced oxidative stress (see hypotheses 3 and 4) were studied using this setup.
- Essential oils (EOs) are aromatic biologically active oily liquids originated from plants. These substances have been known as a natural remedy since Middle Ages, and are widely used not only in food preservation industry nowadays. Besides their successful utilization and high ability of microosrganism suppression, their maximal concentration in food should be carefully controlled due to their strong odors. The author hypothesizes that plasma can increase EOs' biocidal efficiency (see hypotheses 5). Transient spark discharge was used to activate EO aqueous solution, that was simultaneously electrospayed onto bacteria inoculated surfaces *in vivo* and *in vitro*, in order to explore its bactericidal properties.

The thesis is divided into three parts: state-of-the-art; materials and methods; results and discussion. The first part is covered by chapters 2, 3, 4 and 5, and provides the reader with a review of plasma sources commonly used in the field of plasma decontamination; describes antibacterial agents of plasma and plasma activated solutions; and finally brings the basic information regarding microbiology and bacteria damage mechanisms. The part called "Methods" (chapter 6) informs the reader about analysis and assays used to obtain relevant data in order to support discussion on bactericidal pathways induced by plasma in liquids. Results and discussion part consists of three chapters (chapter 7, 8 and 9). Each chapter contains information regarding experimental setup, explanation of experimental procedure, and results and discussion concerning each experiment. The last mentioned part provides the reader with hypotheses on possible bactericidal pathways based on experimental results and reports of other researchers working in the field. Experiments were performed separately under different experimental conditions and their results are hardly comparable. Nevertheless, the last chapter called "Conclusion" provides the reader with summarized results of the work.

Chapter 2
Non-thermal atmospheric pressure plasma sources for microbiological applications

Plasma occurs naturally and composes 99% of observable matter in the known Universe, for example the solar corona or solar wind, ionosphere and polar lights are all plasmas. The common discharge channel, visible from the Earth surface — lightning — is also plasma; as well as St. Elmo's fires seen by sailors on sharp ends of masts during thunderstorms on the sea. Human curiosity and desire to understand mechanisms of plasma generation led to invention of discharge devices. The first frictional charge discharge was obtained by Greek philosophers; although, the first steps in understanding of processes governing plasma ignition were not made until the seventeenth century. For example, a corona discharge, first described as a "pencil of electric light", was presented by Priestley in 1734 [7]. Later on devices for spark discharge were investigated by Leyden (1734) [8], and only with invention of electrochemical battery by Volta (1800) [9] and progress in electricity generation and storage it was possible to invent more powerful devices, e.g. a powerful continuous arc discharge discovered by Petrov (1803) [10].

During the nineteenth century with progress in knowledge in storage of electric energy and vacuum systems Michael Farraday developed the direct current (DC) glow discharge (1831–1835) [11]. Several decades later (in 1879) Sir William Cooker identified plasma as a radiant matter, but did not yet named it [12]. Then J. Townsend in 1900 came with the breakdown theory and laid the foundation of modern plasma research [13].

But a term *plasma* was introduced for the first time by Irving Langmuir in 1928 with a definition written as follows: "Except near the electrodes, where there are sheaths containing very few electrons, the ionized gas contains ions and electrons in about equal numbers so that the resultant space charge is very small. We shall use the name plasma to describe this region containing balanced charges of ions and electrons" [14]. The definition commonly used to describe plasma nowadays does not differ much from the initial one and describes plasma as a quasineutral particle system in the form of gaseous or liquid-like mixture of free electrons, ions and neutrals which all together behave collectively. Quasineutrality means, that the amount of positive and negative charge carriers in plasma should be approximately equal, but at the same time ionization of all particles is not necessary [15–17]. Plasma, used in biomedical applications and plasma medicine, is weakly ionized with degree of ionization (ratio of charge carriers to all particles) in range of 10^{-7}–10^{-4}. Moreover, Langmuir in his definition [14] mentioned a plasma boundary region, called plasma sheath. Sheath has different properties in comparison with plasma and forms an electrical screening separating plasma and outer atmosphere. In this region many chemical reactions take place producing of reactive species, which are highly important in biomedical applications [18–20].

Except the degree of ionization plasma can be characterized by an average energy of its compounds. Moreover, corresponding thermodynamic temperatures of electrons, ions and neutrals can be different. Particles in electric field are accelerated and gain energy in the periods between inelastic collisions (mean free path). During inelastic

collisions with heavy particles electrons lose a small part of their energy, hence their thermodynamic temperature is initially higher. If applied electric field is strong enough, electrons can acquire energy to ionize heavy gas particles and start the avalanche to induce the discharge. Subsequently, the temperatures of all plasma compounds can be equilibrated through electrons collisions with heavy particles. Depending on the temperature of electrons (T_e), ions (T_i) and neutrals (T_n) low- or high-temperature plasma can be distinguished (see table 2.1).

Low-temperature plasma (LTP)		High-temperature plasma (HTP)
Non-thermal plasma (NTP)	Thermal plasma	
$T_i \approx T \approx 300$ K $T_i \ll T_e \leq 10^5$ K	$T_e \approx T_i \approx T \leq 2 \times 10^4$ K	$T_i \approx T_e \geq 10^7$ K
e.g. corona discharge	e.g. arc plasma	e.g. fusion plasma

Table 2.1. Subdivision of plasmas [16].

In following section we restrict to plasma sources, which are reported to be effective against microbiological contaminants, mostly by non-thermal plasma with low temperature of heavy particles. Sources are classified by the frequency of power supply and electrode configuration: corona and transient spark (DC or pulsed DC), dielectric barrier discharges (DBDs); atmospheric pressure plasma jets (APPJ); and microwave (MW) driven plasmas in the gigahertz range.

Plasma sources described below can be constructed in different scales depending on characteristic dimension (L) of generated plasma. Normal scale sources produces plasma with $L > 1$ mm, while micro scale ones generates it with $L \leq 1$ mm [21]. Majority of normal scale plasma sources can be modified to micro-scaled ones. However, there is one special source with rectangular electrode arrangement, which was produced to be a reference plasma jet initially in microscale: micro atmospheric pressure plasma jet.

2.1 Corona and transient spark

Corona discharge usually appears around thin wires or pin electrodes with small radii of curvature. The discharge is ignited when electric field in the close proximity of the electrode is large enough to accelerate electrons up to the ionization energy of the surrounding gas [22]. Since the gradient of electric field in the close vicinity of sharp electrode reached breakdown value, the luminosity as well as excitation take place in its surrounding. In the case of bipolar corona discharge, where both electrodes are sharp the luminous plasma region can be extended even out of the electrode proximity [23]. With increase of applied voltage the streamer is formed and corona discharge changes to a streamer corona and than to a transient spark discharge [17, 24].

Point-to-plane configuration is commonly used in the biomedical applications [23, 25] (see figure 2.2(a)). The point electrode connected to high voltage is usually constructed using a sharpen rod or a needle, while the plane electrode can be realized as any conductive surface or liquid; e.g. a solidified cultivation medium inoculated with microorganisms or bacterial suspension.

In the case the plane electrode is realized with an inoculated agar surface, microorganisms are treated by plasma directly and experience an electron current flow [4]. The

most efficient bacteria inactivation is observed within the region with maximal current density [26]. Its distribution corresponds to the Warburg's law [27]:

$$j(\theta) = k\frac{V(V - V_{cr})}{d^n}\cos^m\theta, \tag{2.1}$$

where θ is an angular coordinate of the point on a plane with respect to longitude axis, d is a distance between electrodes, V is applied voltage and V_{cr} is critical voltage needed for discharge ignition in the used working gas (see figure 2.1). The value of parameter n was experimentally assigned to 3 [28–29]; parameter m depends on the corona polarity and was examined experimentally by Warburg: $m = 4.82$ for positive corona and $m = 4.65$ for the negative one. The constant k corresponds to the actual parameters of the setup and surrounding gas.

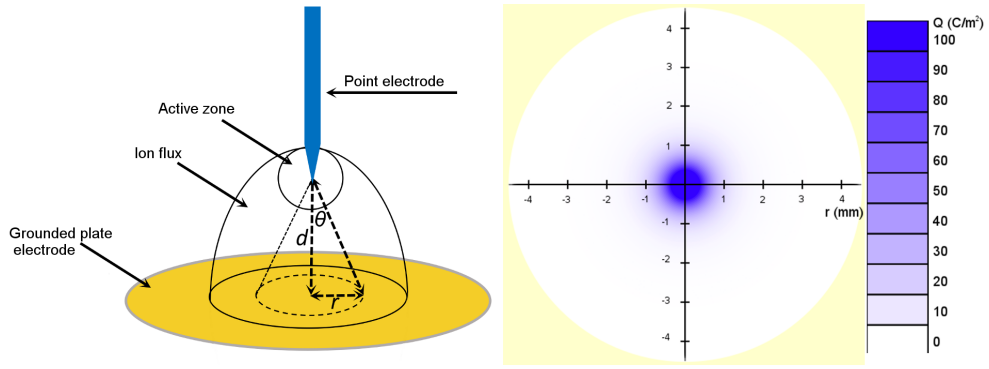

Figure 2.1. The ion and electron distribution along the gap between the electrodes (left). The dashed circle on the plane electrode of the figure on the left represents the zone with maximum of current density (the imminent zone of the direct treatment). The $\theta = \operatorname{atan}\frac{d}{r}$ and r parameters depend on the shape of the point electrode. The figure on the right shows the charge distribution on the grounded electrode for negative corona discharge generated using copper electrodes, $d = 10$ mm, $U = 10$ kV and exposition time of 3 minutes [26].

With rising energy corona changes to a streamer, and further to a transient spark discharge [17]. Despite DC applied voltage they are characterized by repetitive pulses with frequency up to several tens of kHz. The streamer corona appears when the high voltage applied to the point electrode is several kilovolts higher than the breakdown voltage of the working gas. With further voltage increase the transient spark discharge is established [30]. Amplitude of current pulses in this case is higher, but the pulse duration is in range 10–100 ns [31].

Briefly, streamers are filaments rapidly extended from high voltage electrode generated by strong electric field. They are usually ejected out of very localized ionization seeds or if the electric field is above the breakdown threshold in a small area of the electrode, where the free charge carries begin to avalanche [32]. After initiating, the streamer can propagate to the rest of the gap, where the field can be too weak for its initiation. It is propagated under influence of external electric field augmented by its self-generated field.

Mechanism of streamer propagation depends on its polarity. Free electrons for negative streamer drift from its ionized channel, while positive streamer needs a constant source of free electrons in the surrounding gas. The major source of electrons for positive streamer are photo- and background ionization [32, 17].

Inactivation of microorganisms induced by plasma generated with corona or transient spark discharge has been studied by different authors.

Julak et al. [33] presented a bipolar corona discharge, called cometary discharge for its shape similarity with a tail of comet (see figure 2.2(c)). The cometary discharge was ignited between two point electrodes connected to a DC high voltage power supply. Authors reported up $7\log_{10}$[1]) *E. coli* inactivation *in vitro* and significant surface decontamination *in vivo* (e.g. guinea pig skin, human skin) [33–34, 23].

Bussiahn et al. [25] used a point-to-plane electrode arrangement to ignite streamer corona discharge (see figure 2.2(b)). The pin electrode was realized by a stainless steal needle insufflated with pure argon and created a hairline plasma (as authors called it). The discharge was characterized by selfpulsing, with pulses of the amplitude of several milliamperes lasting for nanoseconds with high repetition rate of 1.8 kHz. Authors reported its ability to enter small cavities e.g. tooth channels and *E. coli* inactivation in there.

Machala et al. [24] used point-to-grid electrode configuration to ignite streamer corona or transient spark discharges (see figure 2.2(d)). They used deionized water with and without bacteria, streamed through the needle with a constant flow rate of 0.5 ml/min. Water was electrosprayed through the transient spark discharge, which induced production of reactive oxygen (ROS) and reactive nitrogen species (RNS) in it. Authors reported up to $6\log_{10}$ of *E. coli* reduction caused by membrane lipid peroxidation and other oxidative processes.

2.1.1 A note regarding electrospraying

Electrohydrodynamic atomization (EHDA) technology, or simply electrospraying was first explored and recorded in 1600 by William Gilbert [35]. However, the precise description of physics behind the electrospraying was gained after centuries of scientific investigations. There are several considerable milestones in research of EHDA: in 1750 Jean-Antoine (Abbe) Nollet reported observation of the process and provided it terminology; a century later Lord Kelvin proposed the setup with several kilovolts of potential differences and achieved electrospraying; in 1882 Lord Rayleigh theoretically predicted a maximum electric charge that could be carried by a liquid droplet ("Rayleigh limit" [36]). The limit was experimentally confirmed after a century by Taylor, who developed a mathematical description of EHDA process (Taylor cone [37]); John Bennet Fenn got the Nobel Prize in Chemistry for his contribution to electrospray ionization for analyzing biological macromolecules [38]. Nowadays, EHDA is a well-practiced technique for generation of very fine mono-dispersed droplets [39].

Typical EHDA setup contains a syringe pump, a syringe and a conductive nozzle, which is connected to DC high voltage power supply. The grounded collector is placed underneath the nozzle in a certain distance. The principle of EHDA processes is based on applying electric force to atomize liquid: a drop of liquid at the end of a nozzle is abducted electrically to the grounded collector, forming the liquid jet, which further becomes a source of fine drops [40] (see figure 2.3).

2.2 Dielectric barrier discharges

One of the disadvantages of point-to-plane electrode arrangement used for generating corona discharge is small treatment area. On the contrary, dielectric barrier discharges (DBDs) allow large areas and volumes or surface treatment.

[1]) $n\log_{10}$ is a common notation of bacterial reduction, where n stands for orders of magnitude number. Mathematically correct notation $\log_{10} 10^n$ is not used in microbiology. For example bacterial reduction of $7\log_{10}$ means that 1 bacterium out of 10 000 000 survives

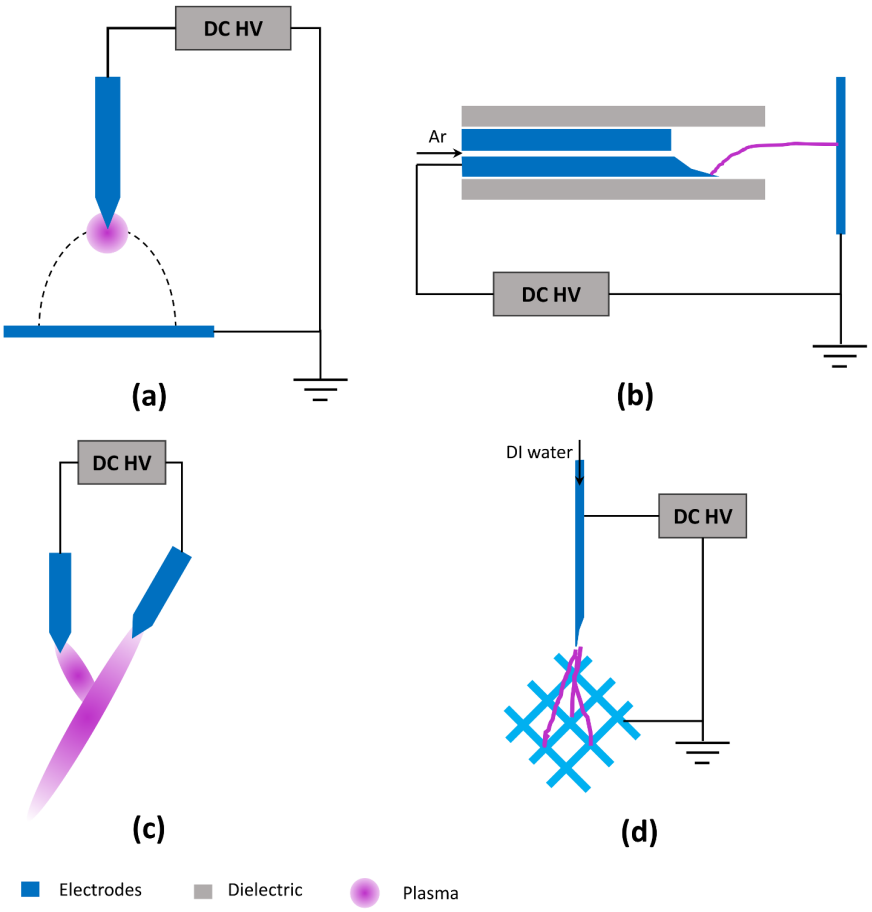

Figure 2.2. Electrode configurations of DC plasma sources: (a) point-to-plane electrode arrangement; (b) insufflated needle-to-plane geometry; (c) bipolar cometary discharge; (d) electrospraying of aqueous solution through transient spark discharge.

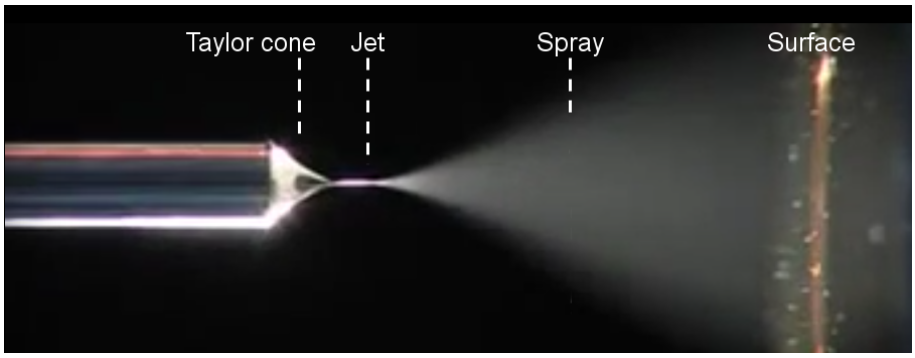

Figure 2.3. Photo of the electrospraying process [41].

DBD is ignited between two electrodes insulated by dielectric barrier. This barrier can be either in contact with one or both electrodes, or places somewhere between them (see figure 2.4(a–c)). The arrangement shown in figure 2.4(c) is not common in medical applications. The DBDs are powered with alternating current, as the DC cannot pass the dielectric barrier. The voltage needs to be high enough to cause the breakdown in working gas and ignite plasma in the inter-electrode gap. One of the main advantage of

DBD is possibility to use almost any gas mixtures (from atomic gas, through ambient air to liquid vapors [42]).

Moreover, DBD can be realized by planar or coplanar electrode arrays generating surface DBD discharge. Coplanar arrangement can be realized by embedding both electrodes inside a dielectric barrier, while planar one is achieved by embedding one electrode into the dielectric barrier and placing the second one on it (see figure 2.4(d–e)) [43].

DBD can be characterized by its homogeneity (filamentary, discerned or diffuse). Typical voltage needed to ignite plasma depends on the particular device parameters, but usually is not less then 10 kV with frequency varying from several kHz to the order of MHz. DBDs can be used for direct or remote plasma treatment.

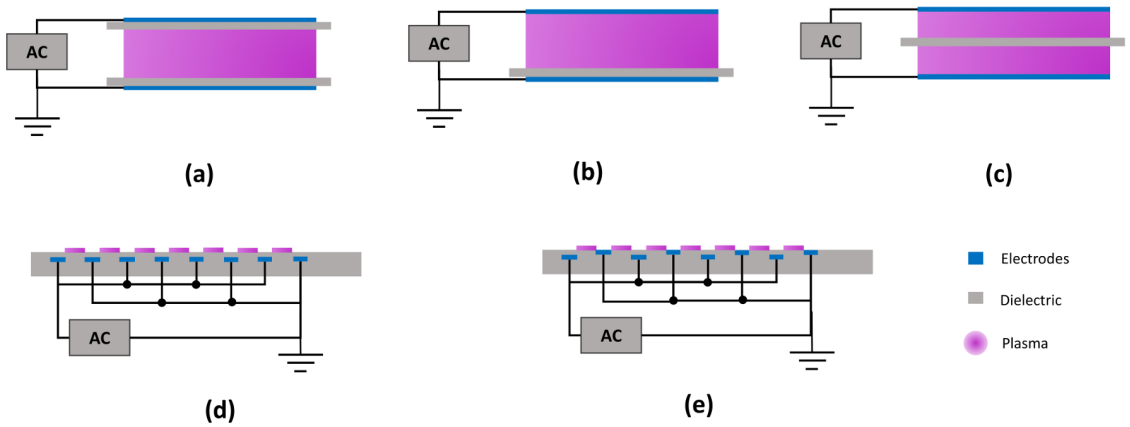

Figure 2.4. Possible electrode configurations of DBD plasma sources. Volume DBD discharge with dielectric barrier placed on one (a) or both (b) electrodes, or in the inter-electrode gap (c). Surface DBD discharge in coplanar (d) and planar (e) electrode arrangements.

DBD is especially interested for industrial applications mainly due to effortless discharge ignition, no need of huge gas flows while almost any combination of gases can be used. The main disadvantage is high ignition voltage ($>$ 10 kV) and a need of high-quality isolation [21].

Different configurations of DBD plasma sources are widely used in research and biomedical applications. For example, Fridman et al. [44] reported the floating electrode DBD (FE-DBD) designed to treat human skin. The power electrode was covered with isolator with large dielectric constant, while the second virtual electrode was human skin. They reported up to $8\log_{10}$ *E. coli* reduction on the surface. Polak et al. [45] designed a DBD source to inactivate bacteria inside up to 5 m long tube with inner diameter of 2 mm by equidistantly twisted electrodes inside the tube wall. They reported $4\log_{10}$ reduction of *B. atrophaeus*[1]) spores inside after 10 minutes of exposition using Ar as a working gas.

Planar or coplanar electrodes arrangement allows creating DBD plasma sources to cover large areas. For instance, the remote impact of surface DBD in ambient air on *B. atrophaeus* spores resulting to $4\log_{10}$ reduction in 60% air humidity after 150 s was reported by Hahnel et al. [46]. The planar DBD discharge with electrode arrangement

[1]) *Bacillus atrophaeus* is a gram-positive, aerobic rod-shaped bacterium. It has been widely used in biomedical applications as an indicator for heat- and chemical-based decontamination regimens.

realized as the concentrate circles was reported by Oehmigen et al. [47] and was used to treat aqueous solutions to investigate bacteria inactivation pathways.

Detailed review of dielectric barrier discharges and their applications is out of scope of this thesis, and the reader is asked to find more information in review articles, e.g. [21, 48–49]

2.3 Atmospheric pressure plasma jets

Winter et al. [50] proposed the definition of the term *plasma jet* as follows: "The gas discharge, which is operated in a non-sealed electrode arrangement and projected outside the electrode arrangement into the environment". It can be also called plasma plume or plasma flame. It is usually expelled from the open electrode or a routing tube by a gas flow or by electric field depending on electrode configuration. The commonly used abbreviation APPJ was derived from the Atmospheric Pressure Plasma Jet and was first used by Schutze et al. [51]. Plasma jets can be classified by the discharge geometry, type of plasma, power supply frequency and working gas or gas mixture (see figure 2.5). Lu et al. [52] in his article focused on plasma jets used in bioaplications defined 4 groups of plasma jets:

- dielectric free electrode (DFE) jets,
- DBD jets,
- DBD-like jets,
- single electrode (SE) jets.

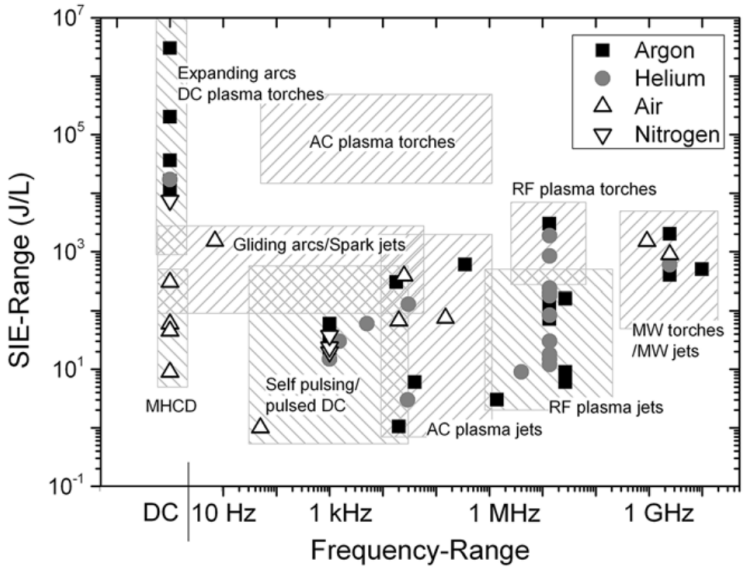

Figure 2.5. Classification of different plasma jets regarding to the estimated SIE (energy per working gas volume) [50].

The configuration of **DFE jet** was reported by the Hick's group [53–54] (see figure 2.6). The jet is driven by RF power supply with peak-to-peak voltage of several volts, i.e. electric field in the plasma plume is relatively low and the plasma is blown out the device by gas flow. The DFE jet is characterized by high power delivered to plasma (in comparison with DBD and DBD-like jets), that leads to high temperature of plasma,

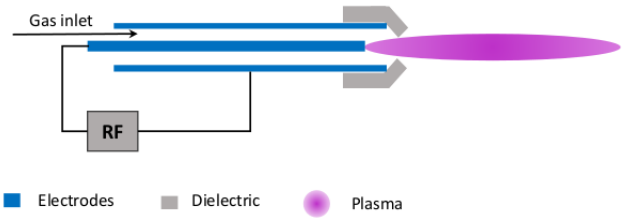

Figure 2.6. Dielectric free electrode (DFE) plasma jet designed by Hick's group [53].

which is not acceptable in biological applications. DFE plasma jet can be suitable for non heat-sensitive material treatment as the generated plasma is highly reactive.

Common **DBD jets** consist of one or two electrodes in a coaxial or special ring arrangement. In the case of coaxial setup plasma is ignited at the sharp end of the inner electrode, while the outer one is realized as a ring on a dielectric tube routing the working gas flow (see figure 2.7(c), [55]). The pin electrode is powered by RF power supply, while the ring one is grounded. However, virtualization of the grounded electrode is also possible and is shown in figure 2.7(d), [56].

The DBD jet with ring electrodes placed on the dielectric tube was first reported by Teschke et al. [57] and is shown in figure 2.7(a). High voltage is connected to one of the ring electrode, while the second electrode placed closer to the tube end is grounded. The geometry shown in figure 2.7(b) is reduced to a single electrode setup, therefore the discharge inside the tube is weakened [58].

Arrangements shown on figure 2.7(a) and 2.7(c) generate stronger electric, which makes plasma more reactive. Moreover, noble gases (like Ar, He) are usually used to expel plasma outside the jet. Plasma generated in these gases is known to produce VUV radiation [59]; nevertheless, plasma properties depend on particular jet geometry.

And finally in figure 2.7(e) is shown the microhollow electrode arrangement, when electrodes are placed on the outer side of dielectric chamber supplied with a hole. The plasma plume blown out with a working gas can reach several centimeters [56].

A typical **DBD-like jet** consists of a pin or capillary electrode and the ring electrode outside the outer dielectric tube. These jets can be powered either by AC (kHz or RF) or DC power supply. Unlike DBD plasma jets, the inner electrode is not covered with dielectric. That is why when the jet operates against the dielectric surface or gas, it works basically as DBD discharge. In the case the treated sample or tissue is conductive the discharge is running between the high voltage (HV) electrode and the sample and the risk of sparks with high current density occurs. This fact should be taken in account when working with biological material or living tissue.

Possible electrode arrangements are shown in figure 2.8. Pure gases or gas mixtures are usually used to expel plasma outside the jet. Inner capillary electrode allows to feed the discharge with two gases avoiding their mixing together. This setup was reported to be more effective for reactive species generation [60], in comparison to application of gases mixed in advance (see figure 2.8(b)) [61].

The **SE jets** are rather similar to previously mentioned DBD-like jets, but they lack the ring electrode. The outer dielectric tube used in configurations shown in figure 2.9(a) and 2.9(b) guides the working gas. These jets are usually powered by DC voltage and can be characterized as DC or pules-DC corona discharge. Moreover the electrode arrangement shown in figure 2.9(c) was already mentioned in the section 2.1. Treated sample should be conductive and again there is a risk of local increase of current density leading to thermal effects. Nevertheless, this kind of jets is applicable for example in

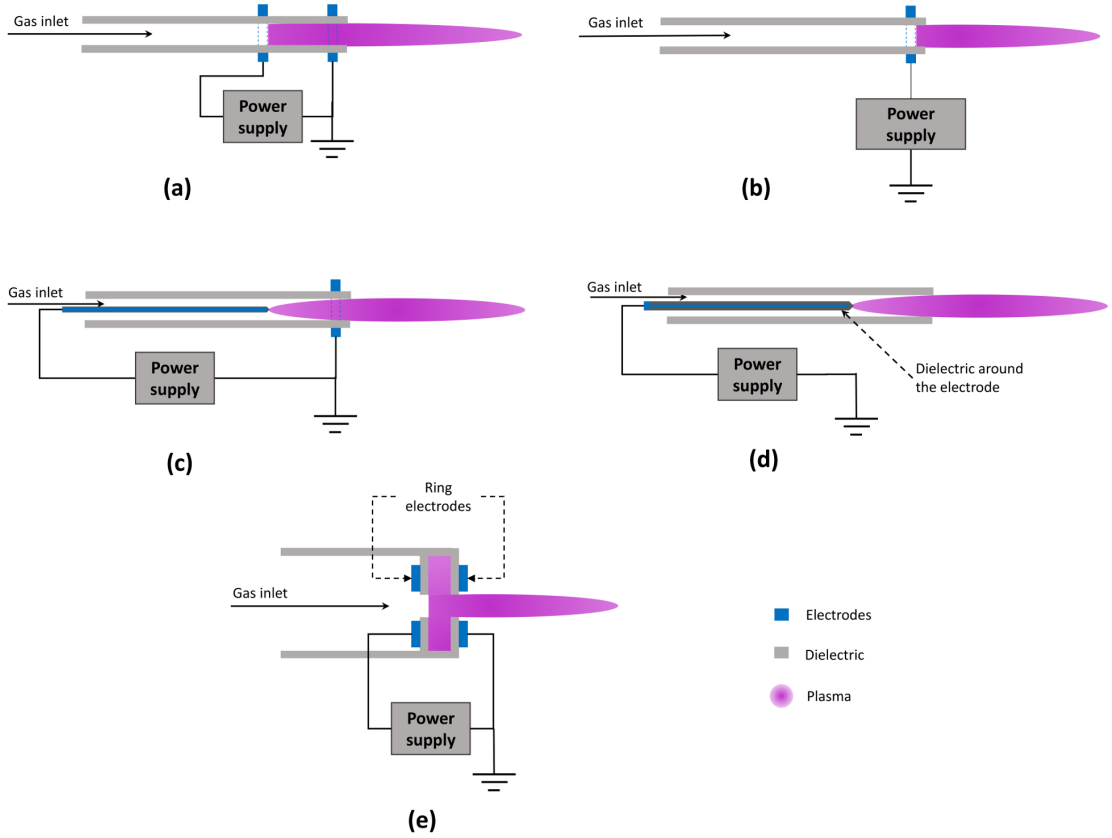

Figure 2.7. Electrode configuration of DBD jets: using RF-driven ring electrode with (a) and without (b) the second grounded ring electrode; consisting of RF-driven pin-electrode with (c) and without (d) grounded ring one; microhollow electrode arrangement (e).

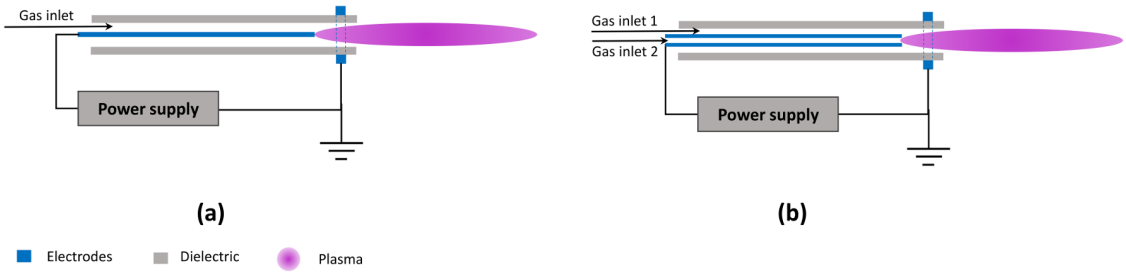

Figure 2.8. DBD-like plasma jets: with pin (a) and capillary (b) powered electrode and a grounded ring one.

dentistry, where the very thin plasma plume is necessary to be applied inside the teeth channel [62–63].

2.3.1 µAPPJ

Plasma jets described above are constructed using coaxial or outer rings electrode arrangements; nevertheless, the rectangular one with symmetric, coplanar, stainless steal electrodes is also possible (see figure 2.10). Schulz-von der Gathen and co-workers [64] used this arrangement to design a µatmospheric plasma jet (µAPPJ). Their goal was to create a jet which is easy to calibrate and modify plasma jet, and it is based on the original APPJ introduced by the group of Hicks and Selwyn [51].

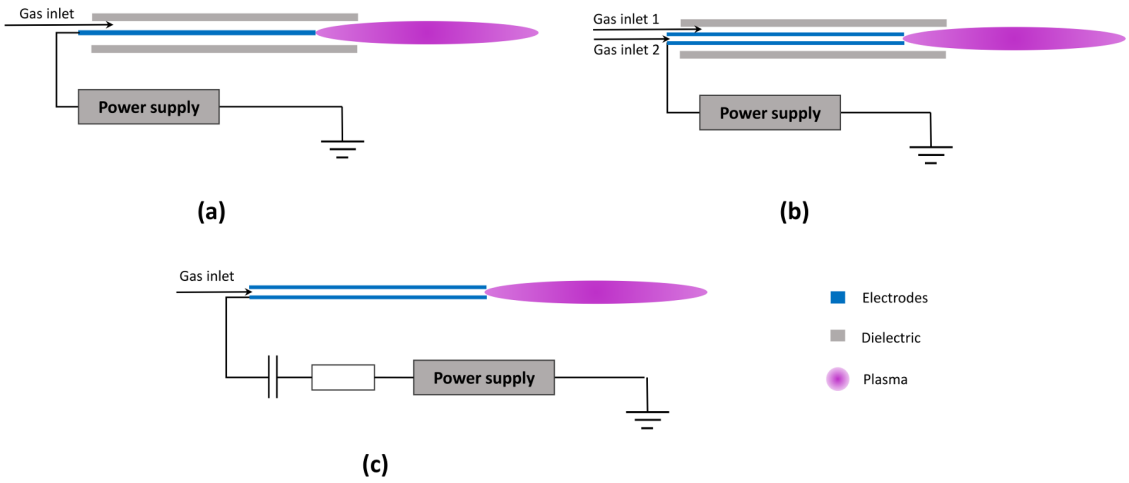

Figure 2.9. Single electrode plasma jets.

μAPPJ has been and is actively investigated at several institutes, and about 40 articles describing experimental measurements, models and simulations have been published [65]. Characterization of physical and chemical phenomena occurring in micro-scale APPJ were provided taking advantage of the simple device geometry.

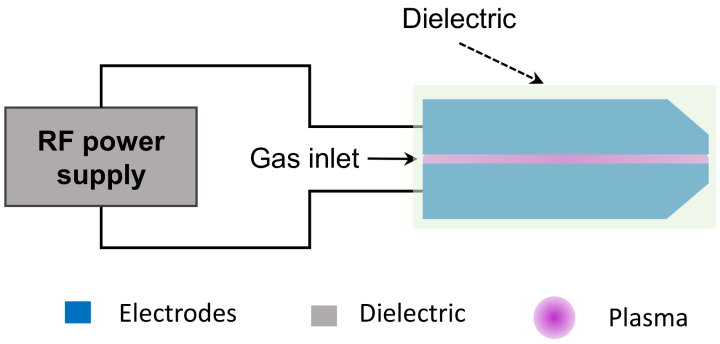

Figure 2.10. Schematic of the rectangular electrode arrangement of the μAPPJ.

The working gas of the jet is He, however different admixtures (e.g. $He + O_2$, $He + N_2$) have been used to evaluate plasmachemical and biocidal processes. Quantitative and qualitative characterization of atomic nitrogen density depending on nitrogen admixture to the working gas was reported [66–68]; the complex plasma chemistry was modeled [69–70]; helium metastables in plasma and jet afterglow[1]) were measured [72]. μAPPJ was also used to investigate the plasma induced chemistry of treated aqueous solutions, and the pathways of hydrogen peroxide and hydroxyl radicals generation were proposed [73]. Discharge propagation dynamics in modified jet, when glow and constricted discharges co-existed was described [74–75].

Moreover, bacteria inactivation pathways were studied using modified μAPPJ [76–77] to study reactive species and emitted photons separately. Authors concluded, that the damage of bacteria envelope was caused mainly by plasma produced particles, while DNA modifications were induced by both particles and emitted photons.

Results of experiments provided to evaluate bactericidal pathways in plasma treated aqueous solution using μAPPJ are summarized in section 8.2.

[1]) "The radiation emitted from plasma after the discharge is not maintained anymore." [50, 71]

2.3.2 DC driven plasma jets

Plasma jets driven with DC power supply are usually constructed using the electrode arrangement shown in the figure 2.11(a). The most commonly used DC-driven plasma jet was reported by Kolb et al. [78]. The inner capillary electrode is insulated with alumina tube and the second grounded electrode makes the cover; although, the jet is driven with positive or negative DC voltage, the outer electrode is not completely insulated from the inner capillary one, and makes a chamber where plasma is generated. The distance between the electrodes, a diameter of inner capillary electrode and working gas parameters are crucial for plasma ignition. Material and feeding gas varies in dependence on the particular parameters in each scientific group. For instance, Sun et al. [79] used the micro scale electrode arrangement and Ar with admixture of O_2 or N_2 to investigate inactivation pathways of plasma treated aqueous solutions. They inactivated more than 97% of *B. subtilis*[1]) in the treated water and assigned inactivation to reactive oxygen species, namely to $OH^{\bullet}, O_2^{-\bullet}, O_2(^1\Delta_g)$). Zhu et al. [80] used similar gas mixtures and reported options to control plasma compounds via the working gas. Kolb et al. [81] and Li et al. [82] reported inactivation of several microorganism strains (one gram positive, two gram negative bacteria and one yeast) and concluded, that inactivation was achieved by plasma generated reactive species, since single effect of heat and UV-radiation was excluded.

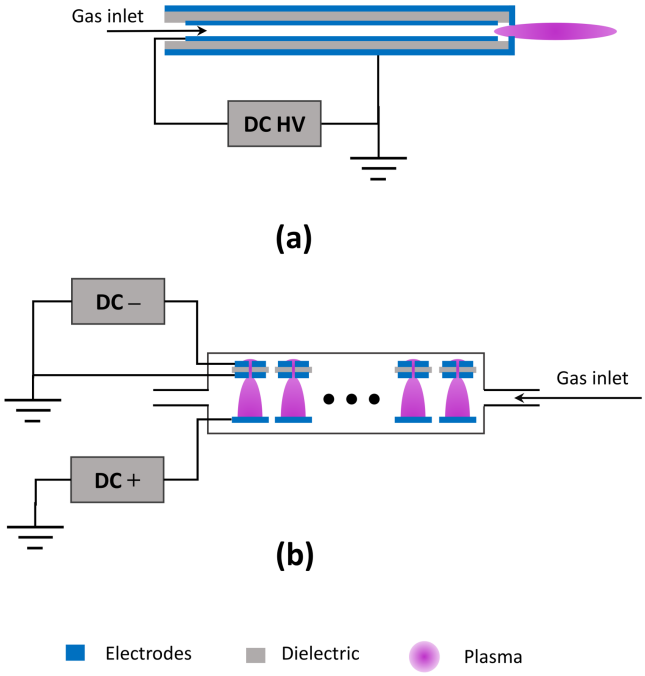

Figure 2.11. Schematic of DC jets commonly used to investigate of plasma induced biocidal effects. (a) shows typical electrode arrangement of widely used jet, first invented by Kolb et al. [81] and (b) shows DC driven array of 20 microcathode sustained discharges [83].

Moreover, Li et al. [82] reported lipid peroxidation, DNA damage and modification of protein of *E. coli* induced by plasma generated with DC-driven plasma jet operated in pure oxygen. There are even more authors, who used similar setup for their

[1]) *Bacillus subtilis* is commonly used in biomedical studies as a characteristic representative of Gram-positive spore-forming bacteria.

investigations. For instance, Deng et al. [84–85] used the nitrogen with admixtures to deposit inorganic films; Xian et al. [86] investigated formation and propagation of plasma bullets with electric field.

Arrays of microcathode sustained discharges (MCSD) driven with DC power supply were reported by Sousa et al. [84]. A single array consists of 20 MCSD units, while each unit is created as a microhollow cathode discharge first developed by Schoenbach et al. [83]. The electrode arrangement is shown on figure 2.11(b). All micro units are placed in the chamber and the plasma is expelled from it by the gas flow (He with admixture of O_2 or NO). Authors were able to produce $1.0 \times 10^{17}\mathrm{cm}^{-3}$ of singlet delta oxygen.

2.4 MW-driven plasmas

In order to exhaust all possibilities plasma sources used in biomedical applications MW-driven plasma sources should be mentioned.

Microwave (MW) plasma are generated in electrodeless setup. The plasma is ignited and sustained by the electromagnetic radiation with frequency 2.45 GHz. Free electrons absorb the MW energy and ionize gas particles via inelastic collisions. As a result, power consumption increases and a number of free electrons rises. Energy of electrons in such plasmas does not usually exceed 2 eV and their density reaches values of about 3×10^{21} m^{-3} [87].

There are several commonly used setups of MW plasma sources. They usually use a magnetron, that generates microwaves at 2.45 GHz. Waves are transmitted by a coaxial cable or rectangular waveguide to a discharge chamber. Discharge can be insufflated with different gases, gas mixtures or air with gas flow of moderate rate of several slm. Amount of generated reactive oxygen species (ROS) and reactive nitrogen species (RNS) depends on used working gas; e.g. Shimizu et al. obtained 2 750 mg/l of NO and 400 mg/l of ozone using ambient air [88].

Nowadays, MW sources are realized as self-ignited plasma jets by inserting a quartz tube to lead the gas flow into the discharge space [89–90]. Moreover, downscaling of MW plasma torches allows to decrease power consumption down to several tens of watts [91–92].

Different studies on the MW plasma sources report inactivation of *B. cereus* spores[1]) up to $5\log_{10}$ reduction after 10 s of direct air MW plasma treatment of the contaminated surface [93]; or inactivation of $2\log_{10}$ of *E. coli* contaminated surface by indirect treatment [94], etc. Moreover, at least $5\log_{10}$ inactivation of *E. coli, S. aureus* or *A. brasiliensis*[2]) in PET bottles was reported [95]. Authors of a recent study in which bacteria inactivation pathways of MW-driven Ar plasma jet [96] claimed UV-C radiation and hydrogen peroxide species as main inactivation factor. Experiments were held on *E. coli* UV-sensitive mutants and wild stains [97].

More information regarding MW-driven plasma sources and schema of particular setups can be found in the review article [21].

[1]) *Bacillus cereus* is a gram-positive, heat resistive food borne pathogen.
[2]) *Aspergillus niger* is a fungi, causes black mold of onions.

Chapter 3
Plasma agents for bacteria inactivation

Non-thermal plasma induces a complex gas-phase chemistry, while the gas temperature remains low. This phenomenon makes NTP attractive for many applications, such as biomedical (e.g. sterilization of heat sensitive materials, wound healing), food preservation, etc. The gas phase chemistry in NTP is induced by energetic electrons, while the heavy particles remain at low energy. Electrons collide with gas atoms and molecules causing excitation, dissociation, and ionization. Gas plasma induction is associated with generation of various species, energetic particles (e.g. electrons, ions and photons), reactive species (e.g. free radicals and metastables), and transient fields (e.g. heat, shock and acoustic waves, electrostatic and electromagnetic fields). Interactions of these agents with living metter is a topic of great interest nowadays and due to its complexity is still not completely understood. Moreover, particular chemical and physical processes induced by plasma depend on a plasma source, experimental setup and surrounding conditions in the laboratory. Treated medium plays an important role as well. This makes comparing of achieved results even more problematic.

3.1 Charged particles

The atmospheric pressure discharges produce charged particles mainly in their active region. Charged particles are involved in bactericidal processes during direct plasma treatment, when the treated substrate is a part of electrical circuit [4]. On the other hand cell experiences zero total charge during indirect treatment, as plasma falling down onto the cell is quasineutral [98]. Charged particles play essential role in microorganisms inactivation causing ruptures of the outer membrane of bacterial cells [99–100].

Changes in gram-negative bacterial membrane morphology induced by charged particles were ascribed to processes occurring in their thin cell wall [101–102]. The cell wall is rough and can accumulate charged particles on the surface and gets charged. Bacteria experience an outward electrostatic force due to each charge carrier being subjected to the repulsive forces of charges with same polarity [102, 59]. This force is proportional to the square of charge potential:

$$|\phi| \geq 0.2\sqrt{rdF_t}, \tag{3.1}$$

where r is the radius of the surface curvature, d is a cell membrane thickness and F_t is an electrostatic force. The period of charge accumulation needs to be long enough to cause cell death.

Another hypothesis was offered by Digel et al. [103]: cell wall modifications might be explained by chemical processes induced by plasma born charged particles on proteins. Moreover the hydroxyl radical was proposed to play a major role in protein damage. Guo et al. ([59]) discussed both mentioned inactivation mechanisms and proposed that chemical and electrical processed simultaneously lead to the cell death. The charge accumulated on a cell wall surface increases a transmembrane potential

and leads to modifications of protein conformation. It allows to open membrane ion channels (Na^+, K^+, Ca^{2+} and Cl^-)[1]) and to push ions in- or outside the cell (with respect to partial pressure gradient). Charge accumulation increases further because NTP generated ions are too large to pass through opened ion channels and leads to crucial proteins conformation changes, which can result in their exclusion from a cell membrane. Once a protein is displaced, a huge pore remains on its place, big enough to let plasma produced reactive species get inside the cell and disturb the activity of proteins and enzymes. It was suggested that cytoplasm would leak out through these pores and induce the cell death (see figure 3.1).

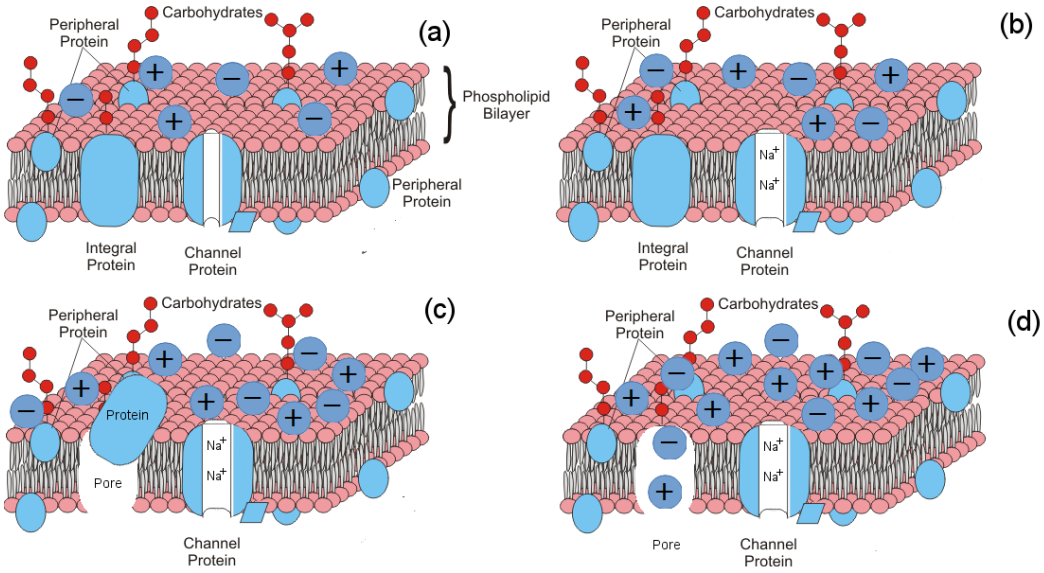

Figure 3.1. Mechanism of bacteria inactivation with charge particles proposed by Guo et al. [29].

3.2 Reactive species

Plasma produced reactive species differ with an operating gas mixture and surrounding in which plasma is generated (gas or gas-liquid interface). Reactive species generated by plasma, especially reactive oxygen and nitrogen species (ROS, RNS and RONS; see table 3.1), are extremely important biologically, as they are generated enzymatically within bacteria metabolism. However, the RONS added to bacteria externally by plasma can act differently, comparing to those, created by the cell [2].

The brief overview on published results shows that obtained bacterial reduction rate and assumed inactivation mechanisms strongly depend on the working gas mixture composition, as well as on atmosphere in the reactor. If one uses helium-driven plasma jet, molecular oxygen should be added in order to inactivate bacteria, even though O_2 increases a breakdown voltage. For instance, Laroussi et al. [104] suspected reactive species (e.g. NO, NO_2, O, O_3, OH) to play a major role in spores inactivation. This conclusion was made after comparison of *Bacillus subtilis*[2]) spore decontamination with a jet of pure He plasma or a gas mixture $He + O_2$. They observed significant improvement

[1]) Ca^{2+} channels present in the membrane of eukaryotic cell

[2]) *Bacillus subtilis* is gram-positive, one of the best understood prokaryote, and it is used in a wide range of microbiological studies as a model organism.

Reactive oxygen species		Reactive nitrogen species	
Radical	Non-radical	Radical	Non-radical
$O_2^{-\bullet}$	H_2O_2	$NO^\bullet$	HNO_2
$OH^\bullet$	$O_2^1\Delta_g$	$NO_2^\bullet$	NO^+
$HO_2^\bullet$	O_3	$NO_3^\bullet$	NO^-
$RO_2^\bullet$	ROOH	$N^\bullet$	N_2O_3
$RO^\bullet$	$ONOO^-$		N_2O_4
$CO_2^{-\bullet}$	O_2NOO^-		N_2O_5
$^1O_2$	ONOOH		ROONO
$O^\bullet$	CO		RO_2ONO

Table 3.1. List of various reactive oxygen and nitrogen species produced in plasma or plasma-liquid environment [32, 2].

in quality and quantity of spores inactivation caused by oxygen addition. Experiments were performed in ambient air, that is why presence of nitrogen species were expected.

Lai et al. [93] claimed plasma generated atomic oxygen plays an important role in bacterial inactivation, while Timoshkin et al. [105] asserted both nitrogen and oxygen reactive species play a key role. Differences in their conclusions were due to different plasma devices. Timoshkin et al. used two-points to metallic mesh DC corona discharge to treat inoculated surface indirectly using ambient air as a working gas. While Lai et al. used a microwave plasma torch working in ambient air to inactivate spore forming bacteria in the agar surface treated indirectly.

Deng et al. [106] and Kim et al. [107] independently studied the effect of gas mixture He and He + O_2 used as a working gas for a plasma jet on bacteria and obtained quantitatively different results. However both groups concluded, that mixture of helium and oxygen appeared to be a suitable gas mixture due to high production of reactive species in plasma.

Lu et al. [108] performed experiments with plasma jet using He + N_2 and He + O_2 working gas and indirectly treated substrate. They attributed antibacterial impact to reactive species, including oxygen atoms, ozone, and metastable state O_2^* in both cases.

Authors using plasma sources working with N_2 and O_2 containing gases (e.g. ambient or synthesized air) ascribed essential role in bacteria inactivation to reactive oxygen species (H_2O_2, O, O_3, $OH^\bullet$, O_2^1, $O_2^{-\bullet}$) and their reaction with RNS [109–110, 82, 111–114]. These species are known to induce oxidative stress in bacteria, which leads to membrane degradation (e.g. lipid peroxidation) and DNA damage [2].

3.3 UV light

It is widely reported, that various plasma sources generate ultraviolet (UV) radiation; however, its role in inactivation processes is also not definitely understood yet. The spectral density of UV light depends on the configuration of plasma source, working gas composition, power supply, etc. Only UV light with wavelength in range of 200–300 nm and doses of several millijoules per square centimeter are known to cause bacteria inactivation [115, 4]. However, smaller doses of UV radiation can cause sublethal damage to bacteria and induce changes in its DNA.

Possible effects of UV light generated by plasma was described by Boucher [116] in 1980. He proposed, that photons of energy in range of 3.3–6.2 eV induced strong bactericidal effect, as the energy corresponds with the maximal DNA absorbance wavelength. They showed, that UV radiation was more effective in inactivation of small

non-sporulated bacteria, because the depth of UV-light action is restricted to micrometers. Additionally, in the case of cell culture, which grew on the surface in layers, UV-light was absorbed by the cells of the top layer preventing those underneath from destruction. In the case of spores, which are bigger and highly resistant, it was assumed that UV light may contribute to partial alteration of disulfide-rich protein coat and allow diffusion of free radicals into the cell [116]. Nowadays, it is well known, that UV light is absorbed by nucleic acid of the cell, resulting to formation of thymine dimers, that stop DNA replication. Moreover, the results of recent studies confirmed, that the lethal effect of UV-A radiation is caused primary by protein damage [117].

The role of UV light in non-thermal plasma induced bacteria inactivation is still a topic of discussions. It is reported, that UV light plays a major role in the microwave driven plasmas or plasma generated by gliding arc discharge.

Moisan et al. [118, 111] in their review article summarized information considering changes in bacterial survival curves[1]) induced by plasma treatment of surface (see figure 3.2). Major role in plasma induced bacteria inactivation was ascribed to UV light.

They assumed three phases of bacteria inactivation process:

1 direct DNA damage induced by UV light;
2 erosion of the microorganism through the intrinsic photodesorption, which is induced by breaking chemical bonds with UV light photons leading to formation of volatile compounds and destruction of the cell. Authors who worked with microwave plasma devices usually use Ar or N_2/O_2 as a working gas. Devices operating in Ar are more sufficient with the dominant role in bacteria inactivation assigned to UV [119, 109, 120].
3 erosion of the microorganism through etching, resulting from the reactive species adsorption from plasma.

Non-thermal plasma devices operating in lower than microwave frequencies (with some exceptions) are assumed to generate UV radiation of insufficient intensity to cause bacterial death. Several authors confirmed this hypothesis experimentally: for instance, Hermann et al. [122] performed experiments with APPJ and a quartz glass window to screen out all plasma agents except the UV light. They did not recognize any inactivation or at least sublethal reduction of *Bacillus globigii*[2]); Machala et al. [24] performed similar experiment with his plasma spraying DC-driven device. They obtained similar results with no inactivation of *E. coli* on the surface. Analogous experimental results were obtained by Dobrynin et al., Deng et al., Lu et al. and other groups working with different non microwave driven NTP sources [123, 106, 108]. The author of this thesis also investigated, whether the UV light plays a significant role in surface decontamination with corona discharge in point-to-hollow electrode geometry. Her results confirmed results described above — UV light did not play the major role in bacteria inactivation [124].

[1]) Survival curve is a dependency of bacteria reduction on treatment time. This curve is characterized by the D value, which can be described as an inactivation rate, i.e. bacteria reduction rate as a function of time.

[2]) *Bacillus globigii* has been called *B. subtilis* var *niger*, it is gram-positive, spore-forming and is commonly found in dust, soil and water. It is a human pathogen and it is usually used as a tracer organism or biological indicator.

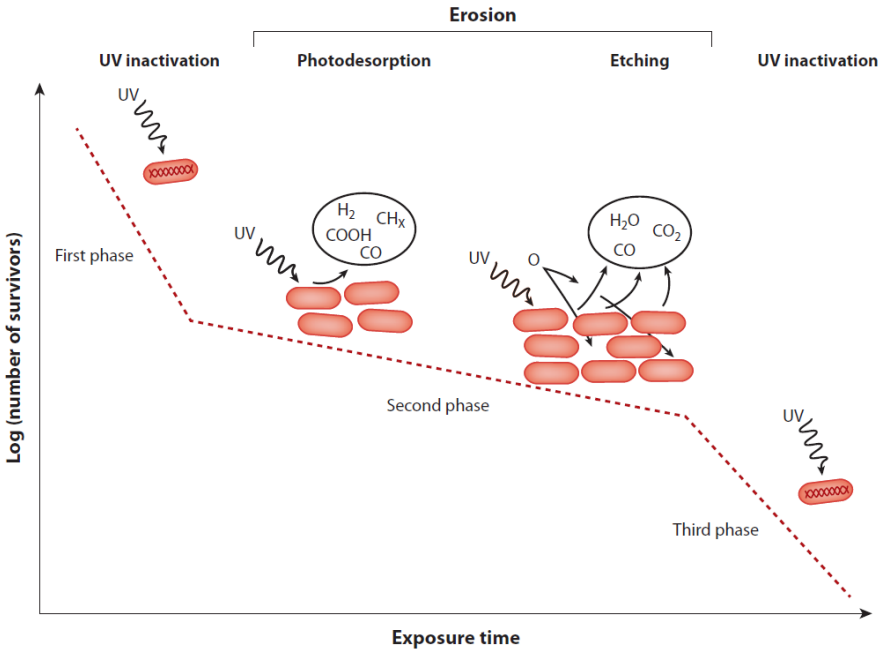

Figure 3.2. Mechanism of bacteria inactivation proposed for microwave driven discharges, where UV irradiation play a major role [121, 118].

3.4 Heat

There are two kinds of conventionally used heat sterilization: moist and dry ones. Moist heat sterilization technique includes autoclave method, when temperature of 121 °C under large pressure is used to sterilize surfaces and liquids [125]. The dry heat sterilization needs even larger temperatures (up to 170 °C) to inactivate most of known microorganisms [126]. However, smaller temperatures are sufficient to cause sublethal damages or stress response to most known bacteria. E.g. microorganisms used in this study (*E. coli, S. aureus, C. albicans*) show heat shock response already at 42 °C, and it results to 2 $\log_{10}$ bacteria reduction. The fourth microorganism used in this study, *D. radiodurans*, is less heat sensitive and is able to resist even 85 °C heat-shock [127]. Hence to provide heat sterilization ($> 5 \log_{10}$ bacteria reduction) temperatures over 100 °C should be used [128–129].

Most non-thermal plasma devices operate at low temperatures; however, in the case of APPJ, temperature of expelled plasma plume changes with distance from the nozzle. Temperature distribution of the DC-operated plasma jet used in this thesis, was evaluated by Mohamed et al. [130]. They measured temperature of the expelled plasma in dependence on the distance from the jet nozzle, used carrier gas, its flow rate and electrical parameters (supply voltage and current). Temperature decreased with increase of the gas flow rate and distance from the jet nozzle, while the current and voltage were kept constant. In the case when the gas flow rate and distance were kept constant, the temperature of expelled plasma increased with increasing current (see figure 3.3).

Analogous situation can be observed for different plasma devices in the case of remote treatment [131]. As one can see in figure 3.3 plasma temperature in close vicinity of the nozzle can reach even more than 100 °C. However, it is not common to place treated sample within 2 mm distance from the nozzle.

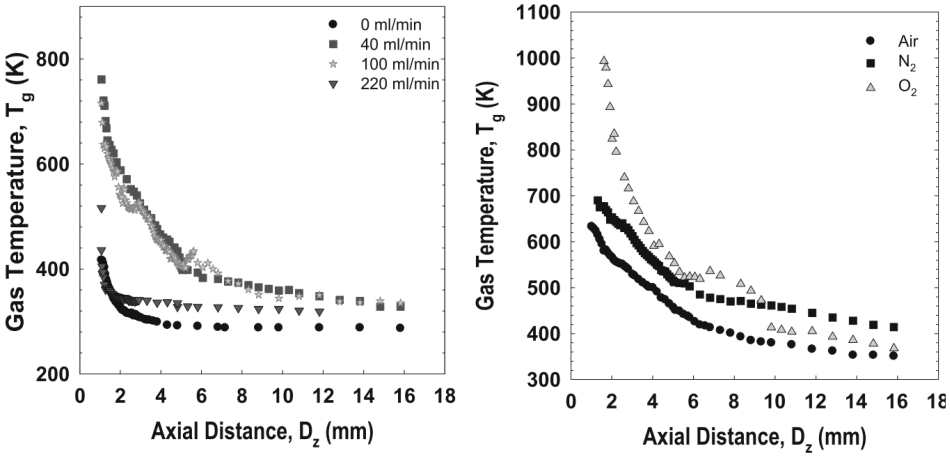

Figure 3.3. Gas temperature along jet axis for different flow rates (left) and working gases with flow rate 0.11 slm flow rate (right) measured on DC-operated plasma jet [130].

Nevertheless, there are several plasma sources (e.g. microwave ones, gliding arc or dielectric free electrode plasma jet) when the heat should be consider as a possible inducer of bacteria shock state [59].

3.5 Electric field

The intensity of electric field generated by non-thermal plasma sources is not sufficient to provide bacteria inactivation. It reaches the maximum values in a close vicinity of the electrodes. When the sample is treated remotely, it is usually placed 5–100 mm from the device nozzle, so the electric field can be neglected. However, in the case of direct plasma treatment, when the sample acts as an electrode, electric field can significantly contribute to bacteria damage. Intensity of electric field up to 20–30 kV/cm and 50 kV/cm was reported for dielectric barrier discharge and glow discharges respectively [132–135]. Moreover, direct plasma treatment with DC discharges leads to charge accumulation on the cellular surface, which rises potential difference between the intra- and extracellular space and induce membrane ruptures.

Critical intensity of electric field required for membrane destabilization is 10–14 kV/cm [136–137], because microorganisms decline its ability to close pores formed on the membrane. Porous membrane becomes hydrophilic, fails in its barrier function, and allows molecular flow through it. The current flow corresponding with Joule heat contributes to membrane destabilization and loses of its integrity. Loss of membrane integrity can result in a cell death.

Chapter 4
Bactericidal effects of plasma activated water

Interaction of plasma agents with living matter usually takes place in the gas-liquid interface, e.g. directly in bacterial suspension, or under humid conditions. NTP induces various chemical and physical processes in the gas, gas/liquid interface and liquid resulting to formation of reactive compounds. Variety of primary and secondary species depends on the discharge type, surrounding environment and properties of treated liquid. For example, the plasma working gas and energy dissipated in plasma influences reactivity of species, while composition of the treated liquid can affect plasma induced reactions through presence of electrolytes.

Prolonged post-discharge bactericidal properties of treated liquids were referred differently by various researchers: e.g. "the water of death", plasma activated water (PAW), plasma acid, plasma pharmacology, or prolonged microbial resistance of water [138–142]. The term "*Plasma activated water*" or PAW proposed by Kamgang-Youbi et al. [139] will be used in this thesis, as it is widely used worldwide considering any plasma treated aqueous solution, e.g. plasma treated phosphate buffered saline, or plasma activated essential oil can be also referred as PAW.

Bactericidal effects induced by plasma in liquids were demonstrated for: unbuffered solutions such as deionized (DI) water [143–145, 3], normal saline [47, 146] or buffered solutions [1, 147–148, 145]. However understanding of post-discharge processes in aqueous solutions is challenging due to diversity of both gas and liquid environments. Moreover, liquid evaporation or its eminent contact with electrode can change plasma parameters or affect formation of species in gas phase.

Acidification of unbuffered solutions induced by gas-phase plasma has been reported [149–159] (see table 4.2). One of the first studies referring this phenomenon was published in 1990 by Brisset et al. [150]. They used DC corona discharge established at point-to-plane electrode arrangement over the aqueous solution surface. They attributed acidification to excited nitrogen species (NO_2^-, NO_3^- and singlet oxygen.

The major role on pH changes was ascribed to weakly acidic HNO_2 as well as to HNO_3. Nitrous acid does not dissociate completely in low pH solutions, and can give rise to spontaneous formation of nitrigen monoxide ($NO^\bullet$) and nitrogen dioxide ($NO_2^\bullet$). Both $NO^\bullet$ and $NO_2^\bullet$ are cytotoxic and are more likely to be known as acidified nitrites. It has been reported, that acidic conditions are good prerequisite for nitrites to act as an antimicrobial agent [160].

Formation of hydrogen peroxide in PAW might also contribute to pH decrease. Nevertheless, concentration of accumulated H_2O_2 rarely increase over 2 mmol/l (see table 4.2) and it might be too low to cause observable pH changes [32].

Plasma induces formation of transient RNS in gas-liquid interface, which are expected to play a major role in bacteria inactivation [47, 162–163, 143–144, 164, 145, 165, 1]. Pathways of short-lived RNS generation are depicted on figure 4.1, right dashed box [161] and can be summarized through following oxidizing reactions [32]:

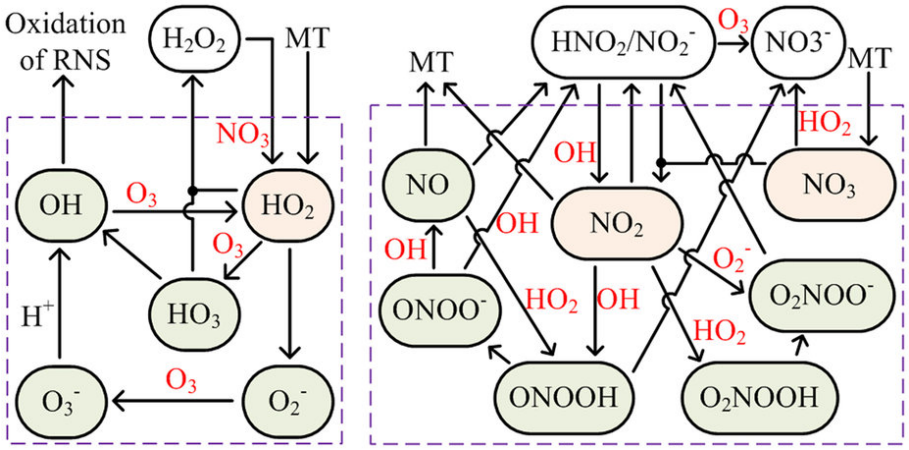

Figure 4.1. Pathways of short-lived ROS and RNS generation induced by gas-phase plasma in gas-liquid interface proposed and simulated by Liu et al. [161]. Abbreviation "MT" corresponds to the mass transfer.

$$O_2^{-\bullet} + NO^{\bullet} \rightarrow O{=}N{-}OO^{-} \tag{4.1}$$

$$NO_2^{-} + H_2O_2^{\bullet} \rightarrow O{=}N{-}OO^{-} + H_2O \tag{4.2}$$

$$OH^{\bullet} + NO_2^{\bullet} \rightarrow O{=}N{-}OO^{-} + H^{+} \tag{4.3}$$

Reactivity of peroxinitrites is strongly pH dependent, and under acidic conditions the protonated form of peroxinitrite predominates and it decays into $HO^{\bullet}$ and $NO_2^{\bullet}$ radicals:

$$O_2^{-\bullet} + NO^{\bullet} \leftrightarrow O{=}NOO^{-} \overset{\pm H^{+}}{\longleftrightarrow} O{=}NOOH \leftrightarrow^{\bullet} OH + NO_2^{\bullet}. \tag{4.4}$$

Reactive nitrogen species are recognized to play variety of important biological roles [166], e.g. they are involved in the cell signaling pathways, or redox chemistry [2]. Formation of peroxynitrites under acidic condition can catalyze reactions of other reactive species with fatty acids on cellular membrane and lead to membrane degradation and DNA damage [167–169].

Hydroxyl radical is the major ROS formed by electrical discharges in gas-liquid interface, and its hard to overestimate its impact in bacteria damage. $OH^{\bullet}$ radical among others induces strong oxidative stress, starts lipid peroxidation, and is involved in DNA damages (see chapter 6). It is short-lived molecule with half-life of approximately 200 µs and high oxidizing power $E^0 = 2.85$ V, that makes it the strongest oxidant in aqueous environment. Nevertheless, due to its short life-time it should be in close vicinity with biological material or to be generated inside the cell to induce cell damage. $OH^{\bullet}$ radicals formation in PAW is caused both by their diffusion from gas phase plasma, or by direct formation in aqueous solution in contact with discharge attributed to photochemical reactions [32].

Direct impact of UV-radiation to a microorganism is very limited since it needs to sufficient dose of radiation to be damaged. There are several main processes resulting in formation of hydroxyl radical induced with photolysis. Photolysis of ozone, taking place in 200–280 nm region:

$$O_3 + h\nu \rightarrow O_2 + O(^1D) \tag{4.5}$$

$$O(^1D) + H_2O \rightarrow 2OH^{\bullet}; \tag{4.6}$$

the photolysis of hydrogen peroxide in the 200–300 nm region [32, 170]:

$$H_2O_2 + h\nu \rightarrow 2OH^{\bullet}. \tag{4.7}$$

Generally short lived ROS are very important in bacteria inactivation processes, as they induce oxidative stress. Ozone is another powerful oxidant, which dissociates from the gas-phase into liquid. Ozone is unstable in solutions; moreover, hydrogen peroxide accelerates its decomposition and increases generation of $OH^{\bullet}$ radical via peroxone process [32, 161] (eq. (4.8), (4.9) occurs very slowly in low pH (see figure 4.1, left dashed box).

$$O_2 + HO_2^- \rightarrow HO_2^{\bullet} + O_3^{\bullet -} \tag{4.8}$$

$$O_3^{\bullet -} + H_2O \rightarrow OH^{\bullet} + OH^- + O_2 \tag{4.9}$$

The role of ozone in bacteria inactivation in PAW was discussed by several authors, as despite it short life-time ozone is highly reactive and is known for its cytotoxicity. Pavlovich et al. [148] reported a good correlation of O_3 concentration in PBS with *E. coli* reduction rate, and concluded an important if not dominant role of ozone. They prepared PAW by remote surface DBD treatment in ambient air. Machala et al. assumed ozone contribution to antibacterial effect in PAW prepared with transient spark discharge [145].

The diversity of plasma reactors, experimental conditions and ways of bacteria treatment make the question even more challenging and bring a question of comparability of results of different scientific groups worldwide. A short review of bacteria inactivation with chemical composition of PAW across different plasma sources is provided in tables 4.1 (bactericidal properties) and 4.2 (chemical composition).

There are several commonly used ways of bacteria exposure to PAW that are:

- bacterial suspension is added to treated solution prior to plasma treatment, i.e. bacteria are treated with plasma in the liquid media;
- bacteria suspension is added to the solution within 1–3 minutes after the plasma is turned off, i.e. bacteria are exposed to post-discharge chemical processes in PAW;
- bacteria suspension is added to PAW within hours (or even days) after plasma treatment.

The key role in bacteria inactivation with PAW is usually prescribed to synergistic effects of hydrogen peroxide and nitrites, through formation of transient nitrogen species in acidic environment. The dominant role of hydrogen peroxide is excluded according to evidence that the minimal inhibitory concentration of this species investigated for example by Penna et al. [171] is at least one order of magnitude higher then its concentration generated in PAW (see table 4.2). Moreover, the effect of NO_x^- and H_2O_2 on bacteria in artificially prepared solution with the same concentrations as in PAW is negligible as well [172]. The correlation between bacteria inactivation rate and PAW acidification was observed by different authors [172, 147, 173].

There are several studies, which report very different mechanisms of bactericidal effects of PAW. For example Sakiyama et al. [174] reported inactivation of 99.5% of *E. coli* bacteria in normal saline solution after microdischarge treatment of the sample. In their setup the electrodes were dipped into liquid, while the discharge was generated in the gas-liquid environment. Authors proposed dielectrophoresis to be the leading mechanism of *E. coli* inactivation in 100–500 μm distance from the electrodes, and ascribed it to nonuniform electric field in the reactor. They assumed classical electrolysis

to occur on the electrodes with formation of hydrogen and chlorine gases. Reduction of hydrogen was accompanied with generation of highly reactive OH^-, which could play a significant role in bacteria inactivation.

Bactericidal effect of stored PAW decreases significantly and is ascribed to long-lived species and acidification [138, 144]. At the same time, the role of transient species cannot be excluded, considering the fact, that bacteria are always added into stored PAW in suspension with different concentration of chemicals. Pure DI water is usually not used in order not to cause osmotic shock to bacteria. Bacteria solution insertion and vortexing of PAW with bacteria gives rise to various chemical processes, that still were not deeply examined.

Tables 4.1 and 4.2 contain summary of PAW bactericidal properties and chemical components reported by authors mentioned above.

Plasma source	Medium	t_t min	V_t ml	t_b min	Bacteria	Reduction logs	Reference
Gliding arc	DIW[1]	5	20	30[b]	*H. alvei*	5	Naitali et al. [143]
DBD	DIW	20	10	180[b]	*E. coli*	6	Traylor et al. [144]
DBD	PBS[2]	5	0.15	5[a]	*E. coli*	5.5	Pavlovich et al. [148]
DBD	DIW	15	10	15[a]	*E. coli*	7	Oehmigen et al. [152]
DBD	Saline[3]	12	5	15[b]	*E. coli*	7	Oehmigen et al. [47]
DBD	DIW	10	10	15[b]	*S. aureus*	4.3	Laurita et al. [175]
FE-DBD	Saline	3	0.1	15[b]	*E. coli*	6	Ercan et al. [176]
DC jet (−)	DIW	10	20	10[a]	*S. aureus*	6	Liu et al. [147]
DC jet (+)	DIW	15	50	90[b]	*E. coli*	6	this thesis
Corona (−)	DIW	30	10	10[b]	*E. coli*	4	Julak et al. [138]
RF APPJ	Saline	2	0.1	2[a]	*P. aeruginosa*	6	van Gils et al. [146]
kINPen	DIW	45	6	45[a]	*E. coli*	7	Dolezalova et al. [3]
Transient	DIW	10	20	10[a]	*E. coli*	7	
spark	PB[4]	10	20	10[a]	*E. coli*	4	Machala et al. [145]

Table 4.1. Review of bactericidal effect of PAW prepared with different plasma sources — bacteria inactivation. a — bacterial suspension is added to treated solution prior to plasma treatment, i.e. bacteria are treated with plasma in the liquid media; b — bacteria suspension is added to the solution within 1–3minutes after the plasma is turned off, i.e. bacteria are exposed to post-discharge chemical processes in PAW. (Abbewviations: [1]DIW — DI water; [2]PBS — phosphate buffered saline; [3]Saline — normal saline solution; [4]PB — phosphate buffer)

Plasma source	Treated solution	t_t (min)	V_t (ml)	pH	c(H_2O_2) (mM)	c(NO_2^-) (mM)	c(NO_3^-) (mM)	Reference
Gliding arc	DIW	5	20	3.0	0.01	1.6	0.13	Naitali et al. [143]
DBD	DIW	20	10	2.7	0.1	1.2	1.2	Traylor et al. [144]
DBD	PBS	5	0.15	6.5	0.08	3.5	3.0	Pavlovich et al. [148]
DBD	DIW	15	10	2.7	0.07	0.03	0.8	Oehmigen et al. [152]
DBD	Saline	12	5	3.0	0.07	0.03	0.8	Oehmigen et al. [47]
DBD	DIW	10	10	3	0.3	0.1	3.2	Laurita et al. [175])
FE-DBD	Saline	3	0.1	2.58	0.9	NR	3.86	Ercan et al. [176]
DC jet (−)	DIW	10	20	3.2	2.4	0.65	0.25	Liu et al. [147]
DC jet (+)	DIW	15	50	3.1	0.04	0.15	1.2	this work
Corona (−)	DIW	30	10	2.7	1.7	NR	NR	Julak et al. [138]
RF APPJ	Saline	2	0.1	4.1	0.6	0.01	0.1	van Gils et al. [146]
kINPen	DIW	45	6	3.7	0.9	0.0025	0.01	Dolezalova et al. [3]
Transient	DIW	10	20	3.3	0.7	0.2	1.0	
spark	PB	10	20	6.2	0.4	0.6	0.9	Machala et al [145]

Table 4.2. Review of bactericidal effect of PAW prepared with different plasma sources — chemical analysis, concentrations of routine measured species (H_2O_2, NO_2^-, NO_3^-).

Chapter 5
Microbiology

The term microorganism does not correspond to any precise taxonomic category. It is commonly used to refer to any organism in a small scale, which is impossible to see with a naked eye. However, the term is usually used for macroscopic forms that belong to a group that is largely microscopic (e.g. the fungi, the algae), and it is not used to define some microscopic animals with organ systems. Most microorganisms are unicellular, i.e. the entire organism consists of a single cell. Some microorganisms can organize to create filamentary structures by attaching to each other, but they do not form differentiated tissues and organs [177].

The cellular world is divided into two major groups based on whether or not cells have nucleus or not. Nucleus refers to an internal membrane-enclosed region containing genetic material. Cells that have a well-defined nucleus are called *eukaryotic*, whereas cells that lack a nucleus are called *prokaryotic* [178]. In addition, DNA of prokaryotic cell is not organized into multichromosomal structures as it is in eukaryotes, but it is typically single double-stranded molecule of DNA.

Typical microorganism contains of 70% of water and 30% of "dry-weight". The dry-weight comprises macromolecules, lipids, and various monomeric building blocks, intermediates in biochemical pathways, enzymes cofactors, and inorganic ions. The particular percentage of each compound depends on the microorganism. An example of *E. coli* composition is shown in figure 5.1 [177].

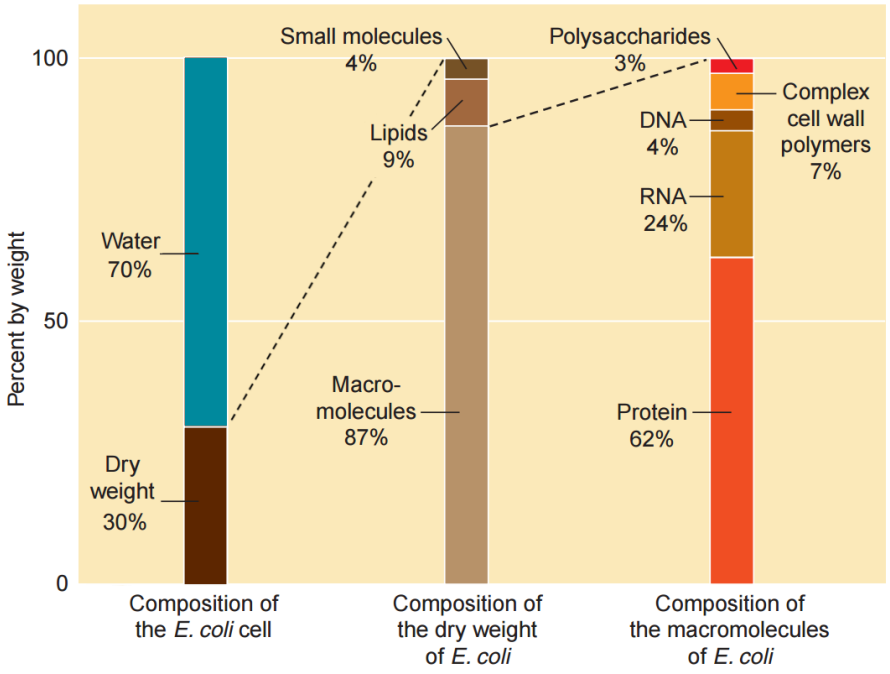

Figure 5.1. An example of the cell composition using *E. coli* [177].

Microorganisms are highly complex and adaptable to changes of their habitat. They have mechanisms to resist damage and adjust to hostile surrounding [177]. Both eukaryotes and prokaryotes employ very similar metabolic pathways to achieve cell growth and maintain viability [178].

Typical prokaryotic cell is small and can assume one of three basic shapes: spherical (coccus, ⌀1 µm, e.g. *S. aureus*), rodlike (bacillus, 2 µm long, ⌀0.5 µm, e.g. *E. coli*), or curved (vibrio, spirillum, or spirochete). All cellular components of prokaryotic cell are gathered in a single cytoplasmic compartment, and are enveloped by the phospholipid membrane and a cell wall [179].

Typical bacteria possess a complex cell wall, which consists of a peptidoglycan structure. This structure is a meshwork comprising sugars and amino acids, and its major roles are to separate interior of the cell from the outer environment, prevent water loss, protect the cell against infections and mechanical stress. Moreover, it gives the cell its definite shape and helps with osmotic-regulation. The cell membrane is composed of phospholipid molecules, which form a thin polar structure called lipid bilayer. The membrane creates as a selectively permeable barrier, restricting the kind and amount of molecules that enter and leave the cell [178].

Depending on the cell wall and membrane molecular structure bacteria can be divided into two groups: gram-positive and gram-negative (see figure 5.2). **Gram-positive bacteria** have thick multilayered peptidoglycan cell wall, which encloses the membrane. Peptidoglycan meshwork is interwoven with polymers called teichoic acids, which play a role of cell surface antigens. **Gram-negative bacteria** have two membranes: the outer membrane and cytoplasmic one. The peptidoglycan layer is located between two membranes in a substance called periplasmic space. In contrast to gram-positive cells, peptidoglycan layer of gram-negative bacteria is thin; therefore, they are more susceptible to physical damage [177–179].

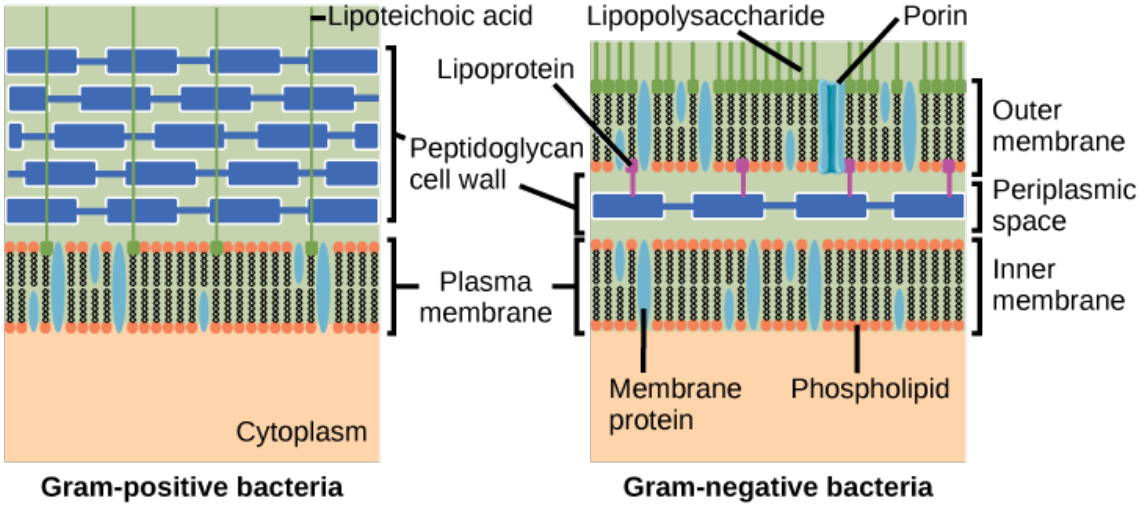

Figure 5.2. Gram-positive and gram-negative bacteria membrane [180].

Contrary to prokaryotes, typical eukaryotic cells have a complex ultrastructure comprising membranous and non-membranous organelles, which serve specific functions within the cell. Eukaryotic cells are larger than prokaryotic ones, due to their capability of endocytosis (a form of nutrients active transport). Endocytosis liberates the cell from constraints of simple diffusion, allowing them to sustain a relatively small surface area to volume ratio. The surface of eukaryotic cells is formed by a plasma

membrane, which is a selectively permeable barrier between the cytosol and the environment [178–179]. The structure of eukaryotic membrane and cell wall depends on the type of eukaryote, e.g. only fungi and plant cells have the cell wall (see figure 5.3). However, this thesis is focused on mechanisms of inactivation of bacteria and the reader can find more information regarding eukaryotes in [177–179, 181].

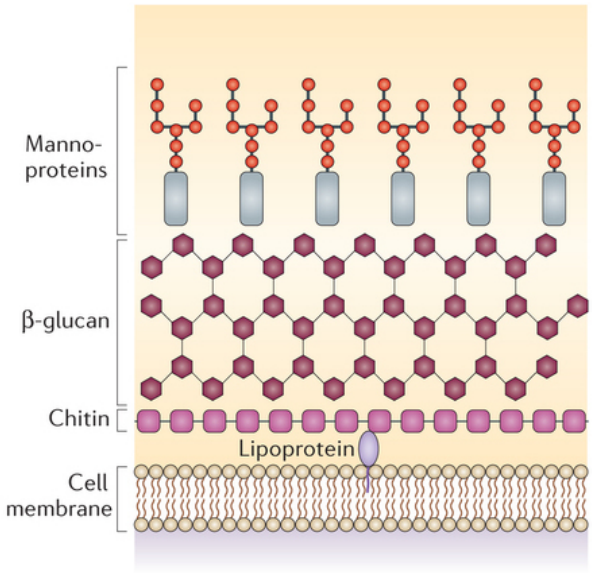

Figure 5.3. The cell wall of eukaryotes [180].

The microorganism's envelope is the first obstacle on the way of biocidal agents. Membrane damage is not necessary lethal to the microorganism, but it increases cells' susceptibility to different stress factors and can lead to cell mutations or even to cell death [177].

In this work four different microorganisms were used: *Escherichia coli, Staphylococcus aureus, Deinococcus radiodurans* and *Candida albicans*. *E. coli* was used to determine bactericidal pathways of PAW prepared with plasma jets. While, all mentioned microorganisms were used as an surface inoculum to determine plasma induced processes in oregano essential oil.

- *Escherichia coli*

E. coli is a typical gram-negative, rod shaped prokaryote. It was named after Teodor Escherich as he was the first to isolate it from the feces of newborns and described it in 1885. *E. coli* colonizes the gastrointestinal tract of most warm-blooded animals within few hours after their birth; for example, it colonizes human newborns within the first 40 hours. Some strains of this bacterium can cause severe infections resulting to illness, e.g. diarrhea, respiratory illness, pneumonia, etc. *E. coli* strains are used as markers of water contamination.

Escherichia coli is very adaptable to its common habitats, as it is able to transform obtained glucose into all macromolecular components. Moreover, it can grow in presence or absence of oxygen, as its metabolism can switch by means of aerobic and anaerobic pathways. This bacteria is able to respond to changes of environmental conditions, e.g. pH, temperature, osmolarity, presence of chemicals in solution, etc. Considering the fact, that entire DNA base sequence of the *E. coli* genome has been read in 1997, it is commonly used as a model organism for different biomedical applications [182].

- *Staphylococcus aureus*

S. aureus is a gram-positive, spherical shaped bacterium. It does not move by itself and can be found as a single cell, in pairs or in clusters, that resemble the bunch of grapes and can form fairly large yellow colonies on rich medium. It was first described and named by Rosenbach in 1884. This prokaryote is facultatively anaerobic, i.e. it grows by aerobic respiration or by anaerobic fermentation. Unlike *E. coli*, it should always be considered as a pathogen. Moreover, it is catalyze-positive, which means it is capable to convert hydrogen peroxide to water and oxygen.

S. aureus colonizes about 30% of human population. It is responsible for food poisoning, skin infections, bacteremia and infective endocarditis [183].

- *Deinococcus radiodurans*

D. radiodurans is gram-positive bacterium, although its envelope is unusual and reminiscent the envelope of gram-negative prokaryotes. It is obligate aerobic, and it is extremely resistive to ionizing radiation, UV light, oxidizing and electrophilic agents; and was first discovered in 1956, as the only surviving bacteria on the ground meat after treatment with high doses of radiation. Many researchers believe, that the reason, why *D. radiodurans* can withstand an acute dose of radiation equal to 5 000 Gy is that it has 4–10 copies of all its genes in its any growth phase. *D. radiodurans* is not documented to be a human pathogen [184].

- *Candida albicans*

C. albicans is an eukaryote, that can be either in unicellular or multicellular form. It gets the violet colour by the mean of gram staining like gram-positive bacteria. This yeast is an opportunistic fungal pathogen and is responsible for candidiasis in human hosts. However, it is found in 70% of the population in gastrointestinal and genitourinary tract of humans and does not cause any harm for non-immunocompromised individuals. *Candida albicans* is the second most described yeast after *Sacharomice cerevisiae* and gained its popularity as a model organisms in middle 90s. It is easy to maintain in laboratory conditions, its cells are dispersed and grow rapidly. *C. albicans* as a typical eukaryote is widely used in *in vivo* experiments prior to investigations performed on human cells [185].

5.1 Phases of bacterial culture growth

Plasma treatment is usually provided to inoculum that is not consisted of a single cell. The growth of bacterial suspension (called bacterial culture) represents a process of sequential division of the cells to form two identical daughter ones. If the cells are stored in medium full of nutrients they can survive for several days or even weeks. The special pattern, called growth curve, can be obtained by measuring bacteria concentration as a function of time. The growth curve is typically characterized by five phases: lag-phase, the delay in growth prior to log-phase; log-phase, when cell division proceeds in constant rate; stationary phase, when bacteria decelerate their replication rate as the habitat conditions stop to be favorable; death phase, when most of cells lose their viability; and long-term stationary phase, that can last for several weeks [186] (see figure 5.4).

When bacteria are placed to the new medium full of nutrients, the lag-phase is observed. The delay of bacteria replicating in the lag-phase can be attributed to the bacterial metabolism adaptation to new habitat conditions. This process can include synthesis of intracellular components, which are necessary for growth; or repairs of

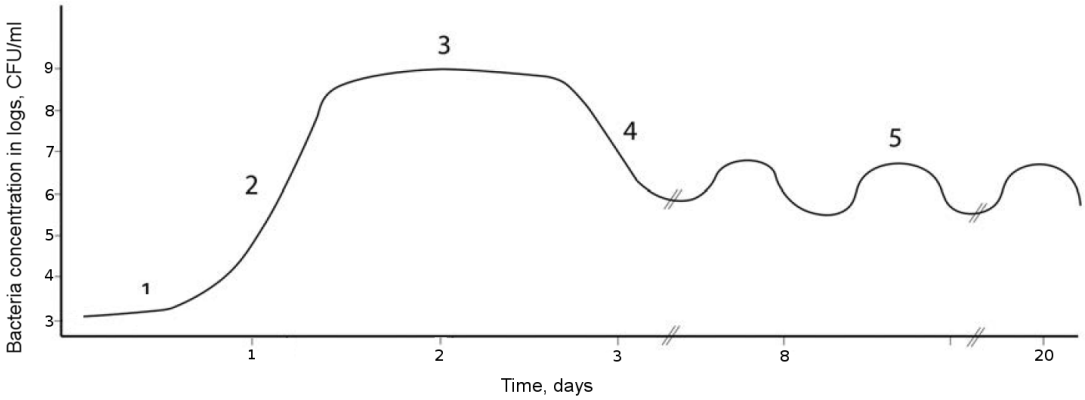

Figure 5.4. Growth curve of bacterial culture: 1 — lag phase, 2 — log or exponential phase, 3 — stationary phase, 4 — death phase, 5 — long-term stationary phase [187].

macromolecular damage accumulated during stationary phase occurred prior to bacteria inoculation into new medium [188]. Bacteria in lag-phase are usually not used in experiments objected to investigate bacterial damage pathways.

Once bacterial metabolism is adapted to new environment, cells start dividing in a constant rate. This rate depends directly on the nutrients in the medium. It is common to use bacterial culture in log-phase for experimental procedures, as metabolism of all bacteria in the culture is synchronized. Moreover, bacteria in this phase are more resistant to any kind of treatment and obtained results can be extrapolated to other phases.

Once nutrients in the medium are exhausted, bacteria replication rate decreases. The culture enters the stationary growth phase, which is characterized by the equilibrium between the numbers of dividing and dying cells. After some time bacteria start to suffer starvation. Moreover the toxic products of their metabolism accumulate in the medium which leads to decline of the number of viable cells. Stationary phase does not start with starvation; however, bacteria lose their viability that can correspond with mutations, changes in metabolic activity and another degradation.

The death phase starts when the number of replicating cells decrease below the number of dying cells. In this phase bacteria in the culture are not resistive to stress factors and are not usually used for biomedical experiments.

The final phase of bacterial culture is the long-term stationary phase, which can last for many days or even months. Dead cells release nutritions into the bacterial culture and survivors can use them to replicate. However, increasing of the replication rate above the dying rate leads to lack of nutrients in the medium and a need for more cells to die. The process is periodical and is called the growth advantage of the stationary phase phenotype. It can be explained by mutations in survivors that lead to their ability to reuse nutritions released from dead cells [187].

5.2 Oxidative stress

The imbalance between the ROS production and antioxidant defense of the microorganism is defined as an oxidative stress. It is not necessarily lethal to bacteria, but it decreases their viability, activity and culturability [189]. Species that induce oxidative stress are, for instance, hydroxyl radical ($OH^{\bullet}$), superoxide ($O_2^{-\bullet}$), nitric oxide ($NO^{\bullet}$), or peroxynitrite ($ONOO^{-}$). Each of mentioned molecule has different half-life and re-

activity, but generally they can be involved in processes leading to a chain reactions producing new reactive species. All biological macromolecules (lipids, proteins, nucleic acid etc.) are possible targets for this process (see figure 5.5). Physiologically reactive oxygen species are produced inside the cell as the result of aerobic respiration [190]. ROS production at physiological level during the cell lifetime does not necessary lead to oxidative stress, as the cell has various of protective mechanisms, which produce antioxidants and can terminate oxidative reactions. However, once ROS production elevates over physiological level bacteria protective mechanisms fail to prevent lethal damages.

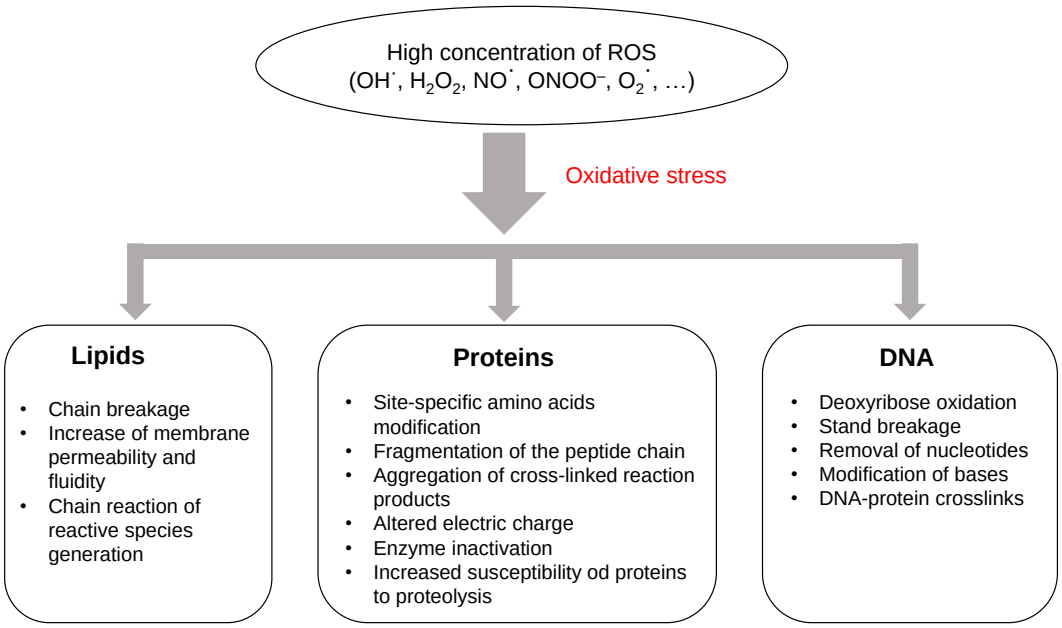

Figure 5.5. Diagram of oxidative stress induced by ROS in high concentrations to lipids, proteins and DNA [191].

5.2.1 Lipid peroxidation as a result of oxidative stress

The strongest oxidant among those mentioned above is hydroxyl radical ($OH^{\bullet}$). It has a high oxidizing power ($E^0 = 2.85$ V), it is water-soluble with half-life close to 200 μs [32]. It is produced in the cell through metabolic reduction of molecular oxygen or under various stress conditions; additionally, it is the major ROS found in electrical discharges in gas-liquid interface. Hydroxyl radical unspecifically attacks macromolecules, and it is involved in a lipid peroxidation process [192]. By the means of oxidative damage, the lipid peroxidation is considered to be the dominant molecular mechanism, that contributes to membrane disruption caused by oxidative stress [193].

Lipid peroxidation is a chain reaction leading to changes in lipid conformation and decline in their functions (see figure 5.6). The hydroxyl radical reacts with fatty acids of cell membrane; notably with polyunsaturated fatty acids (PUFAs), which are susceptible to autooxidation. $OH^{\bullet}$ contacting PUFA detaches one hydrogen atom from the carbon-carbon double bond in order to form a molecule of water changing PUFA into a radical.

Lipid radical ($R^{\bullet}$) is unstable and reacts with molecular oxygen to form the peroxyl radical ($ROO^{\bullet}$), which is also unstable and reactive. $ROO^{\bullet}$ is capable of abstracting

a hydrogen atom from another PUFA forming organic hydroperoxide (ROOH). Lipid hydroperoxide is the first comparatively stable product of the lipid peroxidation [192]. However, in contact with transition metals, e.g. iron or copper, a reductive cleavage of endogenous lipid hydroperoxides (ROOH) of membrane phospholipids to the corresponding alkoxyl ($RO^{\bullet}$) or peroxyl ($ROO^{\bullet}$) radicals can be performed [193–194].

$$Fe^{2+} + ROOH \rightarrow RO^{\bullet} + OH^{-} + Fe^{3+} \tag{5.1}$$

$$Fe^{3+} + ROOH \rightarrow ROO^{\bullet} + H^{+} + Fe^{2+} \tag{5.2}$$

$$Cu^{+} + ROOH \rightarrow RO^{\bullet} + OH^{-} + Cu^{2+} \tag{5.3}$$

$$Cu^{2+} + ROOH \rightarrow ROO^{\bullet} + H^{+} + Cu^{+} \tag{5.4}$$

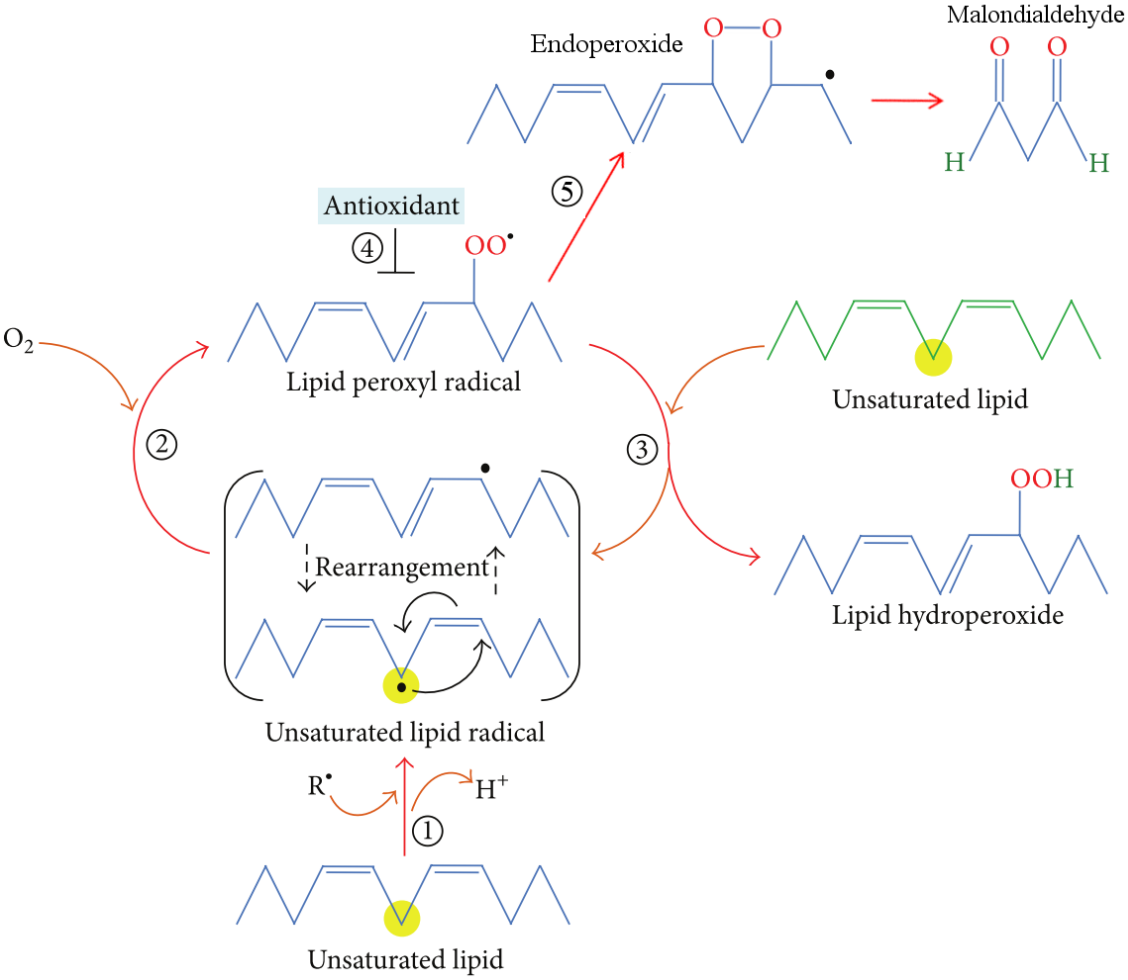

Figure 5.6. Process of lipid peroxidation intermediated with hydroxyl radical. Step 1: hydroxyl radical reacts with PUFA and carries hydrogen out of double bond; step 2: lipid radical reacts with molecular oxygen to form peroxyl radical; step 3. lipid peroxyl radical carries hydrogen out of double bond of another PUFA and form lipid hydroperoxide; step 4: to terminate the process antioxidants donate hydrogen ion. And finally step 5: up to 32 aldehydes can be produced as a result of PUFAs decomposition, one of them is MDA. The image was adapted from [195].

Moreover, lipid peroxidation can be intermediated either with RNS produced by plasma or with nitric oxide metabolism of bacteria [196]. In both cases the molecule involved in the process is $ONOO^{\bullet}$. Mechanisms of its generation induced by plasma in liquid or gas-liquid interface were explained previously. Production of hydroxyl radicals from the peroxynitrite is pH dependent and follows the reaction:

$$ONOO^{\bullet} + H^{+} \rightarrow ONOOH \rightarrow HO^{\bullet} + NO_2 \tag{5.5}$$

Decomposition of PUFAs lead to aldehydes production. About 32 different aldehydes were identified. These aldehydes are highly stable comparing to free radicals and are able to diffuse through the membrane out of the cell. Quantitatively there are two most important aldehydes: 4-hydroxynonenal (HNE) and malonyldialdehyde (MDA). Physiological level of them is low, hence increase of their concentration in extracellular environment is a signal of some pathological processes. Common method to evaluate lipid peroxidation is based on reaction of MDA with thiobarbituric acid and is explained further in the section 6.2.4. Additionally, HNE is able to modulate gene expression, cell prolifiration, differentiation and cell apoptosis [197–202], while MDA contributes to DNA damage and bacteria mutations, stand breakage and cell death [203–205].

5.2.2 Transition metal catalytic ROS production

Plasma device electrodes are usually made of heavy metals, i.g. copper or brass, stainless steel, titanium and others. Considering electrode erosion caused by plasma, reported by various of authors [206, 145, 81, 207], metal ions are released into PAW. In contact with bacteria metal can induce additional bactericidal effect, e.g. oxidative stress, changes in proteins, etc. [208].

The catalytic effect of transition metals improving biocidal properties of PAW was first reported by Sharma et al. [209]. They used corona discharge to induce plasmachemical reaction in liquid and discovered hydroxyl radical generation via Fenton process catalyzed with iron ions (eq. (5.6)).

$$Fe^{2+} + H_2O_2 \rightarrow Fe^{3+} + OH^{-} + OH^{\bullet} \tag{5.6}$$

Since that time a lot of papers have been published on this topic and they have been summarized for example in [32]. The Fenton's process is well known and it can involve different transition metals, e.g. copper or iron. Using M as a symbol for metal the reactions can be written as follows:

$$M^{(n)} + O_2^{\bullet} \rightarrow M^{(n-1)} + O_2 \tag{5.7}$$

$$M^{(n-1)} + H_2O_2 \rightarrow M^{(n)+} + HO^{\bullet} + HO^{-} \tag{5.8}$$

Hydroxyl radical produced by these reactions induces oxidative stress to microorganisms. There are reports suggesting that oxidation of phospholipids depend on the transition metal concentration in liquid and on the transition metal itself (see figure 5.7) [210, 193].

5.3 Bacteria damage induced by transition metals

Nevertheless, metal ions released from the electrode can be toxic to bacteria. For example copper is known to induce bacteria damage even in small concentrations below 10 µmolł.

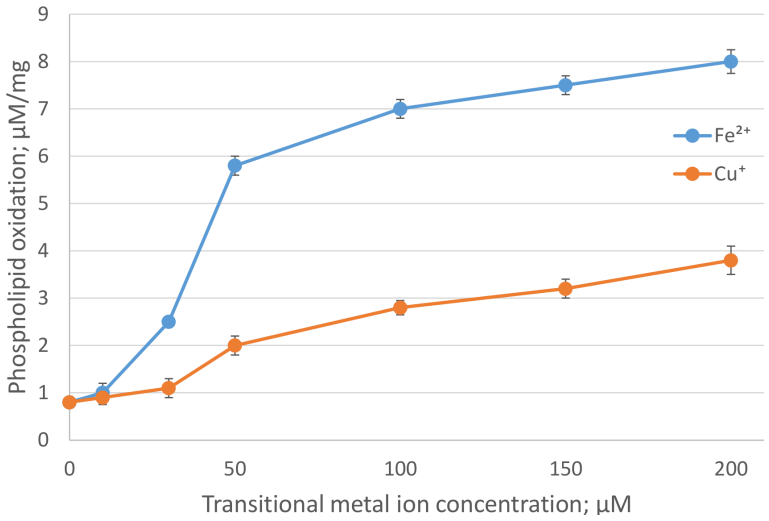

Figure 5.7. Oxidation of phospholipids as a function of transition metals concentration. Each transition metal was used separately. Image was adapted using data reported in [193].

- Copper's toxicity

Copper is an essential metal for most of living microorganisms and physiologically they creates a single copper ion during the lifetime. On the other hand copper becomes toxic once organism is overloaded. Copper catalyze movement of electrons within biological molecules, and due to its high redox potential it serves as a cofactor for proteins in various biological pathways, e.g. respiration or iron metabolism [211, 208]. Microorganisms are highly sensitive to copper impact as they cannot control its concentration in extracellular environment.

The exact mechanism of copper toxicity was long ascribed mainly to the reaction of copper with hydrogen peroxide produced by the cell. Hydroxyl radicals produced by the reaction analog to the Fenton one induce DNA damage, which can cause both mutagenity and lethality [212].

Copper is toxic even in small doses under physiological conditions; however, the minimal inhibitory concentration of this metal in complex medium is in range of mmol/l [213]. In the doses of 10 µmol/l and lower copper causes a branched-chain amino acid auxotrophy, that leads to malfunction of a particular cell signaling process. Moreover, free copper ions are involved in the Fenton-like reaction with production of the reactive oxygen species, that can further induce damage in signaling pathways of the cell [214].

- Iron

Iron is a fundamental element of bacteria metabolism and is involved for instance in bacteria growth pathways. Toxicity of iron is caused by its interactions with reactive oxygen species [215]. Hence, it is extremely important for bacteria to establish iron supplies and, at the same time, ensure the intracellular iron is maintained in a safe, non-toxic form. Iron-sulfur clusters have been recognized as essential and versatile cofactors of proteins involved in catalysis, electron transfer and sensing of ambient conditions [216]. The physiological level of free iron ions in the cell are in trace amount; however, under stress conditions ions can be released for instance from damaged iron-sulfur clusters.

Iron is a major protagonist in redox stress in bacteria; moreover, it activates *fur* gene, which is responsible for iron homeostasis, which rises bacteria sensitivity to the

oxidative stress, as a result of increased concentration of free iron in the cell. This effect can be reversed by iron chelation, by blocking iron uptake or by increasing of iron storage capacity [217]. Mentioned reactions are activated with a trace amount of free iron ions. An amount of iron released to bacterial suspension through electrode erosion can be in range of mmol/l, hence iron toxicity induced by ROS should be considered as a main pathway. The key reactions which lead to ROS production are Fenton (5.9), (5.6) and Habber-Weiss (5.11) ones [32].

$$O_2^{-\bullet} + Fe^{3+} \rightarrow Fe^{2+} + O_2 \tag{5.9}$$

$$Fe^{2+} + H_2O_2 \rightarrow Fe^{3+} + OH^- + OH^\bullet \tag{5.10}$$

$$O_2^{-\bullet} + H_2O_2 \overset{\text{Fe catalysis}}{\longleftrightarrow} OH^\bullet + OH^- + O_2 \tag{5.11}$$

- Titanium

Titanium is recognized for its extremely low toxicity to microorganisms and human cells [218]. Bactericidal effect of titanium has been studied for long time and in early 90^{th} there were rather contradicting results: several studies reported no bactericidal effect [219–220], while others reported small but significant antibacterial properties [221–222]. However, further investigations claimed titanium to have significantly smaller bactericidal impact in comparison with other metals, commonly used in medicine and plasma science (i.e. copper, iron) [218]. Moreover, with respect to physical properties of titanium, release of titanium ions from high voltage electrodes in discharges is rather low and its concentration in media does not exceed inhibitory limits.

On the other hand titanium oxides, particularly titanium dioxide, is known to be toxic to bacteria. Bactericidal properties of TiO_2 corresponds with its photocatalytical activity induced by UV light. Significant increase of bactericidal properties of plasma treated aqueous medium with addition of titanium dioxide powder has been reported [223–225]. However, release of photocatalytically active TiO_2 as well as its generation in medium through the plasmachemical reactions has not been documented yet.

5.4 DNA damage induced by oxidative stress

Reactive species produced by or induced into bacteria affect all compounds of bacterial cytoplasm. Moreover, reactive species are known to be a major source of DNA damage [226]. DNA is a molecule of unique importance as it is a repository of genetic information of the cell. Hence, modification of the DNA can result to malfunctioning or complete inactivation of encoded proteins. Generally speaking, ROS induce oxidation of deoxyribose, nucleotides removal, strand breakage, variety of modifications in DNA-protein crosslinks and organic bases of nucleotides. Additionally, changes in nucleotides of one strand can lead to nucleotides mismatch in another one and result in subsequent mutations [227].

The most reactive, but extremely short-lived ROS is hydroxyl radical, which is the main trigger of DNA damage discussed above. $OH^\bullet$ cannot be inducted inside bacteria cytoplasm directly from plasma; however, there are mechanisms of its generation based on hydrogen peroxide reactions. H_2O_2 is known to be produced in relatively large amount in PAW. Once it reaches the nucleus, chromatin-bound iron catalysis the Fenton reaction (eq. (5.6)) with production of hydroxyl radical. $OH^\bullet$ attacks DNA and DNA associated proteins and creates protein crosslinks, which cannot be repaired and may be lethal [228, 202, 229].

Bacteria and eukaryotes manage enzymes with relative specificity towards ROS induced DNA lesions, which remove modified bases from the DNA sequence and cleave the phosphodiester bond next to the position of the absent base [229–230]; however, mutagenic changes defense mechanism can potentially lead to the cell termination to prevent its replication.

5.5 VBNC state as a response to stress

As it has been discussed above, plasma agents stress bacteria. If the stress is not strong enough to cause irreversible changes to bacteria integrity or their vital functions, they can enter the viable but nonculturable (VBNC) state. This state was first described by Xu et al. [231] as a state, when bacteria fail to grow on routine medium. Bacteria in VBNC state show very low metabolic activity, but they can be regrown once stress factors are eliminated.

Bacteria enter VBNC state as a response to some significant stress factors, e.g. starvation, high or low temperature, oxidative stress or exposition to intense light. Low concentration or intensity are sufficient to induce the state. For instance, copper was assumed to cause *E. coli* switch from viable to VBNC state at concentration of 10 µmol/l, that is 1000 times lower, than minimal concentration to cause lethal bacteria damage [232, 214].

During this state bacteria experience reduction of respiration rate, nutrition transport, and macromolecular synthesis. However, their metabolism does not stop completely, and as a result the starvation and shock proteins are formed [233]. VBNC state is considered to be one of long-term survival strategy used mainly by gram-negative bacteria. Factors, which force bacteria to enter the state are not completely understood, as VBNC can be confused with various bacterial sensitivity states, which are characterized by decline of bacteria viability [234].

There are two possible strategies how to detect bacteria in VBNC state. The first one is complete elimination of stress factors, that should support bacteria to increase their viability, and bacteria regrowth on the routine medium. An the second way is gathering of indirect evidence of VBNC bacteria metabolic activity through e.g. resazurin, LIVE/DEAD or other viability assays applied simultaneously with conventional cultivation method (methods are described in section 6).

5.6 Bacterial damage induced by organic compounds

Plants are capable of synthesizing two kinds of oils: fixed oils and essential oils. Fixed oils consists of esters of glycerol and fatty acids, while essential oils (EOs) are mixtures of volatile, organic compounds originating from a single botanical source, and contribute to the flavor and fragrance of a plant. They have been known for centuries for their antiseptic i.e. bactericidal, fungicidal and medicinal properties. Essential oils can be obtained for example by hydro-distillation, and were used since the Middle Ages as local anesthetic, antiseptics, analgesic, sedative, etc.

Most of EOs are liquid, limpid and rarely coloured. For example, oregano essential oil (OEO) obtained from *Oregano vulgare* that was used in this study has light yellow colour and characteristic strong odor; however, one cannot recognize the OEO by the colour, as, for example, Lemon grass EO has the same one. EOs are lipid soluble and soluble in organic solvents with a general lower density than that of water, e.g. chloroform or benzene [235]. Gas chromatography and mass spectrometry analysis is

usually used to describe a chemotype of the particular EO. Results of general studies are published in analytical monography [236].

Essential oils usually contain about 20–60 different components, that makes them to be recognized as really complex natural mixtures. However, concentration of compounds in this mixture varies: from 20–70% for 2 major components, to trace amounts for others. The components include two major groups of distinct biosynthesized origins: terpenes and terpenoids, and aromatic compounds, which are all characterized by low molecular weight. For example *Oreganum compactum* essential oil's major components are carvaclol (30%) and thymol (27%), both belongs to a group of terpenes and are phenols (see figure 5.8). Generally, these major components determine biological effects of EOs.

5.6.1 Biological effects of essential oils

EOs are reported not to have specific cellular target because of large number of constituents [237], hence affect multiple target in the cell. EOs are reported to affect multiple target in the cell as their action is not specific, nevertheless their primary target is a cytoplasmic membrane [237]. In contact with bacteria cell wall EOs due to their lipophilicity are able to pass through bacteria membrane disrupting the structure of its layers. Moreover, EOs' induced permeabilization of membrane is associated with loss of ions and as a result reduction of membrane potential, collapse of the proton pump and depletion of the ATP pool. Membrane permeabilization can be lethal to bacteria and may lead to lysis and cell death [238–243]. Moreover, EOs provoke damage of mitochondrial membrane in eukaryotic cells by affecting Ca^{2+} cycling or decreasing membrane potential, which results in rapid increase of membrane fluidity and leakage of radicals, calcium ions and proteins [244]. Effects are similar to those of oxidative stress mentioned in previous chapter.

Cytotoxic effects were observed *in vitro* in most of pathogenic gram-positive and gram-negative bacteria, and several fungi stains. Results were obtained by agar diffusion[1]) method using filter paper disc with EO [242–243, 247–250], or the fast screening method using four-sections Petri dish and filter paper [251]. Most of essential oils have been reported to be cytotoxic, but at the same time they are not generally mutagenic. However, several authors reported possible mutagenic effects of *Origanum compactum* in eukaryotes [252–253].

On the other hand, essential oils and their components are reported to have antimutagenic effects. EOs are assumed to prevent mutagens penetration into the cell through its cell wall, or to inactivate mutagens by direct scavenging. Additionally, EOs act like antioxidant by capturing reactive species and radicals produced by mutagen, or induce activation of antioxidants enzymes in the cell. Another reported mechanism is induction of necrosis or apoptosis of the cell with mutated or damaged DNA [253–254]. Namely thymol and carvaclol, the main components of oregano essential oil, are reported to act as strong antioxidants [249, 255].

Imminent contact of essential oil is needed to provoke bacteria inactivation process. According to their high volatility maximal efficiency of surface decontamination can be reached by oils vaporization [251, 256].

- Oregano essential oil

[1]) Agar diffusion method is a common method in microbiology first reported in 1940. The filter paper discs containing test compound are placed on the inoculated agar plate. Antibacterial effect of the chemical compound diffused from filter paper to the agar is evaluated after incubation [245–246].

Oregano is a member of the mint (*Lamiaceae* or *Labiatae*) family and is related to thyme and marjoram. Flavors of oregano (*Origanum vulgare*) and marjoram (*Origanum majorana*) are different, oregano is peppery and zesty, while marjoram is sweeter and more delicate. In this work the author used oregano, as the marjoram does not contain the key ingredient carvaclol, which gives oregano its bactericidal, fungicidal, anti-mutagenic and antioxidant properties.

Oregano is a hardly perennial herb (it prefers colder climates) that grows to about 75 cm tall and wide in the best conditions to harvest. Quality and properties of the essential oil produces from the herb depends on the place of growing, time of harvesting and general environment conditions.

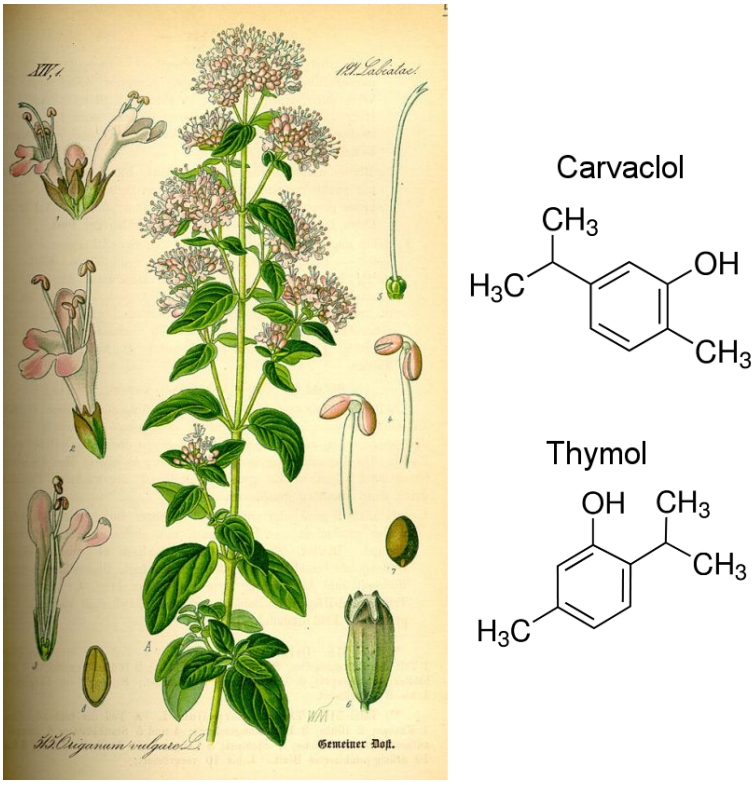

Figure 5.8. *Origanum vulgare L* and its major phenolic components thymol and carvaclol.

Major conmponents of *Origanum vulgare* are thymol and carvaclol (see figure 5.8). For *Origanum vulrage L* used in to provide experiments presented further in the thesis with 90% of carvaclol as a main component.

- Carvaclol

Carvaclol is phenol, which can be found in number of plants, including thyme and wild bergamot, but it is most abundant in *Origanum vulgare*. This chemical is known for its antibacterial and antifungi properties, acting as antioxidant, anti-mutagenic agent [257–259]; talking about humans and human cells, it is known for killing cancer cells [260–262], normalize lipid levels and fight against skin redness and swelling after injections [263]; talking about food contamination and cleaning, carvaclol is as effective as chlorine, that is used to clean for instance grapes tomatoes [264].

- Thymol

Thymol is phenol as well, it has antimicrobial activity due to phenolic structure, and has similar properties as carvaclol [265]. Due to its antiseptic activity, thymol is used as

major antimicrobial agent in toothpaste [266] or it is used as rapidly degradated non-persisting pesticide [267]. Additionally, using thymol and carvaclol at the same time induce synergistic effect of these to chemicals and increase their affect in reduction of bacterial resistance to common drugs like pencilin [268].

Chapter 6
Methods

6.1 Basic chemical analysis

Colorimetry methods were used to determine the concentration of hydrogen peroxide and nitric oxide in plasma activated water. Absorption spectroscopy was used to make pretest of nitrate concentration in solutions. Precise measurements of nitrates were then performed using ion chromatography by Dr. Peter Lukeš; the FTIR GAR and ATR spectra of essential oils were provided by Dr. Pavla Štenclová.

6.1.1 Griess reagent assay

Nitrite and nitrate ions are one of the main reactive species produced by plasma in liquid medium, therefore concentration of NO_2^- and NO_3^- is one of the parameters used to describe the PAW. Concentration of NO_2^- was measured colorimetrically using Griess reagent essay. It is a sensitive method first published by Griess in 1879 in German language [269]. The original reactions was modified and improved through the years. The essential part of the method is a diazotization reaction of two chemicals SA (Sulfanilamide or Sulfanil acid, depends on the kit) and NED (N-1-napthylethylenediamine dihydrochloride). SA and NED under acidic (8% phosphoric acid) conditions form a colorless complex called Griess reagent (see Figure 6.1), which becomes purple/magenta immediately in contact with nitrites with the maximum of absorbency at 540 nm. The colour reaches its maximum approximately 15 minutes after contact with nitrites.

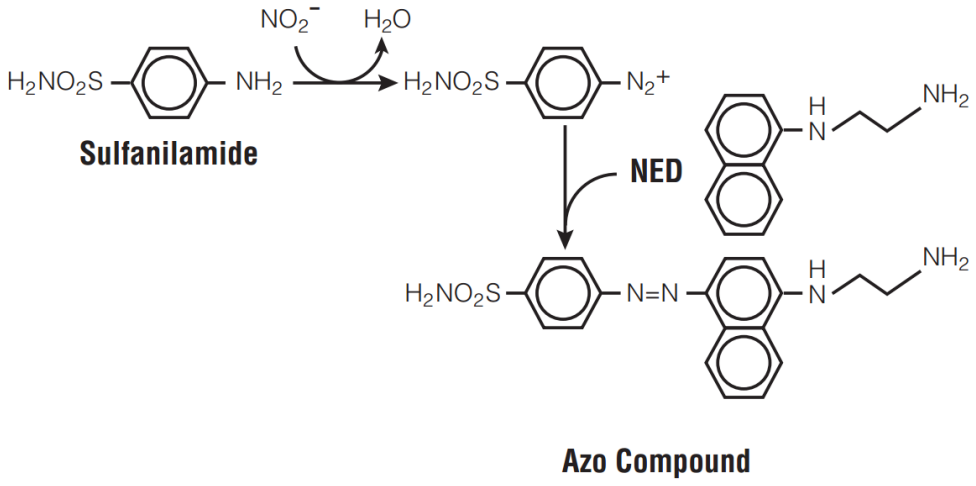

Figure 6.1. Chemical reaction involved in Griess reagent assay designed to provide the measurement of NO_2^- concentration [270].

We prepared the reagent by mixing 8% phosphoric acid with SA or NED; NaOH was added to decrease acidity and reach resulting pH value of 1.9 Griess reagent mixed with a

sample. Griess reagent was kept in the refrigerator at 4 °C to assure its stability in time, nevertheless it was not stored for more than 2 months, as its sensitivity decreases in time. Prepared Griess reagent was mixed with a sample in 1:2 ratio. Purpled substance was then placed into 96-well microtiter plate (330 µl for the well, 3 wells per 1 sample) and the absorbency at 540 nm was measured by the plate reader (Varioscan^{TM} Flash). The absorbance was measured three times.

Eleven points standard curve (see Figure 6.2) was made separately for each experimental day. Detection limits of the method are 1 µmol/l and 200 µmol/l, as the standard curve above the mentioned value is not linear. The standard was prepared by diluting $NaNO_2$ in water.

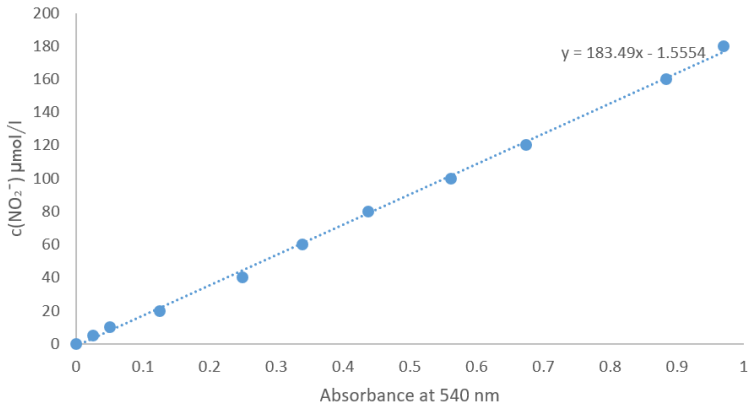

Figure 6.2. Example of the standard curve to measure concentration of NO_2- by Griess reagent.

6.1.2 Detection of hydrogen peroxide

The procedure of H_2O_2 concentration quantification in solutions was first presented by Eisenberg in 1943 [271]. It is based on reaction of titanil ions with hydrogen peroxide which results to pertitanic acid production (see (6.1)). Producted acid has yellow colour with maximum absorbance at 407 nm. The yellow-coloured complexes are stable for at least 6 hours of storage in lowered temperature. Intensity of colour is proportional to concentration of hydrogen peroxide with a molar extinction coefficient of $\varepsilon = 689\ \mathrm{l\,mol^{-1}cm^{-1}}$. This reaction is specific for H_2O_2, and if one uses the modified procedure published by Satterfield and Bonnell [272], no interference with other species occurs. The essential difference of the modified method is that the tested solution is diluted in acid instead of water.

$$Ti^{4+} + H_2O_2 + 2H_2O \rightarrow H_2TiO_4 + 4H^+. \tag{6.1}$$

Plasma activated water consists of nitrites that lead to hydrogen peroxide decomposition via reaction (6.2). That is the reason why the samples were fixed immediately with sodium azide in ratio 1:4 (sodium azide-to-sample) to reduce nitrites to sodium molecules via reaction (6.3) [1].

$$NO_2^- + H_2O_2 + H^+ \rightarrow NO_3^- + H_2O + H^+ \tag{6.2}$$

$$3N_3^- + NO_2^- + 4H^+ \rightarrow 5N_2 + 2H_2O \tag{6.3}.$$

The titanil reagent was then added to fixed sample and the result ratio of sample-to-sodium azide-to-reagent was 4:1:2. Prepared solution was then placed into 50 mm wide cuvette and absorbency was measured with a UNICAM Helios spectrometer.

The method is highly sensitive with the detection limit at 1 µmol/l.

6.2 Bacteria analysis

PAW induced damage to bacteria was evaluated using different tests: cheap and easy cultivation test and drop test performed on the solidified growth medium; expensive but easy Resazurin Viability Assay (RVA), LIVE/DEAD BacLight^{TM} Viability Assay (L/D), and DNA leakage assay; and finally time- and material-consuming TBARS assay and RT-qPCR.

6.2.1 Conventional cultivation test

Cultivation method allows to estimate a number of viable and cultivable bacteria by direct cultivating on the agar surface. The tested sample was prepared in ten-fold dilutions. Samples were diluted in sterile physiological solution. Thereafter, 1 ml of bacterial suspension with supposed concentration of $10^3, 10^2 \text{and} 10^1$ CFU/ml were transferred onto agar surface (solidified in ⌀9 cm Petri dish). The sample was left in the flow box to dry completely and was incubated overnight in the thermostat set to 37 °C. After overnight cultivation a number of colony forming units was calculated. Cultivation test were always done at least in triplicate.

Bacteria load of less then 5 CFU/ml and over 500 CFU/ml was considered as not relevant and were not taken into account in the experiments[1]).

Three different growth medium were used, however all of them were prepared in a similar way. Particular amount (m) of agar powder was suspended in 1 l of DI water and was heat to boiling to dissolve the medium completely. Dissolved medium was autoclaved at 121 °C for 15 minutes, cooled to approx. 60 °C and poured to sterile Petri dishes. All agar powders were purchased from OXOID CZ s.r.o.

- Sabouraud Dextrose Agar ($m = 65$ g) was used to cultivate *Candida albicans*; it is commonly used to cultivate fungi.
- Mueller Hinton Agar ($m = 36.5$ g) was used to cultivate all used bacteria stains; it is a non-selective, non-differential medium and is commonly used for antibiotic susceptibility test.
- m-FC Agar ($m = 52$ g) was used as a selective medium to cultivate *Escherichia coli*. Agar powder was suspended in purified water containing 10 ml of 1% Rosolic Acid in 0.2 N NaOH. According to preparation protocol it cannot be autoclaved, hence sterility was assured by 60 minutes for boiling.

6.2.2 Drop test assay

The drop test is a fast screening method to estimate the bacteria inactivation rate. This test is used in hundreds laboratories worldwide, but each laboratory has slightly different test protocol. Test used in this thesis was adapted from[274].

Figure 6.3 summarize the 4×6 drop test procedure. Briefly, 180 µl of sterile physiological solution (9 g of NaCl diluted in 1 l of water) was loaded to each well of sterile

[1]) Bacteria load < 5 CFU/ml corresponds to pipette error and > 500 CFU/ml is not relevant due to possible overlaying of bacteria [273]

96-well microtiter plate with multichannel pipette. 20 µl of the sample was then loaded to first 4 wells in a column as the primary dilution. Then 5 more dilutions were done by transferring of 20 µl of the sample from column i to column $(i+1)$ mixing 6 times. Afterwards the process was repeated. Thereafter, 4 replicates of 1 µl of the sample from each well were transferred to the 9 cm Petri dish with dry, but fresh agar. Different types of agar were used in different experiments (for particular type check corresponding sections in experimental part). Plates with loaded samples were allowed to dry and placed into the incubator set for 37 °C for overnight cultivation.

Relative decrease of survived bacteria number was estimated in comparison with untreated (control) sample. Conventional cultivation test (described in Section 6.2.1) was done as a reference for the control sample to investigate precise amount of CFU/ml.

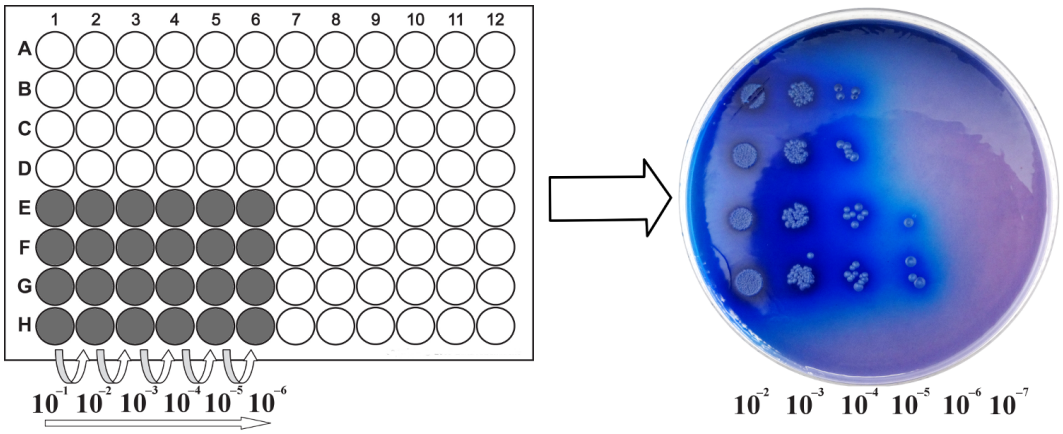

Figure 6.3. The 4 × 6 drop test method. Six 10-fold serial dilutions are made in 96-well sterile microtiter plate by loading 20 µl of the sample to 180 µl of physiological solution. 1 µl drop was then loaded with miltichannel pippete onto dry agar surface and incubated overnight. The photo on the right depicts *E. coli* load on selective m-FC agar.

6.2.3 Resazurin viability assay

Resazurin viability assay is relatively new, quick and sensitive method of detection cell viability, while cells used in the assay can be reused [275]. The test with slightly different protocol have been used for decades to investigate milk contamination with bacteria and yeasts [276].

Resazurin is non-toxic, blue-coloured, nonfluorescent, water soluble dye. In contact with viable bacteria it is reduced to highly fluorescent pink-coloured resorufin (see Figure 6.4). Fluorescence is proportional to a number of bacteria in the sample. Although, with longer time in bacterial suspension resorufin degrades to colourless nonfluorescent hydroresorufin which is responsible for decrease in a measured signal.

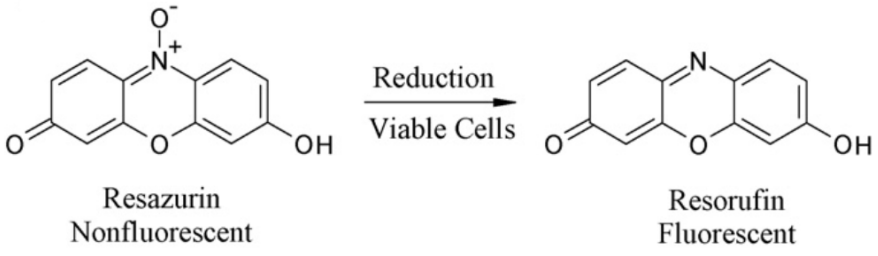

Figure 6.4. Irreversible conversion of non-fluorescent purple-colored resazurin to highly fluorescent pink-colored resorufin.

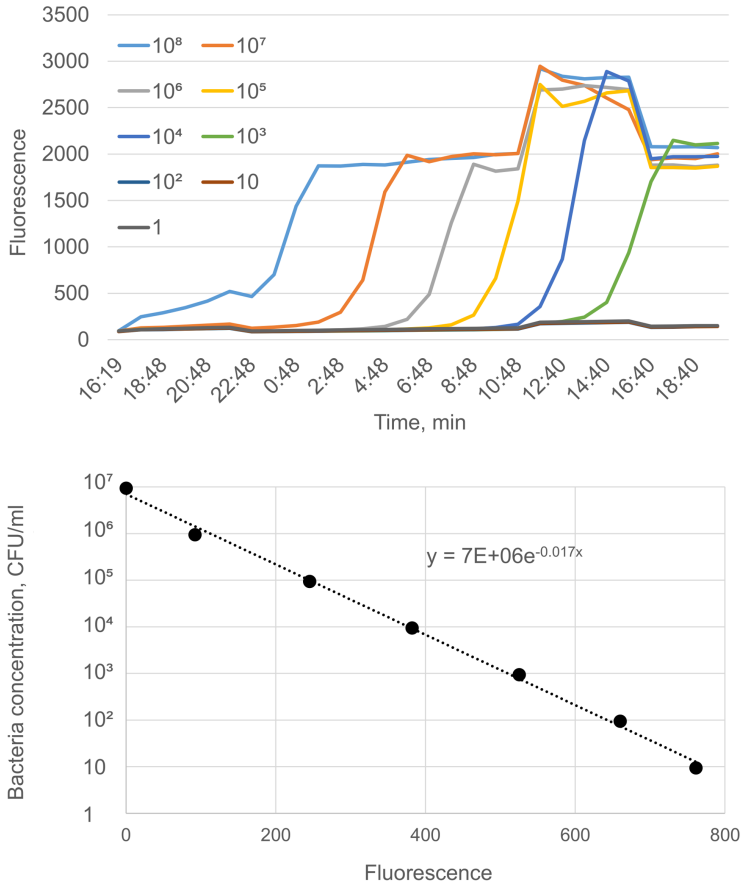

Figure 6.5. An example of preparation of standard curve with the resazurin viability assay: fluorescent signal measured each 60 minutes for 24 hours (top) and a corresponding standard curve (bottom).

Resazurin is reduced to resorufin by the loss of an oxygen atom loosely bound to the nitrogen of the phenoxazine nucleus. This reaction is irreversible by atmospheric oxygen. But the second stage of the reaction when resorufin is converted to nonfluorescent dye is reversible. This fact makes decrease of fluorescent signal small enough to be neglected [277]. Resazurin is very stable medium in absence of cells, but is rapidly reduced inside cell culture. Sensitivity of the method is about 80 cells in a sample, that leads to necessity of sterile atmosphere to prevent contamination.

Assay protocol is as follows: Firstly 100 µl of phosphate buffered saline (PBS) was mixed with the same amount of Luria-Bertani (LB) broth[1]) in each well of 96-well white microtiter plate. Maximal sterility is necessary due to extreme sensitivity of the test. The plate was sterilized by washing with isopropyl alcohol and subsequent irradiating with UV for 4 h prior to load. Loading was then performed in aseptic conditions. 60 µl of a bacterial suspension was then added to the wells. Each sample was loaded in triplicate. And lastly 30 µl of resazurin indicator solution was added to each loaded well and mixed 10 times. Thereafter the plate was placed to the Varioscan^{TM}Flash plate reader and fluorescence was read each 60 minutes for 24 hours. Fluorescence was measured at wavelength of 530 nm excitation and 590 nm emission. 8 point standard

[1]) Luria-Bertani broth contains of 10 g of Peptone 140, 5 g of yeast extract and 10 g of NaCl dilluted in 1 liter of DI water

curve was done for each single plate (measured signals and standard curve are shown in figure 6.5).

Bacteria reduction was then calculated in four simple steps: (i) the reference value of fluorescence (f) was identify as the middle of growth phase for control samples; (ii) the time t_f when f was reached was read from the graph; (iii) standard curve was done as a dependency of t_f on corresponding bacteria concentration in control sample; (iv) time when fluorescence for treated sample reached f was then recalculated using the standard curve.

6.2.4 LIVE/DEAD BacLight^{TM} viability assay

LIVE/DEAD BacLight^{TM} viability assay is based on nucleic acid staining by two compounds SYTO9 and propidium iodide (PI). SYTO9 molecule is small enough to pass through membrane of healthy cells. It stains all cells to fluorescent green by linking their DNA. PI molecule is larger and is able to pass only through porous cytoplasmic membrane [278]. PI displaces SYTO9 in stained DNA and generates red fluorescent signal to mark damaged cells. Although it seems correct to expect membrane-damaged bacterial cells to be considered dead [279], those with undamaged membrane should not be necessarily culturable [280]. There are some intermediate states discoverable with LIVE/DEAD viability assay by different research groups without application of other viability tests [281–282].

The protocol used in this thesis is as follows. 3 µl of SYTO9 dye and 3 µl of PI were added to 1 ml of DI water and mixed together just before the experiment. Then 100 µl of purple-coloured and highly light sensitive resulting solution was added to 100 µl of bacterial sample loaded in 96-well sterile microtiter plate. All samples were done in duplicates. Loaded plate was incubated for 15 minutes at room temperature inside a lightproof box. Fluorescence intensity was measured at 530 ("green") and 630 nm ("red") for centered excitation wavelength of 485 nm. The ratio of live to dead cells was calculated using equation

$$L/D = \frac{F_g}{F_r}, \tag{6.4}$$

where L/D is a ratio of Live to Dead bacteria, F_g and F_r is fluorescence measured for 530 and 630 nm respectively.

Considering a short beam path the optimal amount of bacteria to obtain strong fluorescent signal is 10^7 CFU/ml. Two points standard curve was measured for each plate separately. Dead bacteria for standard curve were prepared using 50 µl of isopropanol added to 200 µl of bacteria suspension.

6.2.5 Thiobarbituric acid reactive substances assay

One of possible type of damage induced on membrane with oxidative stress is lipid peroxidation. One of approximatelly 32 different aldehydes appears in the bacterial solution as a result of lipid peroxidation process is malondialdehyde (MDA). It can be assayed with thiobarbituric acid (TBA) test [283]. The assay is based on the reaction of MDA with 2 molecules of TBA yielding a chromophore with absorbance maximum at 532 nm, as shown in figure 6.6.

The assay used in this study was adopted by Dolezalova et al. [3] from the method published by Slater and Sawyer in 1971 [285]. 20% (w/v[1])) trichloroacetic acid was mixed with the sample in the ratio 1:1 and was cooled down to −20 °C for 20 minutes.

[1]) mass to volume ratio

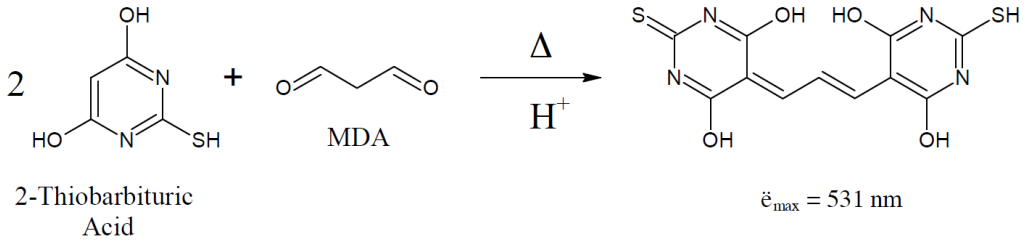

Figure 6.6. Reaction between 2-TBA and MDA under acidic conditions [284].

Then the sample was liquefied at the room temperature and centrifuged. 250 µl of supernatant was mixed with 600 µl of 0.6% (w/v) TBA and heated to 100 °C for 30 minutes. Afterwards sample was cooled down to room temperature and loaded to the sterile microtiter plate. Absorbency at 532 nm was measured with the microplate reader. The background absorbency at 600 nm was measured in advance and was subtracted:

$$\mathrm{c(MDA)} = (\mathrm{A_{532}} - \mathrm{A_{600}}) \cdot 9156 \ \mathrm{lmol^{-1}cm^{-1}} \tag{6.5}$$

Hydrogen peroxide in the solution interferes with MDA-TBA complex; nevertheless concentration of H_2O_2 lower then 1.5 mmol/l does not significantly change resulting fluorescent signal [286]. Maximal measured $c(H_2O_2)$ in PAW was 50 µmol/l and its possible interference was neglected.

6.2.6 DNA isolation protocol

DNA leaked from cells as a result of thermal lysis was analyzed using microplate reader. Protocol of cell lysis was as folows: 1.5 ml of the sample was centrifuged for 10 min at 10 000 rpm. Cells were resuspended in 1 ml of normal saline solution and were centrifuged again for 10 minutes at 10 000 rpm. Washed cells were resuspended in 300 µl of DNA/RNA free water and thermally lysed for 20 min at 90 °C. Suspension was then cooled on ice for 3 minutes, vortexed and centrifuged for 3 minutes at 10 000 rpm. Afterwards, 150 µl of the sample was loaded to UV transparent microtiter plate and the absorbency at wavelengths from 210 to 410 nm was scanned with Varioscan^{TM}Flash. All samples were loaded at least in triplicate to minimize errors. Measured spectras of treated and untreated samples were then compared. Absorbency peak at 260 nm corresponds to DNA and at 280 nm to proteins in the supernatant [3].

6.2.7 Quantitative analysis of DNA changes

Plasma activated aqueous media prepared with plasma sources operated in oxygen and/or nitrogen containing gas mixtures are known to induce changes in DNA. These changes can be detected using the most common technique — polymerase chain reaction (PCR).

PCR is a technique, which serves as a foundation of nearly all genetic tests. It is based on amplifying of a target DNA fragment, which is doubled in each of 20–40 cycles of PCR. The discovery of PCR is credited to Dr. Kary Mullis, who was awarded the Noble Prize in chemistry in 1993 for recognition and improvements of the procedure, that had been discovered earlier [287–288]. Despite remarkable importance of PCR in macromolecular biology it is a relatively simple method, and it is based on three steps cycle of subsequent heating and cooling to facilitate DNA replication by enzymatic reaction. Each thermal cycle leads to doubling of target fragment amount as it is shown in figure 6.7.

The initialization step is needed prior to three-stepped thermal cycling. This step includes reaction through heating it to 94–96 °C for 2–10 minutes and activates DNA polymerase and reagents, as well as denaturates other possible contaminants. Initialization phase is followed by the three stepped thermal cycle consisting, namely denaturation, annealing and extension.

During **denaturation** step, when reaction[1]) is heated to 94–98 °C for 20–30 seconds, DNA is melted by breaking hydrogen bonds between the strands. This process leads to melting of double strand DNA to two complementary single strand ones.

In fact, each primer[2]) is a complementary oligonucleotide[3]) to a specific limiting sequence of the amplified DNA fragment to catalyze DNA polymerase replication. In the **annealing** step primers anneal to the single-stranded DNA template. The reaction typically lasts for 20–40 seconds and its temperature is typically lowered to 50–65 ° C. The optimal temperature of the annealing is 3–5 °C below the primer melting one. Right temperature is extremely important, as if it was too high, the primer would not anneal efficiently but, at the same time, if it was too low, the primer could band to any sequence and the specificity of the reaction would decrease rapidly.

Temperature of **elongation** step depends on DNA polymerase used, but is usually set to 72 °C. In this step the DNA polymerase synthesizes new DNA strand complementary to the DNA template using free deoxynucleotide triphosphates (dNTPs) from the reaction mixture. As a result a number of target DNA sequence is doubled to become a new target for the next elongation step of the cycle.

After 20–40 cycles to yield an amplification of the desired DNA piece **the final elongation** phase takes place. The reaction is kept for 5–15 minutes at 72–78 °C to ensure, that any remaining single-stranded DNA is fully extended after the last PCR cycle. Once all high temperature reactions terminates the temperature of the mixture is cooled to 4–15 °C for an indefinite time for short-term storage of the reaction mixture [289].

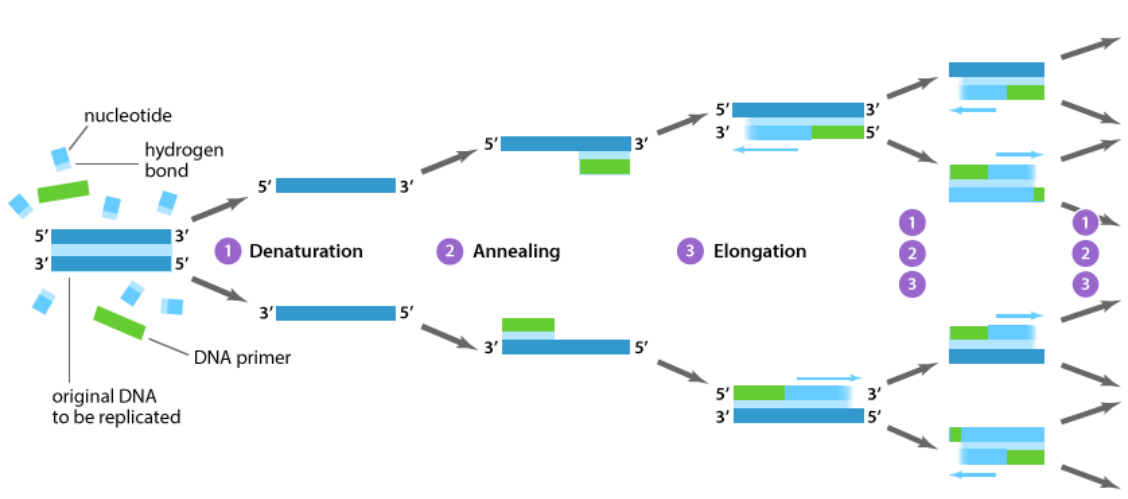

Figure 6.7. Thermal cycle of polymerase chain reaction: 1. Denaturation: breakage of hydrogen bonds between the strands (94–98 °C; 20–30 s); 2. Annealing: primers anneal to the template strands (50–65 °C, 20–40 s); 3. Extension/Elongation: dNTPs addition (72–78 °C). The amount of target sequence doubles during each thermal cycle which leads to exponential amplifying represented by 2^n, where n is a number of cycles [290].

[1]) The word "reaction" refers to polymerase chain reaction.
[2]) Primers are oligonucleotides carrying specific sequence of the DNA replication.
[3]) Oligonucleotides are short DNA or RNA fragments

An ability to generate billions of copies of specific DNA fragment in relatively short time allows analysis of many types of genetic variation of human and nonhuman biological specimens. Many biomedical laboratories use PCR in their testing, as it is possible to adapt this method for various qualitative and quantitative analyses. Qualitative analysis allows detection the presence or absence of a specific gene by using classical PCR reaction.

Theoretically, an amount of DNA doubles in each cycle. To calculate relative increase of DNA concentration it is possible to power 2 with the cycle number in which fluorescence crosses the threshold. However, the reactions are not 100% efficient, and the results require some modifications by using validation protocols. In the case when one needs to determine quantitative information, the real-time (quantitative) PCR (qPCR) should be used. The real-time PCR is based on usage of fluorescent DNA labeling technique allowing detection of generating PCR product by generating fluorescent signal. Once the fluorescent signal crosses the threshold level the measured fluorescent is directly proportional to the concentration of the starting material.

6.2.8 DNA melting curves

PCR products can be determined by their melting curves, as they are dependent on guanine-cytosine (GC) content[1]), length, and sequence. The melting curve of product can be acquired by monitoring the fluorescence of dsDNA specific dye as the temperature passes through the product denaturation temperature. While denaturation can be observed through the rapid drop of fluorescence. Fluorescence signal plot as a function of denaturation temperature is called a melting curve [291].

Precision Melt Supermix purchased from BioRad was used in this study. According to manufacturer it is 2x concentrated, ready-to-use real-time PCR reagent optimized for specificy and post-PCR high resolution melt analysis. Precision Melt Supermix contains two main components: iTaq DNA polymerase, which is an antibody-bound hot-start Taq enzyme that ensures highly specific PCR amplification of target DNA; and EvaGreen dye, which is a fluorescent dye that binds specifically dsDNA [292].

Mastermix was prepared by adding forward and reverse primers corresponding to *uidA* gene (2.6 µl each) to 65 µl of Precision Melt Supermix. The sample with DNA to replicate was then prepared by adding of 4 µl of isolated DNA to 6 µl of mastermix. All samples were done in triplicate. The high resolution melting analysis was provided according the Precision Melt Supermix datasheet [292].

[1]) GC-content is percentage of either guanine (G) and cytosine (C) in the whole target DNA or RNA sequence.

Chapter 7
Pathways of bacteria inactivation with water activated with DC-operated plasma jet

It is well known that the gas phase plasma induces generation of reactive species in water [1, 32, 150]. Plasmas generated in air or N_2/O_2 gas mixtures lead to formation of reactive oxygen and nitrogen species (such as NO_2^-, NO_3^-, H_2O_2, O_2^1, O_3, and other); moreover, plasma acidifies unbuffered liquids [2–3, 152], which all together creates synergistic effect contributing to irreversible changes in living cells exposed to PAW.

The DC-operated plasma jet, have been reported by Kolb et al. [293], as an unique source of gas phase plasma that can be immersed directly into aqueous solution (see figure 7.1). Underwater operation allows direct contact of the grounded electrode with treated solution and plasma at the same time. This feature grants a possibility to examine effects of metal ions on bacteria and aqueous chemistry. Moreover, the jet or its modification has been widely studied by different scientific groups worldwide and as a result various parameters of its operation have been measured, e.g. temperature distribution as a function of distance from the nozzle [81, 130], nitric oxide generation [294], dynamics of the discharge [86], *in vitro* surface decontamination [81, 295] and other.

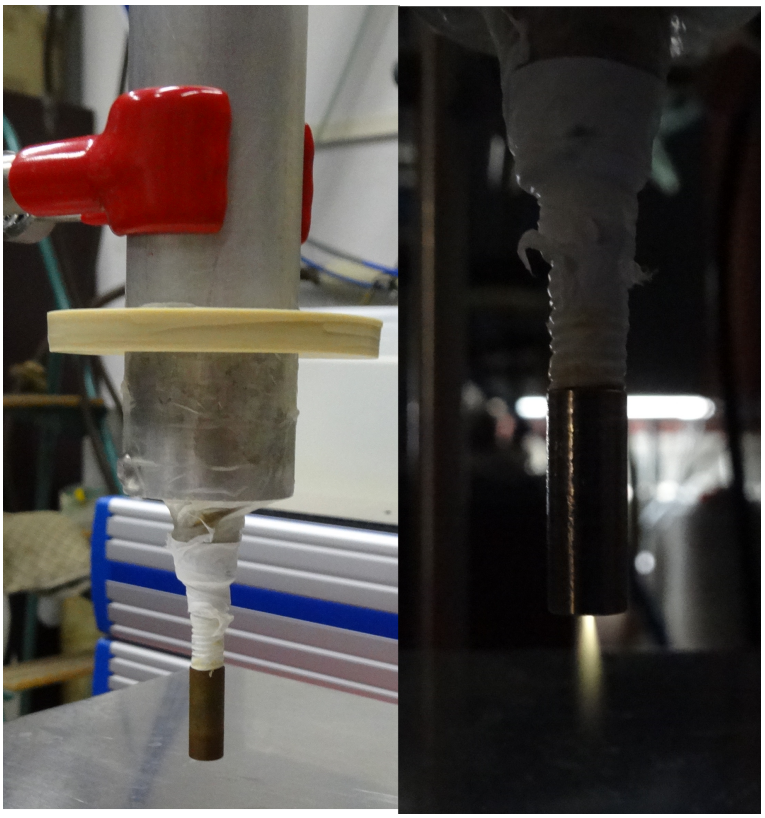

Figure 7.1. DC-operated plasma jet reported by Kolb et al. [293].

The objective of the experiment described below was to evaluate influence of heavy metal particles on PAW bactericidal properties. Heavy metal ions were released from the grounded electrode, which was in the direct contact with treated sample and plasma at the same time. Three different nozzle materials were chosen: titanium (Ti), copper (Cu), and stainless steel (SS) to release titanium, copper, and iron ions respectively.

7.1 Experimental setup

7.1.1 DC operated plasma jet

The plasma was expelled from the discharge ignited in a small chamber between the electrodes, while both electrodes were provided with micro-hollows. The inner high voltage electrode was realized by a titanium capillary with inner diameter of 0.8 mm. It was inserted into 1 mm thick alumina tube which overlapped the electrode for 0.4 ± 0.1 mm. The overlap of alumina tube varied in time due to erosion of both the electrode and the alumina tube. The grounded electrode was realized by a metallic cylinder with a flat closure fenestrated in the middle with a 0.8 mm hollow. The insulator overlap created a chamber between anode and cathode, where the plasma was ignited. A dry synthesized air (N_2/O_2) flowed through described coaxial electrode arrangement with a flow rate of 8 slm. The plasma jet expelled through the hollow in the nozzle was 0.5–1 cm long depending on the initial current (see Fig. 7.2).

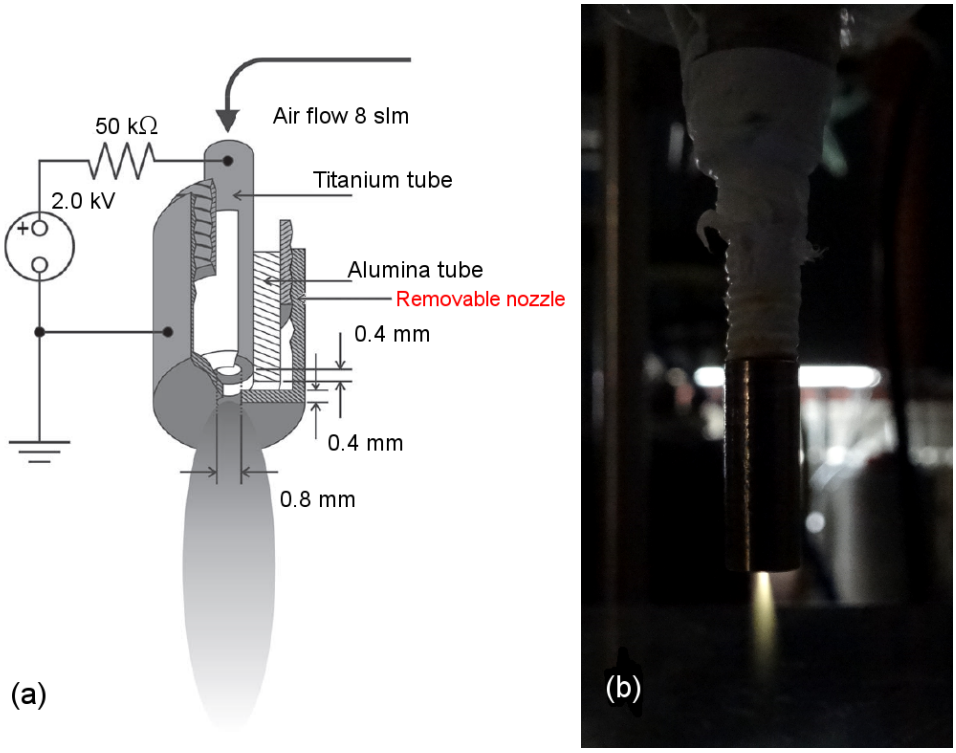

Figure 7.2. Coaxial electrode arrangement to expel the plasma plume [81] (a) and the photo of the working jet with plasma expelling out of copper nozzle (b).

The deviations of ±0.2 mm in all dimensions due to high operational temperatures were measured. No significant erosion of the high voltage electrode was observed; however, because of high working temperature, the insulator became frangible after approximately 50 hours of operation. It was regularly replaced.

Positive DC voltage of 2 kV was applied to a titanium capillary electrode in series with a 51 kΩ power resistor. The discharge current was limited to 10 mA or 20 mA in order to reach better discharge stability and required parameters of PAW. Precision of micro-hollows arrangement was crucial for the stability of the plasma plume and it was regularly controlled at the beginning of each experiment.

In order to prepare PAW, the DC-operated plasma jet was submerged 2 cm deep (measured in steady state) into 50 ml of DI water. A 150 ml glass 10 cm high beaker was used for this purpose. It was not hermetically closed with a rubber isolator. Outer parts of the device submerged inside the beaker were covered with parafilm and teflon tape to prevent corrosion and contact with the treated samples. Plasma jet was always ignited outside the beaker and was operated in ambient air for at least 1 minute in order to stabilize the plasma plume. Afterwards, the device was submerged into the beaker to treat the water for 15 minutes (see figure 7.3). Device was sterilized prior to each experiment with isopropyl alcohol.

7.1.2 Jet stability underwater

A gurgling effect occurred in the beaker during plasma treatment as a result of strong gas flow passing through the tiny hole. Water drops occasionally reached the nozzle and plasma disturbances were observed.

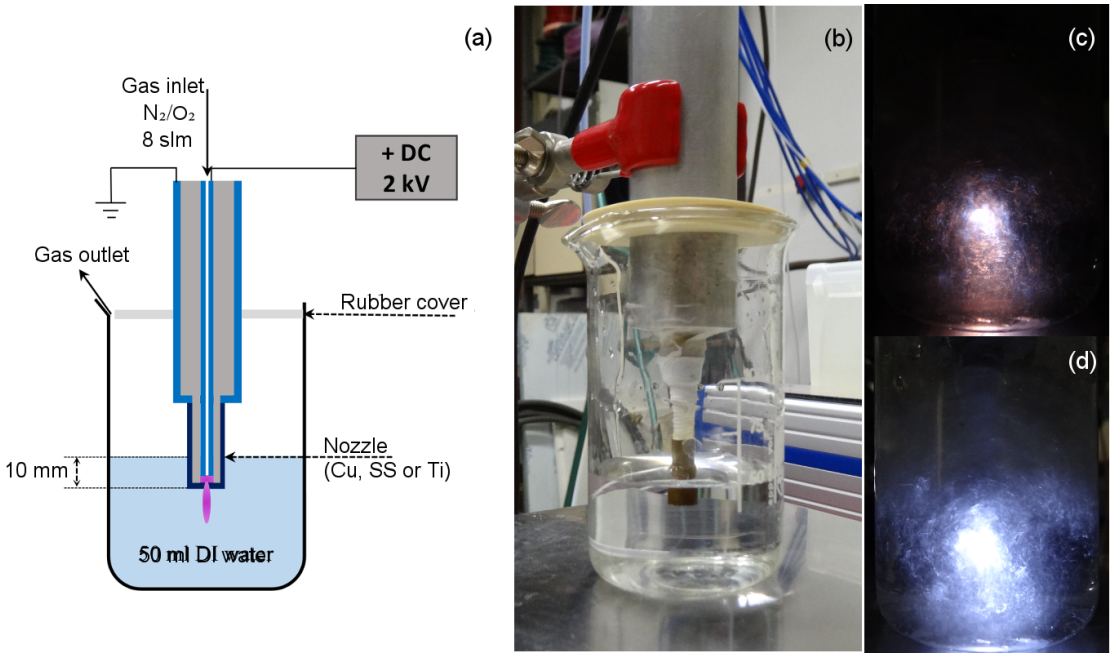

Figure 7.3. A schema (a) and photo of the DC-operated plasma jet dipped into sterile DI water; plasma and gas flow are turned off (b). Photos on the right (c and d) show plasma reflections in water, while jet is operating (8 slm, 2 kV, 20 mA). Photos were taken using different exposition time (1.5 and 3 s for (c) and (d) respectively).

The stability of the plasma plume was monitoring continuously during the whole treatment time. Two differently behaving instabilities were observed: change in plasma plume color (from purple to orange) and discontinuation of jet expelling. There were no disturbances in voltage patterns during plasma plume color change; nevertheless, the experiment was stopped in the case, the color of the expelled jet was orange continuously for more than 15 seconds. The second kind of jet instability, when plasma

plume stopped expelling from the nozzle, caused increase of the nozzle temperature and could be destructive for the device; therefore, in such case the experiment was stopped immediately. Possible reason of plasma plume disappearance could be erosion of electrodes or alumina tube, or water droplets entering the discharge chamber.

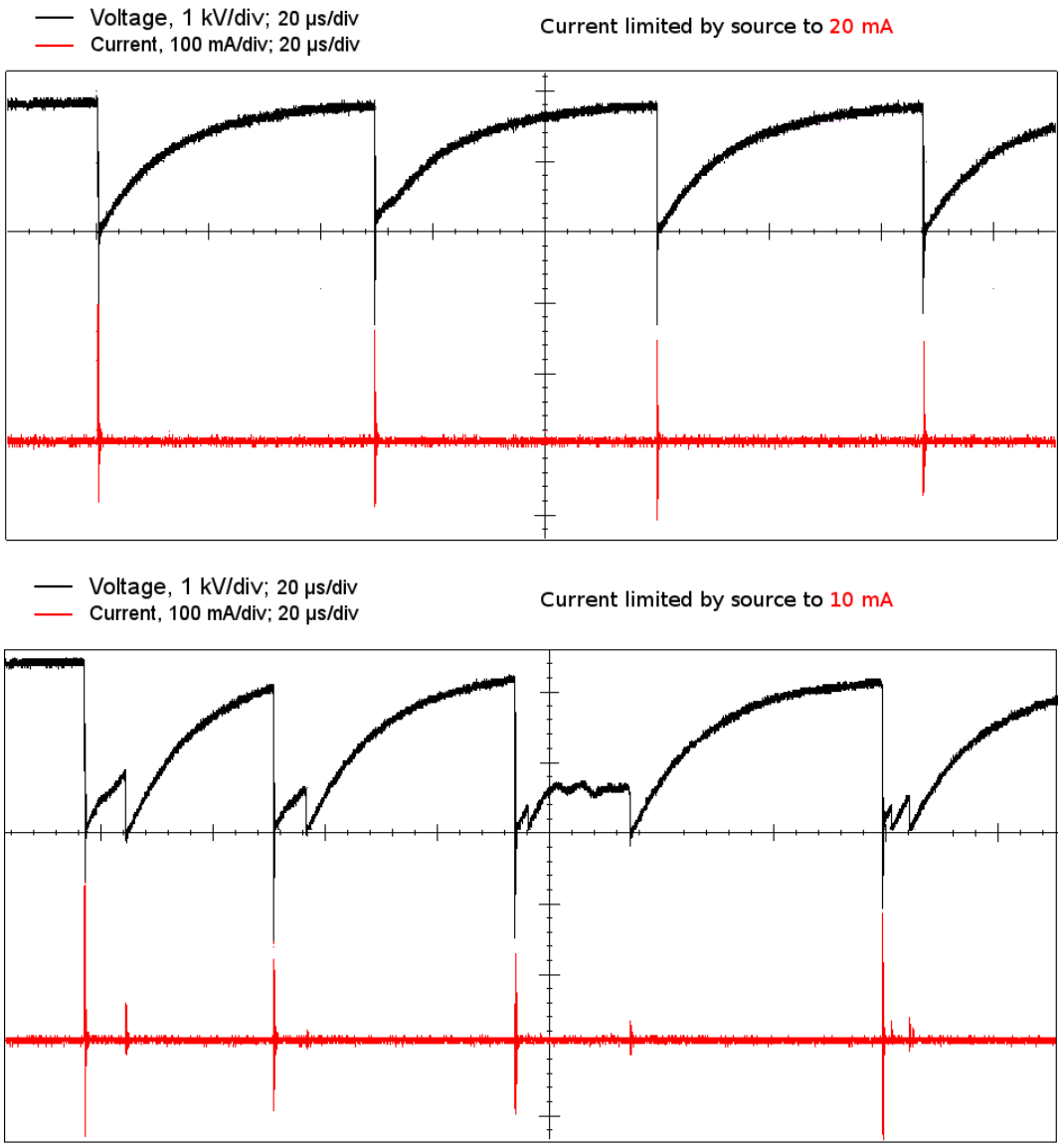

Figure 7.4. Voltage (black curve) and current (red curve) patterns measured with current limited to 20 mA (top) an 10 mA (bottom) for the copper nozzle.

Xian et al. [86] described two different modes of the jet: true DC and self-pulsing modes. They reported that the jet was switching between these modes depending on operating voltage and gas flow. The true DC mode was described as a mode with constant voltage between the electrodes and a corresponding constant current. In the case of self-pulsing mode the voltage pattern was similar to pattern of repetitively charging capacitor. Once voltage reached operating value, the breakdown occurred and the cycle started over. The frequency of pulses was in order of kHz. Self-pulsing mode was observed for operating voltage $\geq$ 7 kV and 2 slm gas flow rate.

Additionally, they reported the DC mode followed the self-pulsing one with voltage increase and unchanged flow rate. They described the mechanism of transition from

self-pulsing mode to the true DC one by the increased power dissipated in plasma and corresponding gas temperature raising. Moreover, with augmentation of self-pulsing frequency the residual ionization between subsequent voltage breakdowns raised as well, up to the moment when the degree of ionization between the discharges and during the discharge became equal and the DC mode (with no pulses) finally established [86].

For our purposes the high flow rate (8 slm) was used, although rather low voltage (2 kV) was set. The current limit was set by the power supply to 10 and 20 mA. Voltage and current patterns were measured by Osciloscope OWON Model PDS50225. The pattern differed depending on the current limitation set on power supply.

When the current was limited to 10 mA, the peak-to-peak voltage and amplitude of current pulses were not constant and varied in a way, that can be seen in figure 7.4 (bottom). Moreover, low amplitude current pulses were observed prior to the current pulses with maximal amplitude. The same observation was made for the voltage pattern. The maximal voltage did not reach 2 kV, despite it was set on the power supply. We assume that pulses of small amplitude were caused by pre-ionization processes, as streamer did not have enough energy to reach the grounded electrode. However, once the residual ionization was enough to connect two electrodes with the streamer, the large amplitude pulse occurred.

When increasing current limit to 20 mA, the energy dissipated in plasma increased. As one can see in figure 7.4 (top), the true self-pulsing mode was established. The frequency of pulses was 20 ± 5 kHz and voltage peak-to-peak amplitude 2.0 ± 0.1 kV.

Slight differences in parameters were observed for different nozzle materials. They could be caused by inaccuracy in hollow positions or different rapidity of material erosion. The true DC mode could not be established due to lack of energy.

Quality and repetition rate of pulses were not correlated to stability or instability of the discharge. Nevertheless, when the jet did not expel from the nozzle, no pulses were observed in the voltage pattern. The color of the expelled jet did not correspond with voltage patterns.

7.1.3 Experimental procedure

Significant inconsistencies in jet operation were observed, thus preliminary experiments were held to control PAW composition. Concentration of nitrites, volume loss and absorption spectrum were set as parameters to optimize. Concentration of nitrites in PAW was measured and are shown in figure 7.5 (top). We did not stop the jet when it experienced the color instability to evaluate its influence on nitrites concentration in PAW. Standard deviation of measured value was incredibly large and increased with operation time.

To predict NO_3^- formation, absorbency measurements were provided. In figure 7.6 there are shown absorption spectra of water treated with plasma for 10 (left) and 15 (right) minutes. Absorbency increase in wavelength range 296–309 nm reflects non zero concentration of NO_3^- immediately after activation.

With respect to all measured parameters the PAW preparation time for all further experiments was set to 15 minutes. Experiment was considered to be successfully finished if the jet was stable for at least 80% of time (12 out of 15 minutes); and if each instability duration did not exceed 15 s. This restriction allowed to maintain the deviation of (cNO_2^-) within 25%. The jet became unstable independently on its operation period; however, duration of instabilities increased with time of operation.

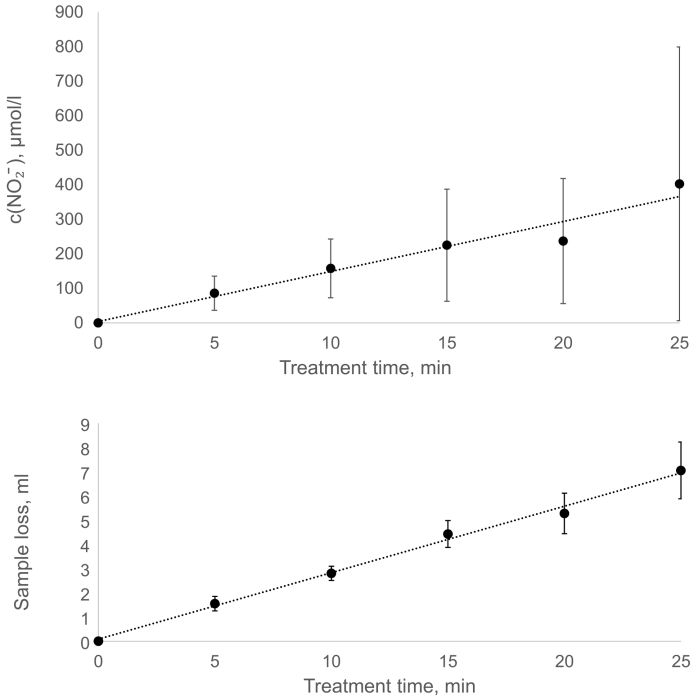

Figure 7.5. Dependence of the NO_2^- concentration (top) and the sample mass loss (bottom) on the treatment time. Presented curves were obtained during preliminary measurements and were used to set the time of treatment. Restriction on plasma plume stability were made to eliminate deviation in nitrite concentration.

7.1.4 Bacteria inactivation procedure

Once PAW was prepared, 10 ml of it was moved to a sterile test glass tube, and *E. coli* suspended in 100 µl of normal saline solution with bacteria concentration of 10^9 CFU/ml was added to PAW within one minute after treatment. Bacteria were left in PAW for 90 minutes. The dynamics of *E. coli* inactivation was investigated with drop test viability assay calibrated with conventional cultivation method four times during the incubation (after 20, 40, 60 and 90 minutes).

We measured following chemical parameters of PAW: pH, sample mass loss, concentration of nitrate, nitrite, hydrogen peroxide, and metal ions concentrations. pH and mass loss were measured with WTW pH330 pH-meter and Kern analytical balance respectively. Concentrations of NO_2^- and H_2O_2 were measured colorimetrically within 5 minutes after treatment, while NO_3^- concentration was measured with ion chromatography within several days after treatment. Due to the low pH (approximately 3.3) of samples they were stabilized with DI water in sample-to-water ratio equal to 1:3. Concentration of metal ions was measured by prof. Vaclav Janda and co-workers.

7.2 Results and discussion

DC-operated plasma jet was used to expell plasma plume into the water while the plasma was generated in the gas-phase. Due to high gas flow rate and gurgling effect induced in liquid activated water was in direct contact with exterior of the jet, which was covered with parafilm and teflon tapes, and the grounded electrode. Moreover, water was vaporizing and escaped from the beaker with the gas. To reduce baterial

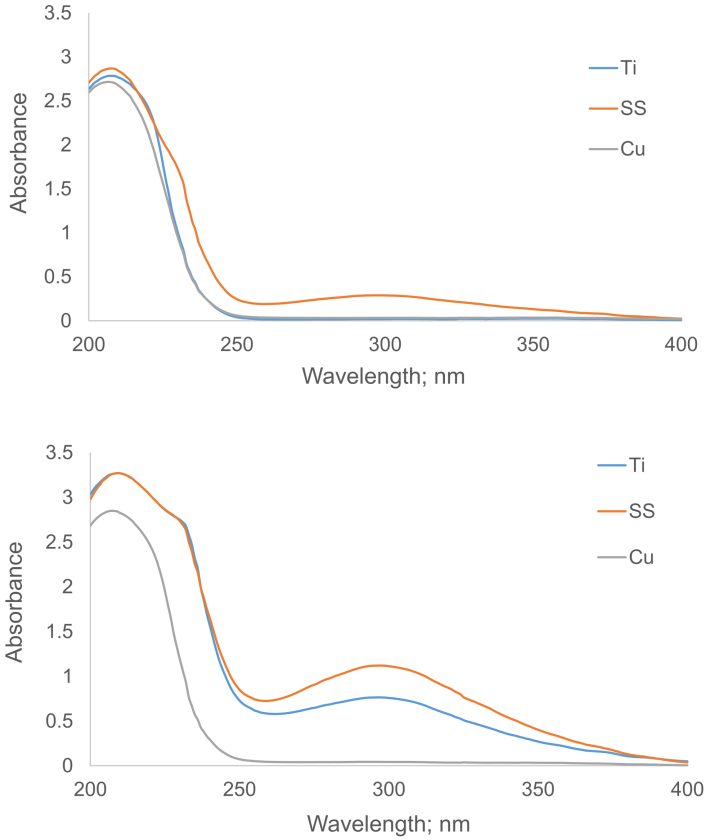

Figure 7.6. Absorption spectra of water activated with DC operated plasma jet for 10 (top) and 15 (bottom) minutes.

contamination of the device and laboratory equipment, bacterial suspension was add to PAW within 5 minutes after its preparation.

7.2.1 Chemical properties of PAW produced by DC-operated plasma jet

Bactericidal properties of plasma activated water depend on concentration and variety of reactive species, pH, and other factors. Three parameters were used as a routine procedure to monitor PAW properties: pH, hydrogen peroxide and nitrites concentrations were measured within 5 minutes after each treatment. Other parameters, such as concentration of metal ions and nitrates were measured for at least 3 samples.

All routine measured PAW parameters varied depending on the current limit set by the power supply. In the case of 10 mA current limit, concentration of hydrogen peroxide was below or on the detection limit of the used method. Nitrite concentration was below 10 µmol/l and pH value was approximately 3.5 (see figures 7.7 and 7.8).

Concentration of hydrogen peroxide in the case of PAW prepared using the jet with current limited to 20 mA was significantly higher comparing with the case described above. Despite the differences in maximal voltage (2.1 kV for Ti nozzle and 2 kV for SS and Cu ones) and minor differences in pulse repetition frequencies for all electrode material, c(H_2O_2) strongly depended on the nozzle material, and was maximal for the stainless steel nozzle. Concerning for example the titanium nozzle, the concentration of hydrogen peroxide and nitrites was low comparing to samples prepared with Cu or SS nozzles. Additionally, nitrites concentration measured in samples prepared with Ti

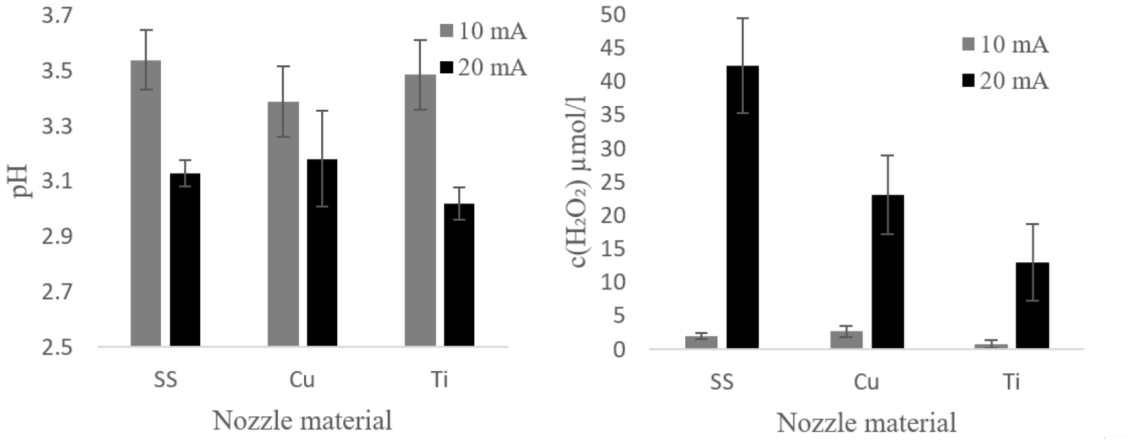

Figure 7.7. pH (left) and hydrogen peroxide (right) concentration in the PAW prepared with DC-operated plasma jet.

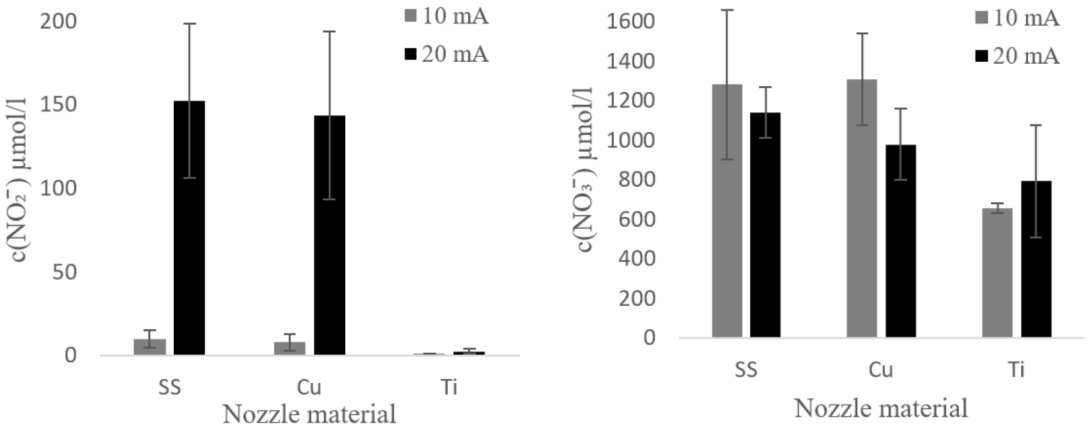

Figure 7.8. Nitrites (left) and nitrates (right) concentration in the PAW prepared with DC-operated plasma jet.

nozzle was below 5 µmol/l, which was the same amount as for the case of 10 mA current limitation (see figure 7.7 (right) and figure 7.8 (left)).

The nitrate concentration, measured separately for 9 samples in each group is shown in figure 7.8 (right). Measured concentration slightly varied with the nozzle material and current limit; however, no significant difference was observed in this case. Plasma jet with titanium nozzle generated the least nitrates in the treated sample.

Particles released from the nozzle within the treatment was measured for 3 sample using each nozzle material and both current limits. Measured concentrations can be seen in table 7.1. Average value of metal ions concentration in treated samples did not vary within measurements for different current limits.

7.2.2 Bacterial properties of PAW without hydrogen peroxide

Bactericidal properties of created PAW strongly depended on concentration of hydrogen peroxide and metal ions released into the sample. Furthermore, period of bacteria exposure to PAW played a significant role.

Plasma activated water prepared using plasma jet with current limited to 10 mA contained only small amount of hydrogen peroxide and nitrites. Concentration of these

Nozzle material	Metal ions concentration	Cytotoxicity limits Without H_2O_2	With H_2O_2
SS (Fe)	4.3–9.7 mg/l	nontoxic	catalyses ROS formation via Fenton reaction
Cu	330–919 µg/l	toxic $\geq$ 100 µg/l	catalyses ROS formation via Fenton-like reaction
Ti	10–14 µg/l	nontoxic	nontoxic

Table 7.1. Metal ions concentration in PAW prepared with DC-operated plasma jet and their toxicity limits.

species was slightly above the detection limit of the used methods ($\leq$ 5 µmol/l). Additionally pH of samples was above 3.3, that means the reaction producing peroxynitrite did not take place [32]. Taking in account all mentioned above, we assumed, that PAW itself should not have any bactericidal effects.

The stress in the case of titanium or stainless steel electrode should not be caused by the metal release, due to nontoxicity of titanium and iron ions. Iron ions did not seem to be toxic in absence of hydrogen peroxide.

Nevertheless, as it can be seen in figure 7.9 (dashed curves), 1 $\log_{10}$ reduction of surviving bacteria was observed for titanium and stainless steel nozzle after 90 minutes of bacteria exposure to PAW. This effect was ascribed to high sample acidity and long term bacteria presence in the medium with no nutritions. *E. coli* is a bacterium isolated from the gastrointestinal tract of warm blood animals and humans, and it has mechanisms, which allow it to survive under highly acidic condition with pH 2.5 and lower [182]. Provided experiments confirmed 90% of survival bacteria after 90 minutes of *E. coli* exposed to PAW, which is in good agreement with results reported elsewhere [296].

Better inactivation results were obtained for the PAW prepared with the copper nozzle. In figure 7.9 the dashed curve for copper nozzle shows 1 $\log_{10}$ inactivation for each 30 minutes of bacteria exposure to PAW. After 90 minutes 3 $\log_{10}$ reduction of *E. coli* was obtained. We subjected this result to toxic effects of copper ions released from the electrode. Measured concentration and toxicity limits of released metals can be found in table 7.1.

Coppers initial site of damage is reported to be at the cell membrane, where copper ions cause membrane disintegration [297]. It is well documented, that copper is toxic to bacteria with minimum inhibition concentration (MIC) reported to be about 250 mg/l [297–300]. This is far higher than the maximal copper ions concentration released to PAW, which was less than 1 mg/l.

Nevertheless, it has been reported, that long exposition (from 30 minutes to 8 hours) of *E. coli* bacterial cells to concentration of 600 µg/l of copper ions induces several irreversible processes in the cell, e.g. lipid peroxidation, substitution of essential metals on membrane, DNA and protein damages [301]. These processes lead to disrupting of membrane integrity of the cell, which should not necessary lead to the cell death, but it makes the cell sensitive to other factors that can cause lethal damages. Moreover, it has been reported, that small concentration of copper might induce a VBNC state caused by stress factors named above [232]. Bacteria in this state fail to grow on the routine cultivation media, and have to be resuscitated in order to be measured conventionally.

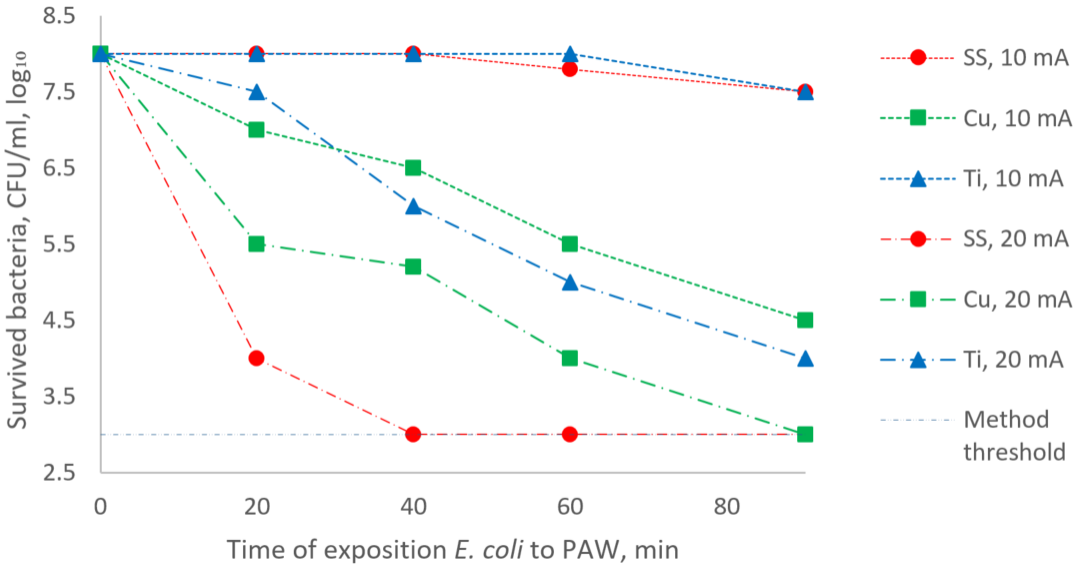

Figure 7.9. Dependence of bacteria reduction rate on time of bacteria exposition to PAW. Error bars were not introduced to the figure; standard deviation of measured values did not exceed 0.25 $\log_{10}$. *The lines in the figure do not correspond to the trend in data, but are drawn for better orientation in measured values.*

7.2.3 Bactericidal properties of PAW with hydrogen peroxide

The concentration of hydrogen peroxide in PAW increased rapidly by setting up the current limitation to 20 mA and establishing self-pulsing mode with stable frequency of several tens of kHz. As it can be seen in the right graph of figure 7.7 concentration of H_2O_2 depended on the nozzle material. Additionally concentration of NO_2^- for stainless steel and copper nozzle increased up to 150 ± 40 µmol/l. And finally acidity of the sample, which is shown in the left graph of figure 7.7, decreased below a value pH = 3.3 for all nozzles.

All mentioned factors participated on enhancing bactericidal properties enhance of prepared PAWs, in comparison with the case described in the previous section. Kinetics of bacteria inactivation is shown in figure 7.9 as solid lines. The most efficient PAW was prepared with stainless steel nozzle, when the bacteria inactivation of $5\log_{10}$ was reached after 40 minutes of bacteria exposure to the medium. Comparing its parameters to other PAWs we should depict higher concentration of chemical compounds (NO_2^-, H_2O_2) and iron ions released from the electrode. Although pH value was comparable with pH of PAWs prepared with Cu and Ti nozzles. We assume two main pathways of bacteria inactivation in PAW: effect of chemical compounds and acidity, and metal ion toxicity.

Lukes et al. [1] performed a detailed study of post-discharge chemical processes in plasma activated water involving formation of peroxynitrous acid ONOOH and its subsequent decomposition into $OH^\bullet$ and $NO_2^\bullet$ radicals via reactions (7.1) and (7.2). Peroxinitrite reactivity is strongly dependent on acidity of the solution, with upper limit of pH value at 3.3.

$$H_2O_2 + NO_2^- + H^+ \rightarrow ONOOH + H_2O \tag{7.1}$$

$$ONOOH \rightarrow OH^\bullet + NO_2^\bullet \tag{7.2}$$

Metal ions released from nozzles start different reactions with generation of ROS. One of the possible mechanisms could be proceeding of the Fenton reaction that occurs both for iron and copper (see equations below). In essence, both Fe^{2+} and Cu^{+} intensifies O toxicity by catalyzing the electron transfer from a donor biomolecule H_2O_2. Furthermore, redox cycling of the metal can consume cellular antioxidants.

$$Fe^{2+} + H_2O_2 \rightarrow [Fe^{2+}H_2O_2] \rightarrow Fe^{3+} + OH^{\bullet} + HO^{-} \tag{7.3}$$

$$Fe^{3+} + O_2^{\bullet -} \rightarrow Fe^{2+} + O_2 \tag{7.4}$$

$$Cu^{+} + H_2O_2 \rightarrow [Cu^{+} - H_2O_2] \rightarrow Cu^{2+} + OH^{\bullet} + HO^{-} \tag{7.5}$$

$$Cu^{2+} + O_2^{\bullet -} \rightarrow Cu^{+} + O_2 \tag{7.6}$$

Iron-mediated Fenton reaction is faster than copper-mediated one. Rate constants of these reactions depend on pH and relative reduction potential of the medium. This difference can be another reason of more effective bacteria inactivation with PAW prepared with stainless steel electrode.

All mentioned processes are the source of hydroxyl radical, which is the most reactive molecule in aqueous solution with oxidizing power ($E^0 = 2.85$ V). In contact with bacteria it induces oxidative stress and membrane damage, via for example lipid peroxidation and pore formation [3]. Moreover, peroxinitrite under acidic conditions might induce oxidizing processes in cell due to their reactivity. All these processes can lead to lethal cell damage or can make cell enter the VBNC state.

Chapter 8
Bacteria inactivation pathways in PAW generated by μAPPJ

There are several possibilities of bacteria inactivation with PAW depending on the moment, when bacteria are added to solution. They can be suspended in treated solution prior, immediately after or within longer (hours, days or weeks) after plasma treatment. Moreover, the period of bacteria exposure to PAW plays significant role in their inactivation in all cases. In previous chapter we demonstrated results of experiment, when bacteria were added to PAW immediately after its activation.

In this chapter we discuss results of experiments, when bacteria were suspended in the treated solution prior to plasma treatment and were washed and analyzed immediately after exposition.

The objective of the study described in this chapter is evaluation of bacterial pathways induced by PAW prepared with μAPPJ in $He + O_2$ atmosphere. Bacteria were added to solution prior to plasma treatment, therefore they were treated with both plasma generated species and post-discharge liquid-phase chemistry. Bacteria were washed and analyzed immediately after plasma treatment, so no long-term exposition to stress factors was considered.

Due to a larger group of people participating on the experiment more precise bacteriological analysis was conducted. Chemical analysis of the model liquids was done by Hefny and Lukes et al. and were already published in [73].

8.1 Experimental procedure

The plasma source used for this experiment was the COST reference jet precisely described and analyzed by various authors. Recent review paper was published by Golda et al. in 2016 [65].

Briefly, μAPPJ generated the capacitively coupled discharge powered with commercial RF power supply at $f = 13.56$ MHz and $U_{RMS} = 230$ V. The discharge was generated in a microchannel between 30 mm long and 1 mm thick stainless steel electrodes covered with two 1.5 mm thick quartz glass plates (see figure 8.1(a)). Distance between the electrodes was 1 mm. The plasma channel dimensions were $1 \times 1 \times 30$ mm^3. Pure helium with gas flow rate 1.44 slm with admixture of 0.6% of O_2 was used. Density of the molecular oxygen species in the gas mixture was determined as 8×10^{14} cm^{-3} when measured using mass spectrometry [73].

Plasma treatment of aqueous solutions was performed in a small chamber tightly separated from ambient atmosphere. The chamber was created with 6 ml glass cylinder closed by an aluminum cover with integrated gas exhaust line. The μAPPJ was fixed to a polyoxymethylene (POM) plate and mounted on a cover of the glass chamber, as shown in figure 8.1. 3 ml of aqueous suspension was treated with plasma jet at a distance of 4 mm.

The gas flow rate induced circulation and mixing of the treated solution, and depression of the water surface for 0.8 mm in the jet axis. This depression was stable in space

and time due to a laminar flux of the gas mixture with plasma on and off [73] (see figure 8.2 (a)). Sample mixing inside the glass cylinder was evaluated by dissolving cornstarch (size ∼10–20 µm) and illumination it with laser beam expanded into a sheath by a prism. Cornstarch movement was than recorded with camera (see 8.2 (b)).

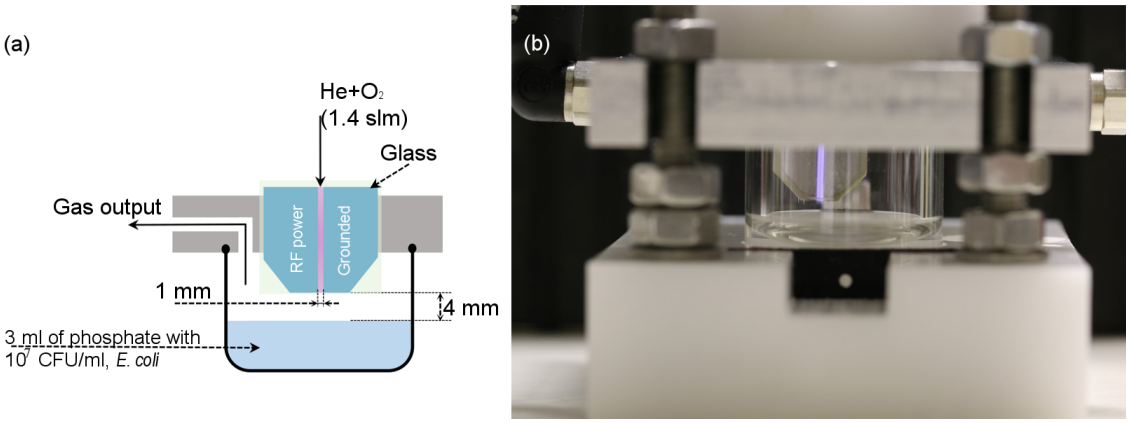

Figure 8.1. Experimental setup to evaluate bacteria inactivation pathways by PAW prepared with µAPPJ, powered by RF generator (a) and a photo of the setup with ignites plasma (b).

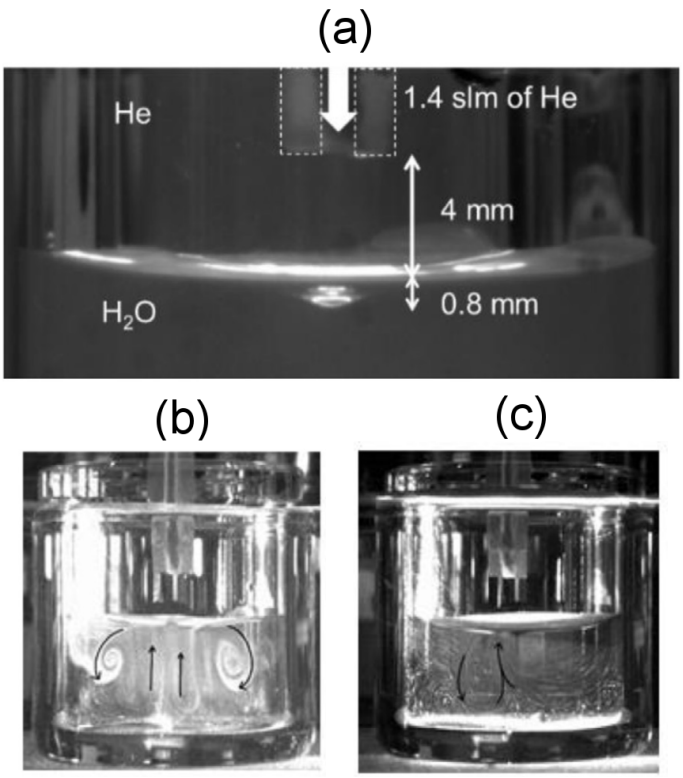

Figure 8.2. Photograph of the effect of the gas flow on the sample level (a). Photographs of vortices in liquid created as a result of laminar gas flow of He 1.44 slm visualized with laser illuminated cornstarch particles suspended in treated sample (b), (c) [73].

To prevent contact of PAW with ambient air, bacteria were added to the aqueous solution prior to plasma treatment. The atmosphere in the closed and tightened glass

cylinder was stabilized for 1 minute with the gas flow, as was described above. Afterwards, plasma was ignited for assigned time. The time series 1, 2, 4, 6, 8, 10 and 20 minutes of treatment were performed to investigate kinetics of bacteria inactivation. The bacterial osmotic shock was prevented by adding 0.9943 g/l $NaH_2PO_4 \cdot H_2O$ into DI water to reach initial conductivity of 500 μS/cm. Normal saline solution was not used due to its strong bactericidal properties after plasma activation [152].

Inoculum was purchased from Oxoid Brno in form of gelatin discs with declared concentration of 10^7 CFU in each. Two *E. coli* gelatin discs were suspended in 40 ml of Luria-Bertani broth[1]) one day before the experiment. Bacteria reached the exponential growth phase during overnight cultivation and their concentration increased to 10^9 CFU/ml. Afterwards, bacteria were centrifuged and resuspended in phosphate solution. Centrifugation and phosphate washing were repeated three times to minimize residual organic compounds pollution. Finally, washed bacteria were diluted in sterile phosphate solution to obtain concentration of approximately 10^7 CFU/ml of *E. coli*.

A number of metabolically active bacteria was measured by a Resazurin Viability Assay (RVA), cultivation bacteria on the specific cultivation media and LIVE/DEAD assay. Concentration of MDA was measured to investigate lipid peroxidation. The oxidative stress, which was assumed to be one of the mechanisms of bacteria inactivation, could cause changes in DNA, hence DNA melting and amplification curves were measured using Precision Melt Supermix and qPCR reaction. Concentration of chemical compounds and pH were measured using the model liquids (DI water and phenol [73]).

8.2 Bacteria inactivation pathways

Membrane degradation, pore formation and DNA damage were assumed to be the main pathways induced by PAW. However, reactive species generated in plasma under helium atmosphere with small oxygen admixture are different, compaing to those generated in nitrogen containing atmosphere. Reactive nitrogen species formation were not supposed to be generated in this case. That means, that degradation processes on bacteria membrane and elsewhere should be induced only by reactive oxygen species.

8.2.1 Reactive oxygen species produced in PAW

The aqueous phase chemistry induced by μAPPJ in aqueous solutions was discussed in details in [73]. Nevertheless we would like to depict conclusions, that are relevant for the study described in this thesis.

‘ Two model liquids were used to detect chemical pathways induced by plasma in liquids: DI water and DI water with 500 μmol/l phenol. Phenol is rather simple molecule with specific analytic advantage, as products of its reaction with OH radical, ozone and NO/NO_2 radicals are known and understood in detail[1].

PAW pH depended on the treated solution (see figure 8.3 (right) for phenol) and did not drop below 5.0 for DI water. pH decrease for DI water with phenol was attributed to formation of organic acids as ring-opened degradation product of phenol.

Formation of $OH^\bullet$ radical strongly depended on water vapors in the plasma channel and was maximal for $He + H_2O$ working gas composition. Nevertheless, the formation of hydroxyl radical was observed in water prepared with the jet operated in $He + O_2$ as a result H_2O impurities vaporized from the treated solution. μAPPJ is a source of high-energy vacuum-UV photons [76, 302]. Their energy is high enough to dissociate or

[1]) Prepared by solution of 10 g of Thryptone, 10 g of NaCl and 5 g of yeast extract in 950 ml of DI water; and autoclaved for 15 minutes.

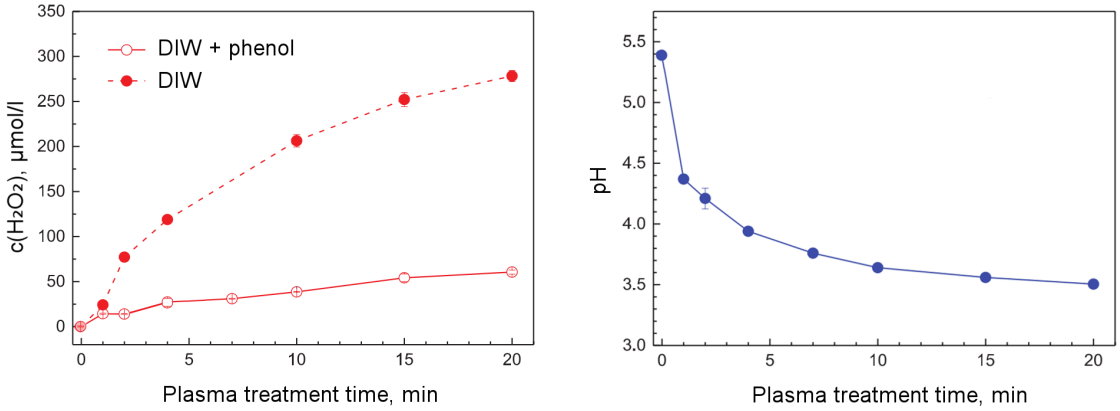

Figure 8.3. Concentration of Hydrogen peroxide (left) and pH (right) measured for aqueous solution treated with µAPPJ. c(H_2O_2) was measured in DI water and DI water with 500 µmol/l phenol, while pH was measured in DI water with 500 µmol/l phenol [73].

even ionized water molecule through absorption in liquid water and induce OH radical formation. This effect was checked using special designed jet modification and no or negligible effect was reported.

Ozone is another species generated in large quantities by He/O_2 plasma. However, authors strongly suggested practically no o negligible role of this species in aqueous chemistry.

And finally, the main reactive species of gas phase plasma generated in He/O_2 is atomic oxygen in ground state, with absolute O-flux into treated liquid of 9.3×10^{15} s^{-1} (assuming 100% O surface loss probability). Nevertheless, its transport into liquid was reported as highly efficient, where more then 50% of O atoms end up inside the liquid. According to recently published results of Kusalik et al. [303–304] and Hefny et al. [73] it was was strongly suggested that solvated oxygen atoms (O_{aq}) do not react with the water molecules, and can directly oxidize phenol and its products; or bacteria and its membrane.

Concentration of hydrogen peroxide in DI water and in DI water with phenol are shown in figure 8.3 (left). The difference in H_2O_2 concentration was explained by direct oxidizing of phenol with the O atoms. Moreover, hydrogen peroxide was assumed to originate from gas phase, where it was produced from H_2O impurities.

8.2.2 Lipid peroxidation induced by ROS

Lipid peroxidation (LPO) was considered as one of mechanisms of bacterial membrane disruption in a medium with high concentration of ROS, particularly OH radical [305] . Briefly, it can be described as a chain reaction of lipid degradation which propagates through the lipid bilayer until antioxidants produced by a cell terminate the process. However, once a cell suffers under stress conditions, the antioxidative mechanisms can fail to stop these reactions soon enough to prevent loses of membrane integrity. Anyway, lipid peroxidation process increases hydrophilicity of lipid bilayer and consequently leads to malfunction of membrane as the intracellular compartment protection. As a result of LPO relatively stable reaction product — peroxidated PUFAs[1]) — are formed.

Peroxidated PUFAs are further decomposed to different aldehydes (e.g. MDA), which can be measured in extracellular liquid. The graph of MDA released to extracellular

[1]) PUFAs (polyunsaturated fatty acids) are the target of lipid peroxidation. LPO is explained in detail in section 5.2.1

liquid can be seen in the figure 8.4. The rapid increase of MDA during the first 5 minutes of treatment corresponded to ongoing lipid peroxidation, which should be caused by an augmentation of reactive oxygen species (e.g. $OH^{\bullet}$, H_2O_2 and O_{aq}) in the liquid. However, after 5 minutes rapidity of MDA release reached the saturation phase.

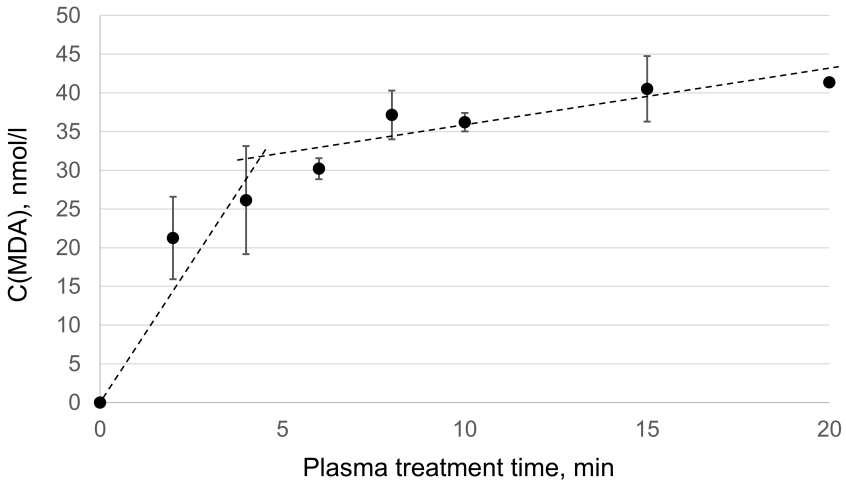

Figure 8.4. MDA concentration in the extracellular environment as an indicator of ongoing lipid peroxidation depending on treatment time. The standard deviation was done for $n = 5$.

Measured values were different comparing to those obtained by another authors. For example Dolezalova et al. [3], who worked with kINPen plasma jet[1]) reported increasing MDA concentration proportional to concentration of ROS and RNS in the liquid. Likewise, Joshi et al. [306] using FE-DBD plasma source in ambient air described that an MDA augmentation correlated with ROS concentration in solution.

8.2.3 Bacterial response to oxidative stress

Bacteria response to PAW exposure was obtained using cultivation on *E. coli* selective medium (m-FC) and Resazurin viability assay (RVA). Results of bacteria inactivation with PAW produced with μAPPJ are shown in figure 8.5.

The solid curves, which were obtained by plotting results of conventional *E. coli* cultivation on a selective medium, can be divided into two parts with different D-values[2]). The first part is characterized by inactivation of less than one $\log_{10}$ and was observed within first 6–8 minutes of plasma treatment. Further, rapid inactivation of 7 $\log_{10}$ reduction during 12 minutes took place. The calculated D-value in this case was 0.58 $\log_{10}$ per minute of plasma treatment.

However, RVA which was performed simultaneously with conventional cultivations, showed slightly different results (see dashed curves in figure 8.5). Survival curve obtained using RVA is again biphasic and the first phase, characterized by slow bacteria inactivation within one $\log_{10}$ lasts 7 minutes longer, i.e. until the 15^{th} minute; while the D-value of the second phase is 1 $\log_{10}$ per a minute.

Bacteria cultivation on selective medium and RVA gives different information about bacteria. Bacteria amount calculated using conventional cultivations indicates the number of cells, that are not damaged and are ready to replicate. While resazurin viability

[1]) kINPen is a DBD plasma jet, that uses Ar as a working gas
[2]) D-value is a slope of a bacteria reduction trend-line

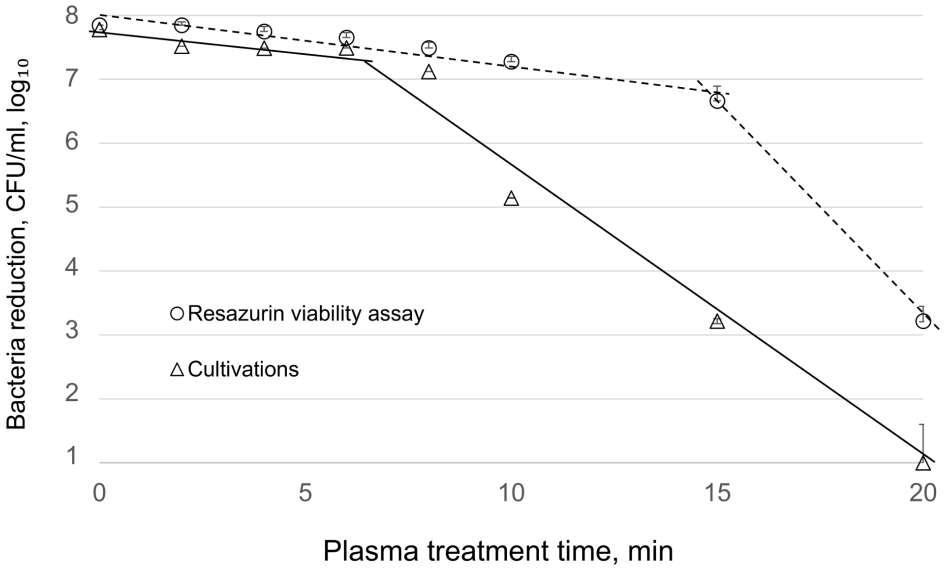

Figure 8.5. Biphasic survival curves evaluated with resazurin viability assay (dashed lines) and conventional cultivations on selective agar (solid lines).

assay detects metabolic activity of bacteria, using non-fluorescent resazurin to highly fluorescent rezorufin conversion. Cells with active metabolism are not necessary able to replicate properly, and as a result they are not detectable via cultivation method.

Differences in results obtained via conventional cultivations and RVA could indicate bacteria entered the viable but non culturable (VBNC), or other sensitive state. Bacteria in VBNC state fail to grow on routine cultivation medium, but can be regrown once the stress factor stops acting; or they can be detected indirectly through metabolic tests. Nevertheless, indirect measurements can give false positive results by detecting bacteria in other sensitive states.

E. coli is aerobic bacterium, which is adapted to certain amount of ROS produced by various intracellular and extracellular biochemical pathways. As a result, *E. coli* cells maintain a strong defense against oxidative stress via two types of superoxide dismutase [307]. Thus, we suggest, that a possible reason, why bacteria survived first 6 minutes of plasma treatment, could be caused by their strong defense mechanisms against stress induced by plasma generated ROS.

Once ROS concentration in the solution augmented above the critical level or if it reached certain cumulative dose bacteria defense mechanism failed, thus the phase of rapid inactivation was observed. The delay of the rapid inactivation phase obtained via cultivation assay and RVA could be explained by assumption, that *E. coli* entered the state, which prevents its culturability.

The VBNC state should be definitely proven by successfully resuscitated cells; however, we did not obtain satisfiable results up to now. The results obtained via RVA, cultivations and additionally via LIVE/DEAD (shown below) endorsed bacteria to enter this state.

Bacteria in VBNC state are reported to be more resistive to different stress factors: among others to oxidative stress, low pH and temperature fluctuations [308, 3]. The maximal difference between concentration of cultivated and viable bacteria was observed within the period from the 8^{th} minute of treatment (see figure 8.5). During this time, H_2O_2 concentration in the solution increased above 40 µmol/l (measured in DI water),

however pH was 5.0 (measured in DI water). Simultaneously concentration of other ROS (mainly atomic oxygen) increased as well [73]. Moreover, it has been reported that *E. coli* under starvation increases its tolerance to sublethal concentration of hydrogen peroxide. The lethal concentration of H_2O_2 was reported to be 1 mmol/l, which is 100 times higher, than the average value detected in PAW [309].

8.2.4 Pore formation as a result of bacteria exposition to PAW

ROS induced oxidative stress could lead to pore formation on the membrane, for example through lipid peroxidation. Concentration of MDA as a result of lipid peroxidation was discussed above. Concentration of MDA leaked out of the cell was comparable with results reported by other authors (e.g. Dolezalova et al. [305]), who concluded, that lipid peroxidation played a dominant role in bacteria inactivation with PAW.

Detection of membrane porosity was provided using LIVE/DEAD (L/D) staining (see 8.6). The L/D assay contains two dyes: SYTO9 and propidium iodide (PI). The first dye is highly toxic small molecule, which can pass through a membrane into an undamaged cell. On the contrary, a large molecule of PI can pass only through damaged (porous) membranes. This reagents belong to marker dyes used in monitoring of the cell membrane permeabilization [310–313]. In figure 8.6 changes in membrane permeabilization depending on plasma treatment time are shown. Measured dependency copies the trend of data obtained with cultivation assay and RVA, when nor significant inactivation, neither membrane permeabilization was detected during approximately 6 minutes of treatment. However, once a c(ROS) in PAW threshold was reached, the percentage of dead cells increased rapidly.

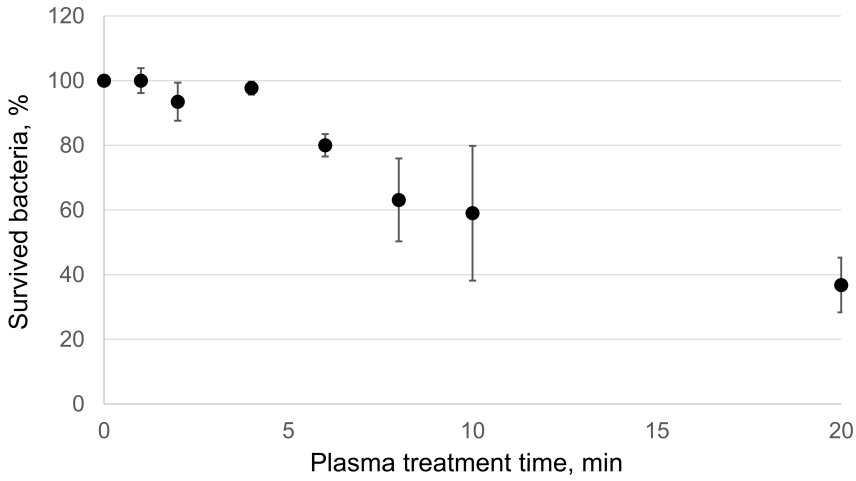

Figure 8.6. Ratio of live to dead bacteria obtained with LIVE/DEAD BacLight^{TM} viability assay with respect to time of plasma treatment. The standard deviation was done for $n = 5$.

Nevertheless, comparing result of bacteria inactivation shown in figure 8.5 with those shown in figure 8.6 we assumed, that permeabilization of the cell was not the main mechanism leaded to the cell death: after 20 minutes of plasma treatment cultivation assay considered 99.9999% of dead bacteria, while RVA gave 99.99%, but L/D assay showed only 55% of cells with porous membrane.

The assumption discussed above was confirmed by recording absorbency spectra of the supernatant obtained as a result of treated cells centrifugation. UV-visible spectrophotometer at wavelength 260 nm (for DNA absorbance) and 280 nm (for protein

absorbance) respectively. Absorption spectra of treated and untreated samples are shown in figure 8.7 and, although, the difference in absorbency of about 0.1 was obtained no peak was detected. Increase in spectra at 260 nm could be ascribed to the DNA leakage, or to residue concentration of different chemical compound of PAW left in supernatant[1]).

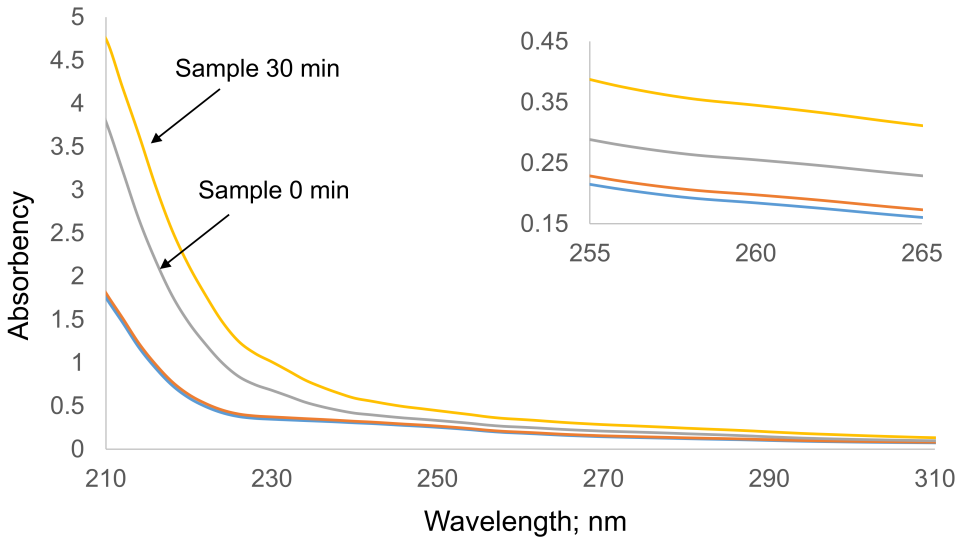

Figure 8.7. Absorption spectra of supernatant of treated and untreated bacteria to examine DNA leakage with a detailed image of the peak absence at 260 nm.

8.2.5 Changes on DNA strands

Changes on DNA were measured by quantitative polymerase chain reaction (qPCR) using the thermal cycler with built in fluorometer. Details of the method are described in section 6.2.7. The method can be summarized as three stepped chain reaction, resulting to doubling of the specific DNA sequence matching the designed primer in each cycle. The fluorescence produced as a result of amplified DNA was monitored in real-time. *uidA* primer, which is complementary to a structural gene commonly used to detect coliform bacteria *E. coli* in solutions, was used in this study. *uidA* gene encodes the B-glucuronidase enzyme, which is present in a small amount of bacteria stains. Initial concentration of DNA in the solution matching the used primer directly corresponds to a cycle number, when fluorescence increases above the threshold value.

In figure 8.8 it can be seen that with increase of plasma treatment time, concentration of DNA matching the primer decreases which indicates DNA changes.

Additionaly DNA melting curves were measured. The melting temperature of DNA indicates the temperature, when 50% of DNA in the measured sample denaturates from the double-stranded DNA (dsDNA) to single-stranded DNA (ssDNA). The study performed by Marmur and Doty [314] on DNA polymer stability presented a linear relationship between the GC content of the polymer and its melting temperature, that was explained by different stability of GC and AT pairs. Two factors contribute to change in DNA melting temperature: (i) hydrogen bonding between complementary strands, and (ii) pi-stacking[2]) between adjacent base [315].

[1]) Supernatant denotes the liquid above the solid residue after centrifugation, or other processes.
[2]) Pi-stacking is non-covalent interaction between aromatic portion of bases

Changes in DNA melting temperature caused by plasma treatment are shown in figure 8.9. DNA melting temperature of treated bacteria increased with plasma treatment time.

Changes in melting curve and quantity of DNA measured using qPCR might be ascribed to several processes: (i) effect of hydrogen peroxide, that is known to cause DNA damage in low concentrations (< 100 μmol/l) [316], (ii) effect of hydroxyl radicals generated directly by plasma, or (iii) hydroxyl radical generated via Fenton reaction directly in the cell as a result of reaction of hydrogen peroxide with intracellular iron.

Moreover, comparing changes on DNA with results obtained via conventional methods we can conclude that the structural and lethal changes on bacteria start to be significant after 10^{th} minute of treatment, once ROS concentration is above the threshold.

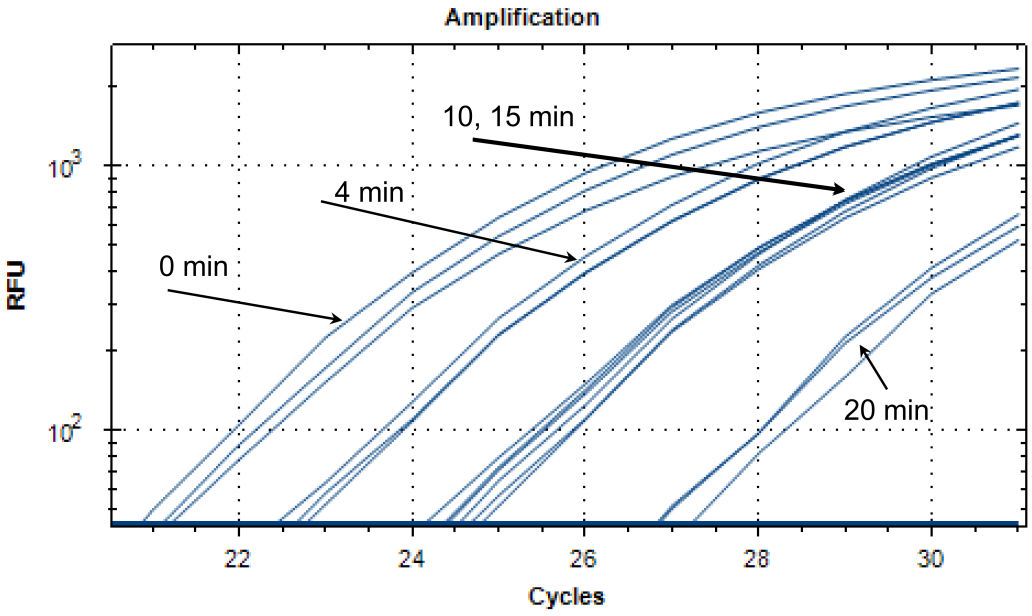

Figure 8.8. DNA amplification curves measured with qPCR depending on plasma treatment time.

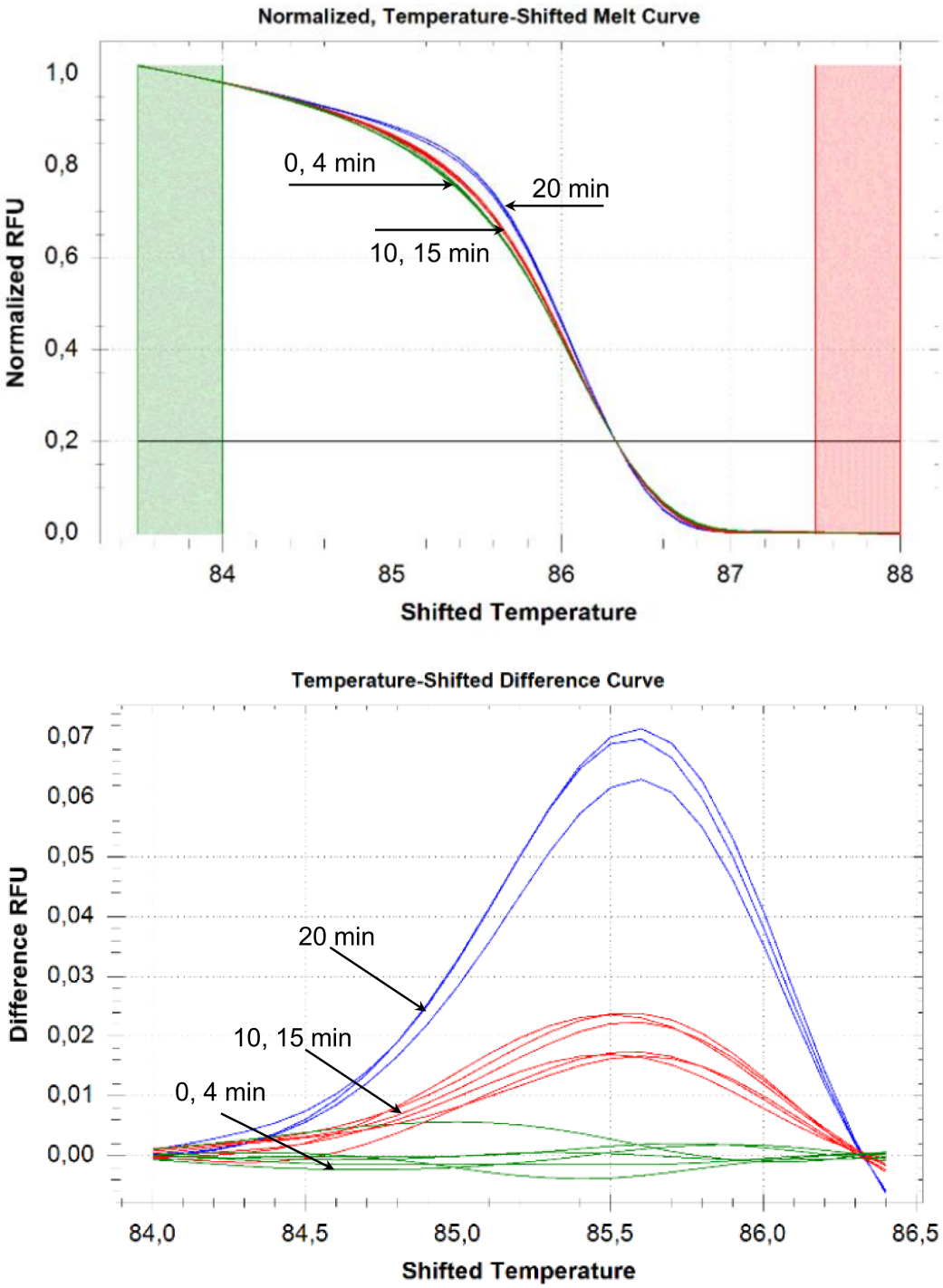

Figure 8.9. DNA melting curves measured with qPCR depending on plasma treatment time (normalized and relative view).

Chapter 9
Bactericidal properties of plasma activated oregano essential oil

Non-thermal plasma is mainly used to activate inorganic aqueous solutions, e.g. DI water, normal saline solution or PBS, while organic one, e.g. phenol is usually used as a probe to detect reactive species. In this chapter the promising possibility of plasma activated organic compound — essential oils — is described.

The objective of the experiment was to design a setup to activate oregano essential oil with non-thermal atmospheric pressure plasma to decrease time period needed for their vaporization in order to inhibit bacterial growth on the surface *in vivo* and *in vitro*.

9.1 Essential oils as natural remedy

Mechanisms of bacteria inactivation by different essential oils (EOs) and their main compounds are described for example in reviews written by Burt et al. [242] or Calo et al. [243] and were summarized in the section 5.5. Moreover, it was investigated that the direct contact between microorganism and EOs or their components is required to cause significant damage to bacteria and fungi [317]. Essential oils are highly volatile, hence it has been suggested that EOs vapors can effectively decontaminate surfaces and gases [318]. The main disadvantage of EOs vaporization is time consumption of the process. It varies from 12 to 72 hours depending on experimental conditions. Electro- or mechanical spraying of OE can be used to accelerate their evaporation through increasing of evaporative surface. Moreover, electrohydrodynamic atomization[1]) can be combined with DC discharge such as corona, streamer or transient spark [24].

Despite the fact that essential oils are natural, a high load of EO in food preservation may imply organoleptic impact, which is caused by changes in food taste by exceeding the acceptable flavor thresholds [319–320]. That is the reason, why the minimal possible concentration of EOs is usually used. Minimal inhibitory concentration (MIC) of essential oils differs for various inactivated bacteria or fungi and depends on the volatile compounds of the used EO. The time and high MIC are factors to be reduced in order to improve EO techniques in food preservation. Author of this thesis used electrospraying through the transient spark discharge to reduce the time necessary for EO to act on bacteria. MIC reduction was not in the focus of this study.

[1]) Electrohydrodynamic atomization is explained in detail in the section 2.1.1 and is usually called electrospraying

9.2 Non-thermal plasma combined with EOs in food preservation and medicine

There is only small evidence of essential oils used simultaneously or subsequently with plasma treatment in order to inactivate microorganisms or molds. This evidence can be divided to three main directions:

- plasma-assisted processing of EOs [321],
- simultaneous sample treatment with plasma generated negative and positive ions, and EOs [319, 322],
- subsequent sample treatment with NTP and EO [323].

Jacob et al. [321] are working on essential oils polymerization in order to produce bio-compatible antibacterial coating. The field of antibacterial coating with addition of essential oils compounds (e.g. capsaicin, curcumin, etc.) develops rapidly. However, these problems are more likely to correspond with plasma-surface modification and activation, and plasma deposition, and are not in the scope of this thesis. More information regarding polymerization of essential oils and its components reader can find at [321, 324–326].

Two groups Tyagi et al. [319] and Guant et al. [322] are investigating synergistic effects of vaporized essential oils and ions generated by an NTP or by a candle. Guant et al. studied inactivation properties of vaporized essential oils in closed volume, where negative and positive ions were induced by corona discharge or candle light. They reached significant decrease of MIC needed to inactivate 80% of *E. coli* and *S. aureus* on the surface with initial concentration of 10^6 CFU/ml. Researchers assumed that changes provided by ions to hydrophobic essential oil could promote their transport through the aqueous film that covers bacteria preventing direct contact of EO vapor and bacteria membrane. Moreover, it is well known, that negative ions with contact with membrane cause its breakdown.

Negative air ions (NAI) produced by Plasma Cluster Ion technology, widely used in air purification and disinfection [103, 327], were used to investigate effect of NAI on bactericidal properties of EOs in the study provided by Tyagi et al. [319, 256, 328]. Researchers concluded that the effect of NAI and essential oils are similar during the first 0.5 h of exposition. However, significant synergistic effect is observed after 4 h for lemon grass oil vapors and NAI against *E. coli*, when bacteria reduction rate increased rapidly [319]. Effects of NAI on bacteria are not completely similar to effects of NTP; however, they correspond with extremely remote NTP treatment .

Matan et al. [323] used Ar-operated plasma jet to treat leaf sheath specimens superior to clove oil or eugenol[1]) treatment. Eugenol is the main volatile compound of the clove oil. They did not use vaporization of the oil, but applied it directly onto the surface contaminated with *A. niger*[2]), *Penicillium sp.*[3]), and *Rhizopus sp.*[4]). Researchers concluded that the subsequent exposition of areca palm leaf sheath to clove oil and remote plasma treatment leads to decrease of minimal inhibitory concentration of EO. Moreover, such treatment prevents the growth of all molds on the areca palm

[1]) Eugenol is the main volatile component of clove essential oil.
[2]) *Aspergillus niger* is a fungus, which cause a disease called black mould on certain fruits and vegetables and is a common contaminant of food.
[3]) *Penicillium species* are filamentous fungi producing penicillin.
[4]) *Rhizopus species* belong to a genus of common saprophytic fungi on plants and specialized parasites on animals.

leaf sheath for at least 15 weeks of storage. They proposed, that NTP generated reactive species activated clove oil on the leaf sheath. Furthermore, according to several reports, plasma treatment leads to increase of surface hydrophobicity, that is followed by a low water or moisture absorption [329–330], and as a result to better adherence of oil components.

9.3 Experimental setup

9.3.1 Electrode system

Oregano essential oil (OEO) dissolved in carrier liquid (CL) was electrosprayed onto the treated surface through transient spark discharge. Experimental setup was inspired by the device reported by Machala et al. [24].

Transient spark discharge was generated between two copper electrodes (see figure 9.1): a tubule anode with inner diameter of 2 mm powered with DC voltage (15 kV), and a plane grounded cathode fenestrated with a 9 mm circular hollow. A Teflon capillary (D_{out}/d_{in} = 2/0.1 mm) was inserted into the hollow anode, in such position that the distance from its end to the anode end was 2 mm. The Teflon capillary was connected to a pump (Harvard Apparatus, 11plus), which injected the liquid into the discharge with flow rate of 50 µl/min. Inter-electrode distance was set to 6 mm.

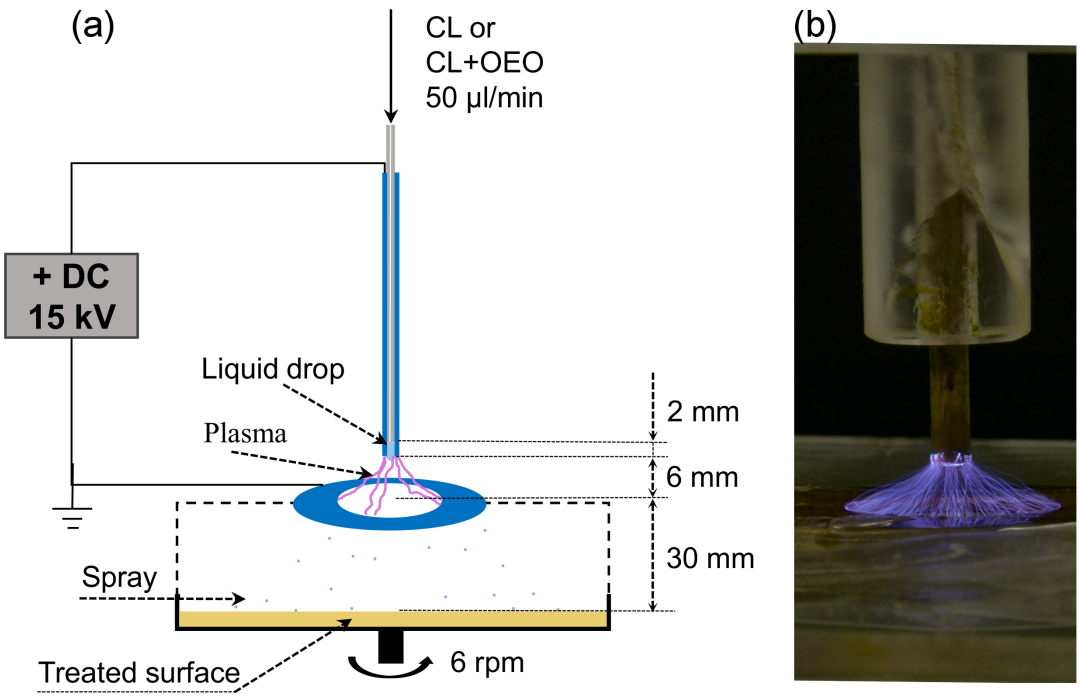

Figure 9.1. (a) Schematic of experimental setup to electrospray oregano essential oil (OEO) diluted in carrier liquid (CL); and (b) photo of transient spark discharge provided with 5 s exposition.

Positive corona discharge was ignited in advance of liquid brought to the end of the electrode. At the moment, when the liquid with conductivity in range 300–350 µS/cm reached the capillary end the discharge current as measured by the power supply increased immediately from 100 to 200 µA, and corona turned to the transient spark

discharge. Despite DC powering transient spark discharge is a self pulsing one with pulses waveforms similar to charging capacitor followed with voltage breakdowns (see figure 9.2). The period between "chargings" and breakdowns were characterized with constant voltage equal to the one set by the power supply. This period corresponded to a positive corona discharge, while the breakdown corresponded to the transient spark [31]. Moreover, low amplitude short pulses were observed as a result of insufficient preionization of the discharge channel. Current pulses were observed during each breakdown and their duration was predicted to be $\sim 10 - 100$ ns, however their amplitude was not determined due to insufficient oscilloscope resolution.

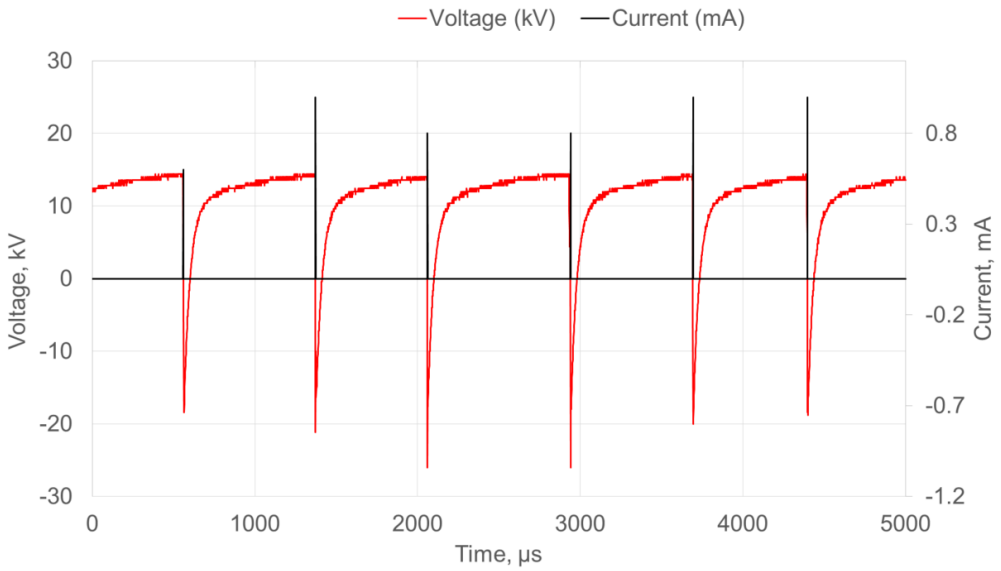

Figure 9.2. Voltage and current pattern of the transient spark discharge during electrospraying of the carrier liquid.

The treated surface was placed on the rotating table 3 cm beneath grounded electrode into the sterile plastic box. The box cover was penetrated with a ⌀ 12 mm hole, where the grounded electrode was glued. The treated surface was rotated with an angular velocity of 6 rpm. Two different kinds of sprayed liquids were used in this experiment: 5% Polysorbate 80 in DI water solution as a carrier liquid (CL) of essential oil; and CL with defined amount of oregano essential oil (OEO). Carrier liquid was prepared by adding 0.5 ml of Polysorbate 80 to 9.5 ml of sterile DI water and was mixed together in the ultrasound bath for 45 minutes. Polysorbate 80 is a polar diluent, which allows to mix water and an oil together to obtain emulsion.

Preliminary measurements of spraying quality were performed by coloring of each kind of liquid with 10 μl/ml of Almar blue; the colored liquid was then electrosprayed onto a filter paper placed on the rotated table in a cover of ⌀9 cm Petri dish. The test was provided before each experimental set to control setup parameters, particularly the distance between the anode end and the Teflon capillary (see figure 9.3). Setup was considered as acceptable if the filter paper surface was sprayed homogeneously and no large drops were observed (see figure 9.3(b)).

9.3.2 Experimental procedure

Essential oils were used in this study as natural compound to inactivate food borne pathogens on the surface *in vitro* (on agar) and *in vivo* (on spinach leaves). As it was

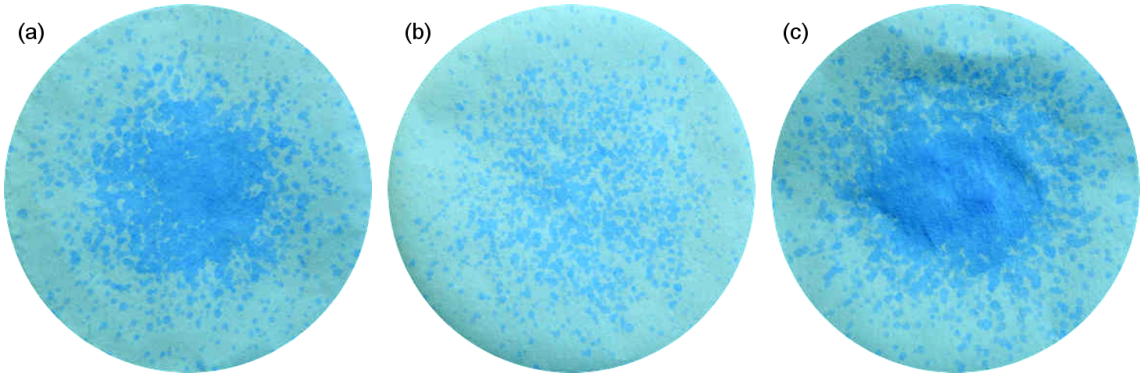

Figure 9.3. Setup testing by electrospraying of the carrier liquid colored with 10 µl/l of Almar blue onto the filter paper for different distances between the ends of anode and Teflon capillary: 1 mm (a), 2 mm (b) and 3 mm (c).

already mentioned, high load of EOs can change the taste of food, that may lead to decrease of its quality. That is a reason, why minimalization of inhibitory concentration of EOs is required.

Information related to MIC of *Origanum vulgare* needed to inactivate microorganisms depends on a bacterial stain and a method used for MIC detection. For example Kloucek et al. [251] in their report dedicated to a fast screening method of MIC indication reported 62.5 µl/l MIC of *Origanum vulgare* to inhibit 10^6 CFU/ml of *S. aureus in vitro*. Minimum inhibitory concentration reported by other authors varies depending on the method used to evaluate MIC, used microorganism and purchased essential oil (differencies were observed either within *Origanum vulgare* thoughout different contries). For example Nedorostova et al. [331] reported MIC of 17 µl/l for *S. aureus* and 66 µl/l for *E. coli* inactivating 10^5 CFU/ml. Eukaryotes are more resistive to EOs and MIC to inactivate them is usually larger comparing to MIC needed to inactivate bacteria. MIC of *Origanum vulgare* to inactivate at least 10^5 CFU/ml of (*C. albicans*) was reported to be 600 µl/l [332].

All reported values were measured using vaporized essential oils in the closed volume of a ⌀9 cm Petri dish with 0.5 cm solidified agar, that corresponds to effective volume of approx. 63.5 ml (considering 1.5 cm as a height of Petri dish).In the performed study 94.4 µl/l was used as corresponding vaporized concentration, or 6 µl of OEO per ⌀9 cm Petri dish. According to medium losses during the electrospraying the exact value was at least 15% lower (e.g. 80.24 µl/l).

- *In vitro* surface decontamination

Decontamination effect of plasma activated essential oil *in vitro* were studied using 4 different microorganisms: a gram-negative *E. coli*, a gram-positive *S. aureus*, a radiation-resistive *D. radiodurans* and a yeast *C. albicans*. Petri dishes (⌀9 mm) with Sabouraud[1]) (for yeast) or Mueller-Hinton[2]) (for bacteria) agar were inoculated with 1 ml of bacterial or yeast suspension[3]) and was dried in the flow

[1]) Sabouraud dextrose medium contains peptone (10 g/l), dextrose (40 g/l) and agar (15 g/l). 65 g of powder purchased from Oxoid CZ s.r.o. was added to 1 l of DI water, autoclaved, loaded onto sterile Petri dishes and solidified before use

[2]) Mueller-Hinton agar contains beef extract (2 g/l), casein hydrolysate (17.5 g/l), starch (1.5 g/l) and agar (17 g/l). 38 g of powder purchased from Oxoid CZ s.r.o. was added to 1 l of DI water, autoclaved, loaded onto sterile Petri dishes and solidified before use

[3]) "Bacterial" suspension will be used to refer the suspension of any type of microorganism further in the text

box prior to the treatment. Concentration of microorganisms in the suspension was $10^3, 10^4, 10^5, 10^6, 10^7$ or 10^8 CFU/ml in order to determine the maximal inactivated concentration. Surface was considered as decontaminated if the inhibition zone (the zone without bacteria) covered at least 80% of the ⌀ 9 cm Petri dish.

Dried agar surface was treated in one of four different ways:

1 electrosprayed with CL;
2 electrosprayed with CL+OEO;
3 mechanically sprayed with CL;
4 mechanically sprayed with CL+OEO.

The period of plasma treatment corresponded to CL amount, while the volume of OEO in CL was always 6 µl per a sample. To evaluate the optimal amount of carrier liquid *E. coli* was used. 1 ml of bacterial suspension was inoculated on the agar surface in different concentrations and was then inactivated by electrospraying of 100, 150 and 200 µl of solution (CL or CL+OEO). Considering the constant flow rate of 50 µl/min these values corresponded to 2, 3 and 4 min of plasma treatment.

Once an inoculated Petri dish was treated, it was closed in-hermetically with its cover and placed into the thermostat set to 37° C for overnight cultivation. The size of inactivation zone was then evaluated.

Maximal inhibitory zone was observed for 4 minute treatment (200 µl of overall volume) and was referred to uniform surface covering with drops of activated liquid (for more information see results section). All further experiments both *in vitro* and *in vivo* were done using 200 µl of CL or 194+6 µl of CL+OEO.

- *In vivo* surface decontamination

In vivo experiments were provided on Spinach leaves. The experimental procedure was as follows:

1 **Sample cleaning**: Fresh spinach leaves were bought in the supermarket in the morning of experimental day. Undamaged leaves were selected, hanged with a needle on a sewing, cleaned with DI water and sprayed with 200 µl of 70% ethanol from each side. Ethanol treated spinach leaves were dried in the flow box.
2 **Preparation**: Cleaned leaves were carefully cut to area of approximately 5 cm^2 and placed to sterile ⌀ 9 cm Petri dish. 50 µl of sterile DI water was dropped underneath the leaf to assure better leaf attachment.
3 **Inoculation**: Each leaf was uniformly inoculated with 100 µl of *E. coli* suspension (concentration 10^7 CFU/ml) using mechanical sprayer. Petri dishes with inoculated spinach leaves were closed with lid (not hermetically) after 15 minutes.
4 **Treatment**: Loaded Petri dishes were then divided into 5 groups: four groups were treated with elecro- or mechanical spraying of CL or CL+OEO and the fifth one was left untreated (control group). All samples were closed immediately after treatment with a Petri dish cover and was coated with an elastic tape to seal activated solution vapor inside. Samples were left at the room temperature (approx. $23 \pm 3°C$) for 10 minutes or 10 hours.
5 **Evaluation**: Each spinach leaf was washed in 3 ml of sterile normal saline solution (9 g of NaCl in sterile DI water) by vortexing it for 60 s. The drop test and classical cultivation test were then provided.

- Chemical or structural changes of oregano essential oil

Concentration of NO_2^-, H_2O_2 and pH of elecrtosprayed solution were measured using DI water as a model liquid. Despite low conductivity of DI water (< 10 µS/cm) the

average current of the discharge reached 200 μA and the self pulsing mode with transient sparks was established using identical experimental setup.

To investigate whether essential oil components changed with plasma treatment, FTIR GAR and ATR spectra were recorded for plasma treated and untreated CL, CL+OEO and pure OEO.

The FTIR spectra were measured for following samples: carrier liquid (5% Polysorbat 80 solution in water), carrier liquid with essential oil and pure essential oil; each sample was measured before and after plasma treatment.

At least 1 ml of the sample was needed to provide measurements of FTIR (GAR or ATR) spectra. Each sample was gathered by parts during 8 separately provided exposition. Concentration of essential oil in carrier liquid was equivalent to 6 μl of OEO in 194 μl CL (3% of OEO in CL). Treated sample was collected to a glass test tube after each single treatment to avoid consequent remote plasma treatment. Samples were then sent to Czech Academy of Sciences, Institute of Physics for spectroscopic measurements.

9.4 Results and discussion

9.4.1 Chemical and spectroscopic analysis

Deminiralized water (σ = 3 μS/cm) was used as a model liquid to investigate basic chemical properties of electrosprayed solution. pH of the DI water electrosprayed into the collecting test glass through the transient spark discharge was equal to 4.2 ± 0.3. Concentration of H_2O_2 and NO_2^- were 87 ± 0.2 μmol/l and 0.512 ± 0.031 mmol/l respectively. We assume presence of nitrates in small concentrations in the solution as a result of dissolution of nitrogen oxides formed in the gas-phase from air.

The amount of hydrogen peroxide measured in the model liquid is below reported lethal threshold for bacteria [309]. Nevertheless, it is an evidence of DNA damages occurred in *E. coli* as a result of Fenton chemistry even when $c(H_2O_2)$ = 50 μmol/l [316, 333]. Transient spark was generated in ambient air and we can assume generation of superoxide radicals in activated model liquid. This assumption predicts formation of hydroxyl radicals through the Haber-Weiss reaction:

$$O_2^{-\bullet} + H_2O_2 \rightarrow O_2 + OH^- + OH^{\bullet}. \tag{9.1}$$

The reaction results with formation of extremely short lived hydroxyl radical, which is highly toxic to bacteria. Moreover, the electrode used in the experiment is made of copper, which is transient metal and is known to induce Fenton reaction, which results to formation of hydroxyl radical as well (see section 5.2.2 for more information):

$$Cu^+ + H_2O_2 \rightarrow Cu^{2+} + OH^- + OH^{\bullet}. \tag{9.2}$$

Plasma generated in liquid or in gas-liquid interface is known to induce phenol degradation, that can play an essential role, due to the fact, that carvaclol is a phenol (see Figure 9.4). The main mechanisms of phenol degradation induced by plasma are summarized in [32]. The oxidation pathways strongly depend on pH and availability of the suitable oxidants and reductants, when there are two basic pathways leading to ring-opened products or to generating of hydroxylated products of phenol such as catechol or hydroquinone. Ozone generated in transient spark discharge in gas-liquid interface attacks the phenol ring and induce its opening or another degradation process. Moreover, presence of nitric ions can lead to nitration and nitrosation of phenol [32].

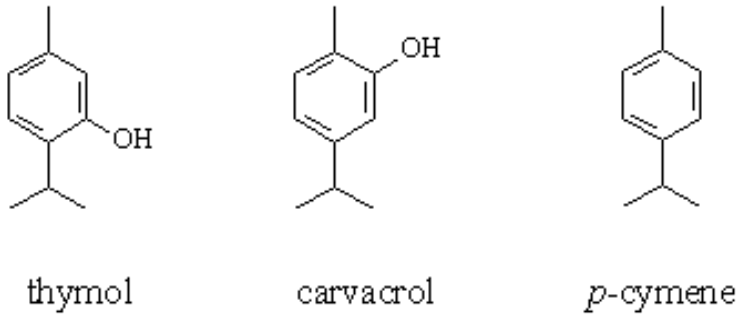

Figure 9.4. Carvaclol, thymol and *p*-cymene.

Changes in phenolic compound of essential oil mentioned above should be seen in the measured spectra. One of the possible changes, could be degradation of carvaclol to *p*-cymene by the loss of hydroxyl group.

Nevertheless, no significant changes in absorbency and a spectra pattern were observed for any samples (see figures 9.6 and 9.7). We assume that no measurable changes on phenols (carvaclol and thymol) were induced as a result of plasma treatment. However, the color of oregano essential oil in Polysorbate 80 solution changed from bright white to lightly yellowish 9.5. More chemical investigations using for example GC-MS technique should be done for deeper understanding of changes in the oil structure.

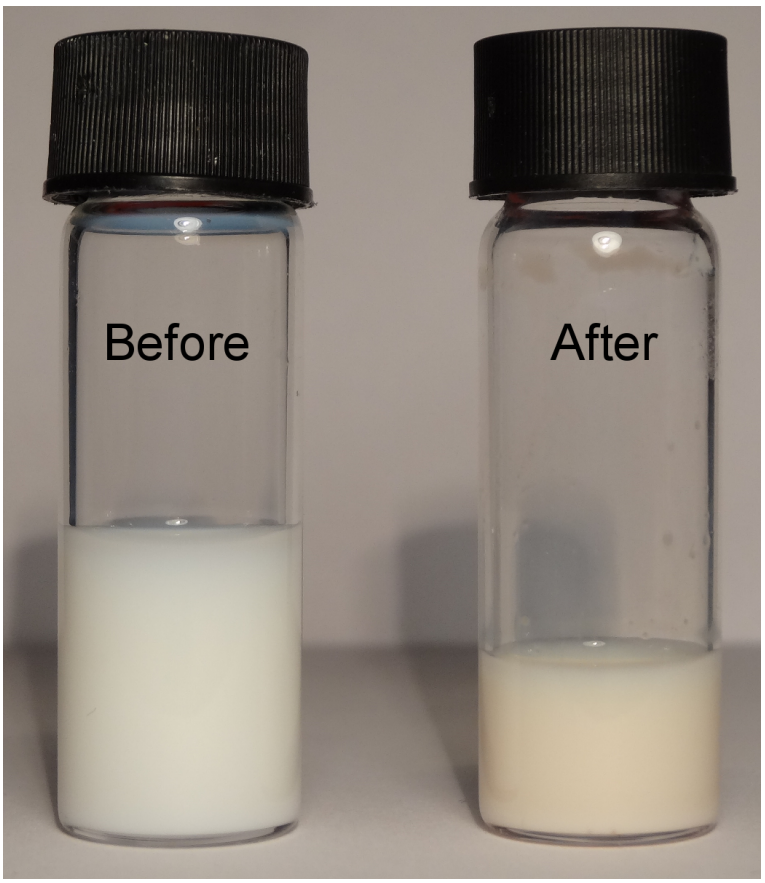

Figure 9.5. Changes in color of oregano essential oil suspended in carrier liquid before (left) and after (right) plasma treatment.

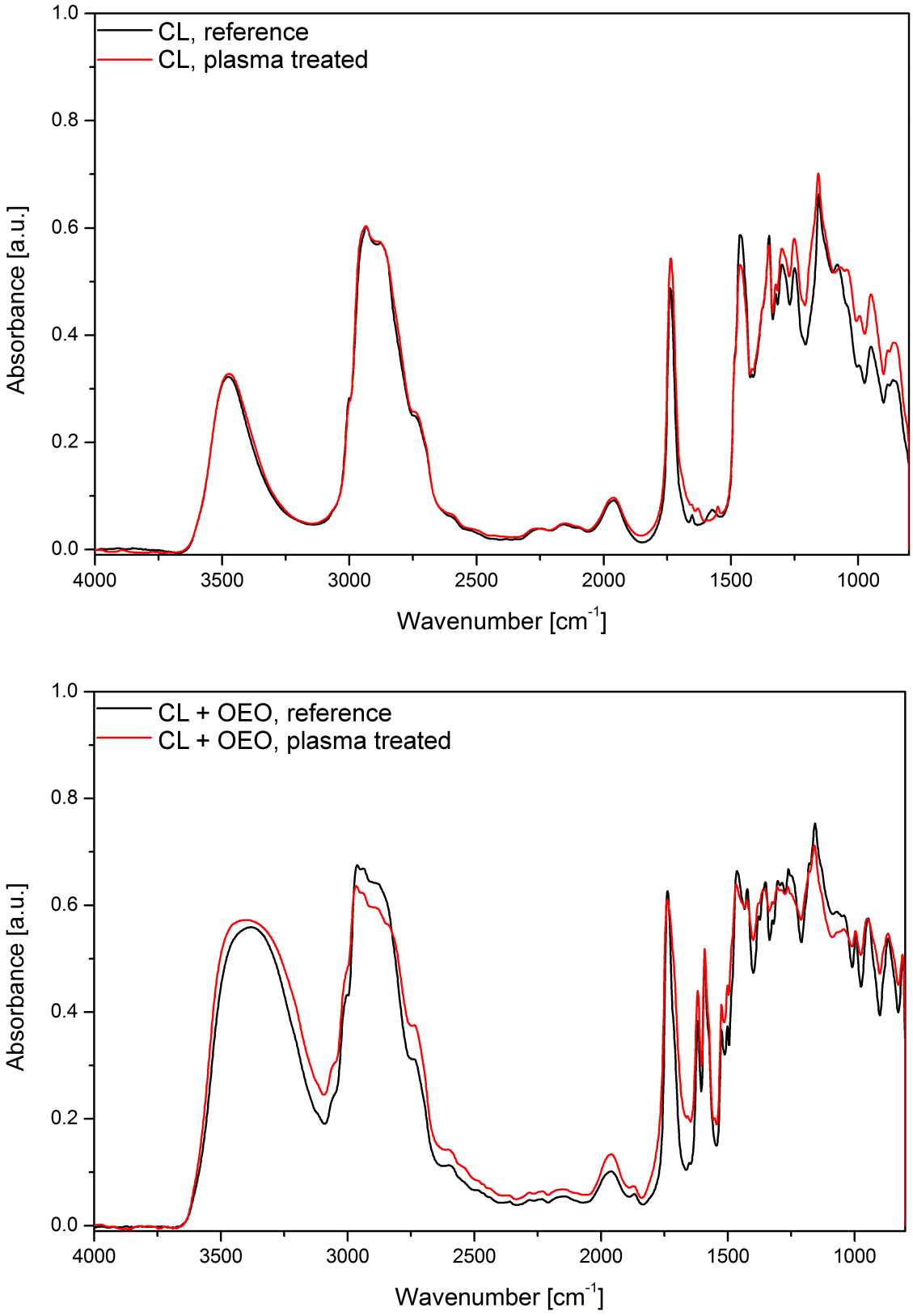

Figure 9.6. GAR FTIR spectra of carrier liquid (top) and carrier liquid with oregano essential oil (bottom) before and after plasma treatment.

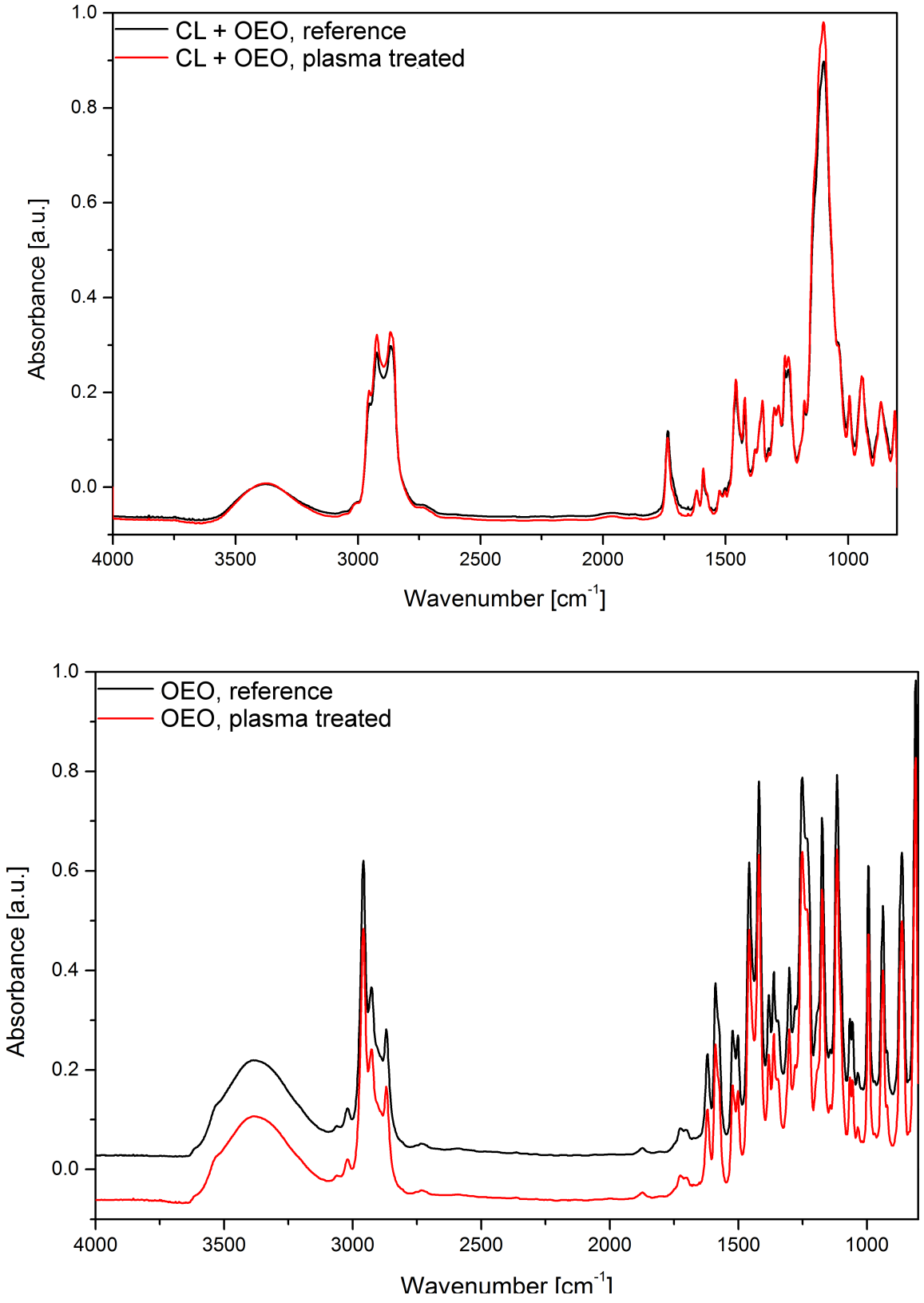

Figure 9.7. ATR FTIR spectra of carrier liquid with oregano essential oil (top) and pure oregano essential oil (bottom) before and after plasma treatment.

9.4.2 Bactericidal effects of electrosprayed OEO *in vitro*

As it was already discussed above (Section 5.6), essential oil should be in direct contact with a microorganism to inhibit its growth [253]. That was the reason for using mechanically sprayed OEO+CL solution onto inoculated agar surface instead of disc volatile method described elsewhere [251, 331–332]. Efficiency of mechanically sprayed OEO+CL was $3\log_{10}$ of bacteria and $2\log_{10}$ of fungi reduction and it was independent on the amount of carrier liquid.

The carrier liquid was electrosprayed onto inoculated agar surface in order to examine its biocidal properties. The test was provided for series of ⌀9 Petri dishes inoculated with 10, 100, 10^3, up to 10^8 CFU/Petri dish. The efficiency of bacteria growth inhibition by plasma activated carrier liquid was less than $3\log_{10}$ reduction and was observed in the middle of the sprayed surface. Bacteria inactivation strongly depended on liquid drop position. We assume, that long-lived plasma generated reactive species in gas phase did not play a significant role in plasma induced bacteria inactivation. On the other hand, plasma activated 5% Polysorbate 80 in DI water carried ROS and RNS, that caused stress to bacteria and decreased their resistance and viability.

Inactivation rate obtained with plasma treated essential oil was significantly higher. It depended on period of plasma treatment and as a result on amount of carrier liquid used to solute OEO. Amount of carrier liquid (CL) corresponded directly to period of plasma treatment due to the constant flow rate (50 µl/min). The size of inhibition zones appeared on agar inoculated with bacteria or fungi increased with respect to the time of treatment, and are shown in figure 9.8. The observed effect was ascribed to better covering of the agar surface with plasma activated solution. Bacteria reduction rate obtained by mechanically and electro-sprayed solutions are shown in table 9.1.

	Mechanical spraying		Electrospraying	
Bacteria	CL	CL + OEO	CL	CL + OEO
E. coli	0	3	2–3	8
S. aureus	0	3	2–3	8
C. albicans	0	1	0	7
D. radiodurans	0	3	2	8
	In vivo surface decontamination			
E. coli (after 10 min)	0	2	2	3
E. coli (after 10 h)	0	2	2	5

Table 9.1. Bacteria reduction induced by electro- and mechanically sprayed carrier liquid with and without OEO. Reduction is written in orders of magnitude ($\log_{10}$). 200 µl carrier liquid or 194 + 6 µl carrier liquid + oregano essential oil was sprayed mechanically or through the transient spark discharge.

The electrospraying process induced reactive species chemistry processes in the treated liquid [145], as it was discussed in the Section 4; hence, treated liquid can be referred as PAW. PAW in contact with bacteria leads to oxidative stress and cause cell membrane degradation. Moreover, bactericidal components of oregano essential oil were also activated with plasma; however, the mechanism of their activation is uncertain.

We suggest the following three stepped mechanism of bacteria inactivation with plasma activated essential oil in aqueous carrier liquid.

Essential oil suspended in the carrier liquid creates an emulsion with micelles, that are activated with plasma and can carry not negligible amount of charge to bacteria.

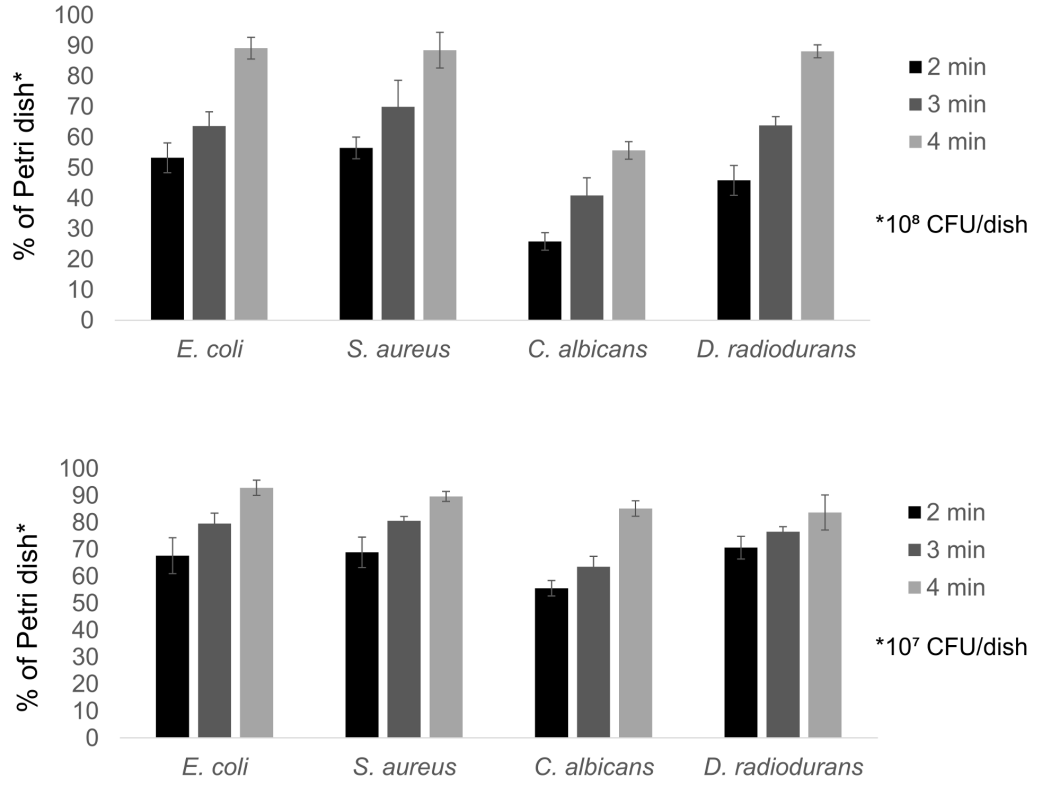

Figure 9.8. *In vitro* inactivation of bacteria and fungi by oregano essential oil electrospraying through a transient spark discharge. Load of the microorganisms per a Petri dish was 10^8 (top) and 10^7 CFU.

Bacteria on the surface are solvated with water molecules, that prevents the hydrophobic essential oil to contact bacteria membrane directly. Nevertheless, the charge carried with micelles and PAW itself may disturb the water screening and open bacterial membrane for carvaclol.

In direct contact with the cell membrane phenolic compounds of OEO can occupy the space between the fatty acids chains in the hydrophobic phase of the cell membrane and lead to changes in conformation of lipids. Moreover, once carvaclol is inserted inside the lipid bilayer it accumulates there, that lead to membrane expansion and as a result causes disturbances of van der Waals interactions between lipid chains resulting with membrane fluidization. An expansion of the membrane may result with membrane destabilization and possible ion leakage outside or inside the cell [240, 334]. This process leads to decrease of cell potential and pH gradient between inner and outer cell environment and may cause lethal cell damage.

Moreover, bacteria cells with fluidized membranes are supposed to be more acceptable to stress factors of plasma activated water, such as reactive nitrogen and oxygen species, or low pH.

9.4.3 Inactivation of *E. coli* on spinach leaves

In vivo E. coli inactivation was performed on the surface of fresh spinach leaves by mechanically and electrosprayed oregano essential oil (see table 9.1). The drop test calibrated by conventional cultivations on M-H agar was used (see figure 9.9).

At least 3 $\log_{10}$ reduction of bacteria was reached after 10 minutes, while 5 $\log_{10}$ reduction was observed after 10 hours of spinach exposure to plasma treated essential

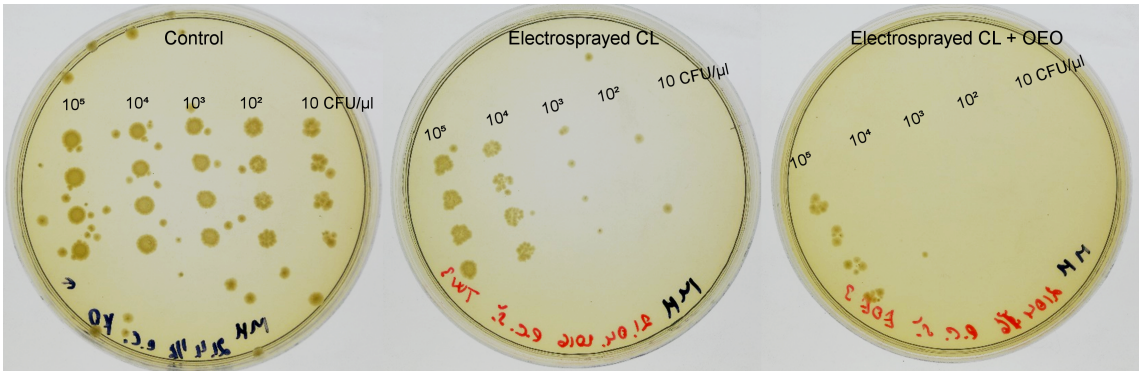

Figure 9.9. Example the 6×4 matrix drop test evaluation of bacteria inactivation *in vivo*. Control sample with 10^7 CFU/ml washed from freshly inoculated spinach leaves (left), bacteria reduction induced by electrospraying of CL (middle) and CL+OEO (right).

oil. 5 $\log_{10}$ reduction is comparable to that one reached *in vitro*. Mechanically sprayed essential oil and electrosprayed carrier liquid inactivated less than 2 $\log_{10}$ bacteria both after 10 minutes and 10 hours of bacteria exposure to treated liquids. Mechanically sprayed carrier liquid did not cause any bacteria inactivation comparing to the control group.

There are several possible reasons of lower efficiency of plasma activated essential oil on bacteria on the spinach leaves surface. Bacterial suspension on spinach leaves was not spreaded homogeneously as it was performed on the agar surface, and as a result it did not dry completely by the time of plasma treatment. Moreover, the leaves surface was not as smooth as the surface of agar. Liquid layer provided bacteria with a better aqueous screening preventing essential oil and its components to interact with the cell membrane.

Moreover, the period of bacteria exposure to plasma activated essential oil seems to play an important role in an inactivation process. One of the possible explanation of this fact is that essential oil is effective as a antimicrobial agent in gas phase and needs some time to vaporize. Carvaclol accumulation in the lipid bilayer takes time as well. Furthermore, bacteria in the liquid medium on the spinach surface migrate and can be deposited in layers.

Nevertheless, bacterial load of ready to eat food is usually less then 100 CFU/ml, that means that 3 $\log_{10}$ reduction can be consider as sufficient.

Possible application of the method described in this section is antimicrobial coating of food packaging prior to its usage with ready to eat leaves (spinach, salad etc.). Leaves are usually packaged hermetically to humidify food properly. According to a test made within this study no significant effect on the wither period of spinach leaves was observed. Several spinach leaves were washed in the sterile aqueous solution (4% NaCl) and were then placed into the ziplock bag. Spinach was then electro or mechanically sprayed with CL, CL+OEO or normal saline solution (control group), filled with some amount of air and closed hermetically. No significant differences in leaves appearance was observed even after 20 days of storage (see figure 9.10).

Figure 9.10. Spinach leaves in ziplock bag treated with different solutions after 10 days of storage in the refrigerator: a. control sample mechanically sprayed with normal saline solution; b. and c. mechanically sprayed with CL and CL+OEO; d. and e. electrosprayed with CL and CL+OEO.

Chapter 10
Conclusion

Non-thermal atmospheric pressure plasma is a source of different plasma agents, such as charged particles, reactive species, UV light, electric field, heat, etc. They can induce bacterial damage, which can lead to bacteria inactivation or entering the VBNC state. Precise mechanisms of bacteria and fungi inactivation are the topic of great interest, as they are still not completely understood. Variety of non-thermal plasma sources makes accurate explanation of plasma induced bacterial damage even more challenging. Moreover, bacteria are usually covered with aqueous layer or contaminates aqueous media that requires understanding of complexity of plasma-liquid interaction and processes.

This thesis is focused on the combination of basic and applied research of processes induced by plasma in liquids, and their effects on bacteria and fungi. Three different plasma sources have been used to investigate plasma induced bacterial damage within three different exeperiments. DC-driven plasma jet working in air designed by Kolb et al. [81] was used to examine influence of electrode material on biocidal properties of plasma activated water. RF-driven micro atmospheric pressure plasma jet (μAPPJ) [65] was used to inspect mechanisms of bacterial damage in $He + O_2$ atmosphere with absence of nitrogen. And finally, the transient spark discharge in ambient air, ignited in the electrode arrangement designed by the author of this thesis and inspired by the setup reported by Machala et al. [24], was used to electrospray oregano essential oil onto spinach leaves surface to figure out possible pathways of essential oil activation with DC discharge.

Bactericidal properties of plasma activated liquids (referred as PAW and discussed in the chapter 4 depend on plasma source, working gas, used atmosphere and activated medium; moreover, inactivation efficiency depends on the microorganism and its growth phase, duration of plasma treatment and the period of bacteria exposure to the activated medium. Mechanisms of bacteria inactivation induced by chemical processes in PAW and can vary with respect to all parameters mentioned above. However, it is possible to generalize that all microorganisms exposed to PAW experience oxidative stress. There are several common parameters, that are used to characterize PAW: concentration of hydrogen peroxide, concentration of nitrites and nitrates and pH. Hydrogen peroxide is generated in the liquid, if plasma and/or liquid is in contact with oxygen. And RNS (nitrites and nitrates) are detected in PAW, in case the working gas or experimental surrounding contains nitrogen. At least small acidification of the unbuffered aqueous solution is observed for any kind of plasma treatment.

The brief recapitulation of each setup and depiction of key conclusions are provided below.

- **Pathways of bacteria inactivation with water activated by DC-operated plasma jet**

  DC-operated plasma jet with coaxial electrode arrangement was operated underwater with imminent contact of treated sample with grounded nozzle. Three nozzles made of different materials (stainless steel, copper and titanium) were used

to evaluate dependency of PAW bactericidal properties on the metal ions released from the electrode. *E. coli* in exponential growth phase was added to the activated water within 5 minutes after plasma treatment.

DC-operated plasma jet is a specific device, which allows to prepare PAW with different properties depending on power dissipated in expelled plasma. PAW prepared with low average dissipated energy did not contain any hydrogen peroxide and only small amount of nitrites (< 10 µmol/l). PAW with these parameters was not supposed to induce lethal bacteria damage. Nevertheless, $3\log_{10}$ reduction of *E. coli* after 90 minutes of its persistent in PAW prepared with copper nozzle was observed. This fact was attributed to the copper toxicity.

On the other hand, plasma plume with raised average energy generated at least small amount of hydrogen peroxide in water; moreover, concentration of measured RNS increased as well with simultaneous decrease of pH below 3.3. Two main bactericidal pathways were proposed in this case:

1. generation of hydroxyl radical through the Fenton reaction of hydrogen peroxide and heavy-metal ions (Fe^{2+} and Cu^{+}). The reaction results in $OH^{\bullet}$ radical formation, that has strong oxidizing potential and extremely short half-life. It is known to be the strongest oxidant inducing various oxidation processes, e.g. lipid peroxidation, DNA damage, etc.
2. Bactericidal effect of peroxinitrite formed by the reaction of H_2O_2 and NO_2^- under acidic conditions. Kinetics of this reaction strongly depends on pH value with threshold at 3.3.

Bactericidal properties of PAW prepared with DC-operated plasma jet strongly depended on the nozzle material. Maximal bacterial reduction rate was observed in the case of stainless steel nozzle and was $> 5\log_{10}$ after 60 minutes of bacteria exposition to the PAW. The same bacterial reduction was reached after 90 minutes bacterial exposure to the PAW prepared with the copper nozzle. In both cases the Fenton reaction proceeded. Nevertheless, the PAW prepared with titanium nozzle was not that efficient with maximal bacteria reduction equals to $3\log_{10}$. This inefficiency was ascribed to the fact, that titanium ions do not catalyze Fenton chemistry, and as a result no or negligible amount of hydroxyl radical was formed. Bactericidal effect of this PAW was attributed to acidified nitrites and mainly to short-lived peroxinitrites, as the pH value was ≤ 3.3.

- **Bacteria inactivation pathways in PAW generated by µAPPJ**

µAPPJ operated in $He + O_2$ gas mixture was used to treat 3 ml of bacterial solution. Treatment was provided in the closed and defined atmosphere with absence of ambient air, i.e. nitrogen. No reactive nitrogen species were supposed to be generated in PAW. Chemical analysis was performed using different model liquids (DI water with 500 µmol/l of phenol and pure DI water) and results were published in [73]. Bacterial inactivation properties were studied in dependence on the treatment time. Bacteria were washed immediately after plasma treatment and no post-discharge treatment was assumed.

According to obtained results, that are discussed in the Chapter 8, bacteria suffered oxidative stress and probably entered the viable but non-culturable state. VBNC state was possibly caused mainly by plasma induced hypersensitivity to hydrogen peroxide. It seemed that increase of membrane permeability as a result of lipid peroxidation and pore formation was not the reason of bacterial death. Nevertheless, oxidative stress induced by µAPPJ prepared PAW caused changes in melting tem-

perature of DNA strands, which indicated damages on DNA and possible bacterial mutations.

- **Bactericidal properties of plasma activated oregano essential oil**

  Electrospraying of natural decontaminant (essential oil) through the transient spark discharge was used to examine bactericidal properties of essential oils activated with plasma. Essential oils in general as well as oregano essential oil in particular are known for their antiseptic properties, i.e. bactericidal, fungicidal, analgetic, sedative, etc., and are usually used in vaporized phase. However, vaporization is highly time consuming process and takes up to 72 hours, depending on experimental conditions. The transient spark discharge was used to decrease the time needed to provide bacteria and fungi inactivation (in this experiment from 12 hours to 4 minutes) and at the same time to induce processes, which can lead to gain more efficient bactericidal effect of OEO.

  Transient spark discharge was used to evaluate possible advantages of plasma treated essential oils in order to decontaminate food borne pathogens *in vitro* and *in vivo* on spinach leaves. 5% Polysorbat 80 solution was used as a carrier liquid to carry essential oils and plasma induced reactive species to the contaminated surface through electohydrodynamics atomization technique. Small amount of essential oil in carrier liquid ($6+194$ µl) was electrosprayed through the transient spark discharge for 4 minutes to cover the contaminated surface completely.

  Up to $8\log_{10}$ reduction of bacteria and $7\log_{10}$ of fungi was observed for *in vitro* experiments. Nevertheless, inactivation rate obtained by PAW electrospraying *in vivo* was equal to 3–4 $\log_{10}$. Author hypothesized that lower inactivation rate was caused by not homogeneous structure of spinach leaves and as a result not homogeneous distribution of bacterial solution on the surface, and short time of bacteria exposure to PAW, as the leaves were washed 10 minutes after the treatment.

  Increase of bactericidal efficiency of plasma activated OEO were ascribed to the charge cumulated on the micelles and transported onto the surface. Such complexes disturb water molecules screening bacterial cell, providing free contact and diffusion of essential oil through the hydrophobic lipid bilayer. Moreover, plasma is assumed to induce acidification and ROS and RNS formation in the aqueous carrier liquid. These factors were supposed to lead to oxidative stress of bacteria and also contribute to the cell death.

References

[1] P. Lukes, E. Dolezalova, I. Sisrova, M. Clupek. Aqueous-phase chemistry and bactericidal effects from an air discharge plasma in contact with water: evidence for the formation of peroxynitrite through a pseudo-second-order post-discharge reaction of H_2O_2 and HNO_2. *Plasma Sources, Science and Technology*, **23**, p. 015019, 2014.

[2] D. B. Graves. The emerging role of reactive oxygen and nitrogen species in redox biology and some implications for plasma applications to medicine and biology. *Journal of Physics D: Applied Physics*, **45**(26), p. 263001, 2012.

[3] E. Dolezalova, P. Lukes. Membrane damage and active but nonculturable state in liquid cultures of Escherichia coli treated with an atmospheric pressure plasma jet. *Bioelectrochemistry*, **103**, pp. 7–14, 2015.

[4] G. Fridman, G. Friedman, A. Gutsol, A. B. Shekhter, V. N. Vasilets, A. Fridman. Applied Plasma Medicine. *Plasma Processes and Polymers*, **5**(6), pp. 503–533, 2008.

[5] S. Bekeschus, A. Schmidt, K.-D. Weltmann, T. von Woedtke. The plasma jet kINPen – A powerful tool for wound healing. *Clinical Plasma Medicine*, **4**(1), pp. 19–28, 2016.

[6] D. Ziuzina, S. Patil, P. J. Cullen, K. M. Keener, P. Bourke. Atmospheric cold plasma inactivation of Escherichia coli in liquid media inside a sealed package. *Journal of Applied Microbiology*, **114**(3), pp. 778–787, 2013. 1388.

[7] J. Priestley. *The history and present state of electricity: with original experiments*. Dodsley, Johnson snd Davenport, Cadell, 1767.

[8] B. Dibner. *Galvani-Volata: a controversy that led to the discovery of useful electricity*. Burndy library, 1952.

[9] A. Volta. On the electricity excited by the mere contact oc conducting substances of different kinds. *Philosophical transactions of the Royal society of London*, **90**, pp. 403–431, 1800.

[10] P. K. Chu, X. Lu. *Low temperature plasma technology*. Traylor and Francis Group, 2010.

[11] M. Faraday. Experimental research in electricity. Eleventh series. *Philosophical transactions of the Royal society of London*, **128**, pp. 1–40, 1837.

[12] A. Andres. Tracking down the origin of arc plasma science-II. Early continuous discharges. *IEEE Transactions on Plasma Science*, **31**, pp. 1060–1069, 2003.

[13] J. S. Townsend. The conductivity produced in gases by the motion of negatively-charged ions. *Nature*, **62**, pp. 340–341, 1900.

[14] I. Langmuir. Oscilation in ionized gases. *Proceedings of the National Academy of Sciences of the United States of America*, **14**, pp. 627–637, 1928.

[15] P. Kulhánek. *Úvod do teorie plazmatu*. AGA (Aldebaran Group for Astrophysics), 2017.

[16] R. Hippler, H. Kersten, M. Schmidt, K. H. Schoenbach. *Low Temperature Plasmas: Fundamentals, Technologies and Techniques, 2nd edition*. Wiley-VCH, 2008.

[17] J. K. J., J. Tobiáš. *Fyzika plazmatu*. Academia Praha, 1966.

[18] A. Fridman, G. Friedman. *Plasma Medicine*. John Wiley & Sons, 2012.

[19] Z. Machala, K. Hensel, Y. Akishev. *Plasma for Bio-Decontamination, Medicine and Food Security*. Springer Science & Business Media, 2012.

[20] M. Keidar, I. Beilis. *Plasma Engineering: Applications from Aerospace to Bio and Nanotechnology*. Academic Press, 2013.

[21] J. Ehlbeck, U. Schnabel, M. Polak, J. Winter, T. von Woedtke, R. Brandenburg, T. von dem Hagen, K.-D. Weltmann. Low temperature atmospheric pressure plasma sources for microbial decontamination. *Journal of Physics D: Applied Physics*, **44**, p. 013002, 2011.

[22] J. P. Reizer. *Physics of gaseous discharge*. Nauka, Moscow, 1992.

[23] V. Scholtz, J. Julak. The "cometary" discharge, a possible new type of DC electric discharge in air at atmospheric pressure, and its bactericidal properties. *Journal of Physics: Conference Series*, **223**, p. 012005, 2010.

[24] Z. Machala, L. Chladekova, M. Pelach. Plasma agents in bio-decontamination by dc discharges in atmospheric air. *Journal of Physics D, Applied Physics*, **43**, 2010.

[25] R. Bussiahn, R. Brandenburg, T. Gerling, E. Kindel, H. Lange, N. Lembke, K.-D. Weltmann, T. von Woedtke, T. Kocher. The hairline plasma: An intermittent negative dc-corona discharge at atmospheric pressure for plasma medical applications. *Applied Physics Letters*, **96**, p. 143701, 2010.

[26] V. F. (now Celedova), J. Jira, V. Kriha. Dependence of bacteria and yeast inactivation on charge transported to the contaminated surface. *32nd International Conference on Phenomena in Ionized Gases (ICPIG)*, **1**, 2015.

[27] J. E. Jones. A theoretical explanation of the laws of Warburg and Sigmond. *Proceedings of the Royal Society A*, **453**, pp. 1033–1052, 1997.

[28] K. Yannalah, F. Pontiga. A semi-analytical stationary model of a poin-to-plane corona discharge. *Plasma Soucrec, Science and Technology*, **21**, pp. 1033–1052, 2012.

[29] Y. Guo, X. Xiang, B. Chen. Investigation of current density distribution model for barb-plate ESP. *11th International Conference on Electrostatic Precipitation*, pp. 359–362, 2008.

[30] E. Marode, F. Bastien, M. Bakker. A model of the streamerinduced spark formation based on neutral dynamics. *Journal of Applied Physics*, **50**, p. 140, 1979.

[31] M. Janda, Z. Machala. Transient-spark discharge in $N_2/CO_2/H_2O$ mixtures at atmospheric pressure. *IEEE Transactions on Plasma Science*, **36**, 2008.

[32] P. Lukes, B. R. Locke, J. L. Brisset. *Aqueous-phase chemistry of electrical discharge plasma in water and in gas–liquid environments Plasma Chemistry and Catalysis in Gases and Liquids*. Weinheim: Wiley-VCH, 2012.

[33] J. Julak, O. Janouskova, V. Scholtz, K. Holada. Inactivation of prions using electrical DC discharges at atmospheric pressure and ambient temperature. *Plasma Processes and Polymers*, **8**, pp. 316–323, 2011.

[34] V. Scholtz, H. Souakova, M. Svarcova, V. Kriha, H. Zivna, J. Julak. Inactivation of dermatophyte infection by nonthermal plasma on animal model. *Medical Mycology*, 2016. Accepted for publication.

[35] W. Gilbert. De Magnete. *Londini, Anno, MDC*, 1600.

[36] G. Taylor. Disintegration of water drops in an electric field. *Proc. R. Soc. Lond. A*, **280**, pp. 383–397, 1964.

[37] G. Taylor. The force exerted by an electric field on a long cylindrical conductor. *Proc. R. Soc. A*, **291**, pp. 145–158, 1966.

[38] J. B. Fenn. Electrospray ionization for mass spectrometry of large biomolecules. *Science*, **246**, pp. 64–71, 1989.

[39] J. Xie, J. Jiang, P. Davoodi, M. P. Srinivasan, C.-H. Wang. Electrohydrodynamic atomization: A two-decade effort to produce and process micro-/nanoparticulate materials. *Chemical Engineering science*, **125**, pp. 35–57, 2014.

[40] P. Mehta, R. Haj-Ahmad, M. Rasekh, M. S. Arshad, A. Smith, S. M. van der Merwe, X. Li, M.-W. Chang, Z. Ahmad. Pharmaceutical and biomaterial engineering via electrohydrodynamic atomization technologies. *Drug Discov. Today*, **22**, pp. 157–165, 2016.

[41] D. B. Victor. ELECTROSPRAY mov, 2013.

[42] K.-D. Weltmann, M. Polak, K. Masur, T. von Woedtke, J. Winter, S. Reuter. Plasma processes and plasma sources in medicine. *Contributions to Plasma Physics*, **52**, pp. 644–654, 2012.

[43] H.-E. Wagner, R. Brandenburg, K. V. Kozlov, A. Sonnenfeld, P. Michel, J. F. Behnke. The barrier discharge: basic properties and applications to surface treatment. *Vacuum*, **71**, pp. 417–436, 2003.

[44] G. Fridman, M. Peddinghaus, M. Balasubramanian, H. Ayan, A. Fridman, A. Gutsol, A. Brooks. Blood coagulation and living tissue sterilization by floating-electrode dielectric barrier discharge in air. *Plasma Chemistry and Plasma Processing*, **26**, pp. 425–442, 2006.

[45] M. Polak, J. Winter, M. Stieber, U. Schnabel, J. Ehlbeck, K. D. Weltmann. DBD source. *Proc. 28th Int. Conf. on Gas Discharges and Their Applications (Greifswald, Germany)*, pp. 436–439, 2010.

[46] M. Hahnel, T. von Woedtke, K.-D. Weltmann. Influence of the air humidity on the reduction of *Bacillus* spores in a defined environment at atmospheric pressure using a Dielectric barrier surface discharge. *Plasma Processes and Polymers*, **7**, pp. 244–249, 2010.

[47] K. Oehmigen, J. W. M. Hahnel, C. Wilke, R. Brandenburg, K.-D. Weltmann, T. von Woedtke. Estimation of possible mechanisms of Escherichia coli inactivation by plasma treated sodium chloride solution. *Plasma Processes and Polymers*, **8**(10), pp. 904–913, 2011.

[48] S. Bekeschus, A. Schmidt, K.-D. Weltmann, T. von Woedtke. The plasma jet kINPen – A powerful tool for wound healing. *Clinical Plasma Medicine*, **4**(1), pp. 19–28, 2016.

[49] G. Y. Park, S. J. Park, M. Y. Choi, I. G. Koo, J. H. Byun, J. W. Hong, J. Y. Sim, G. J. Collins, J. K. Lee. Atmospheric-pressure plasma sources for biomedical applications. *Plasma Sources, Science and Technology*, **21**, p. 043001, 2012.

[50] J. winter, R. Brandenburg, K.-D. Weltmann. Atmospheric pressure plasma jets: an overview of devices and new directions. *Plasma Sources, Science and Technology*, **24**, p. 064001, 2015.

[51] A. Schutze, J. Y. Jeong, S. E. Babayan, J. Park, G. S. Selwyn, R. F. Hicks. The atmospheric-pressure plasma jet: a review and comparison to other plasma sources. *IEEE Transactions on Plasma Science*, **26**, pp. 1685–1694, 1998.

[52] X. Lu, M. Laroussi, V. Puech. On atmospheric-pressure non-equilibrium plasma jets and plasma bullets. *Plasma Sources, Science and Technology*, **21**, p. 034005, 2012.

[53] S. E. Babayan, J. Y. Jeong, V. J. Tu, J. Park, G. S. Selwyn, R. F. Hicks. Deposition of silicon dioxide films with an atmospheric-pressure plasma jet. *Plasma Sources Science and Technology*, **7**(3), p. 286, 1998.

[54] J. Y. Jeong, S. E. Babayan, V. J. Tu, J. Park, I. Henins, R. F. Hicks, G. S. Selwyn. Etching materials with an atmospheric-pressure plasma jet. *Plasma Sources Science and Technology*, **7**(3), p. 282, 1998.

[55] J. L. Walsh, M. G. Kong. Contrasting characteristics of linear-field and cross-field atmospheric plasma jets. *Applied Physics Letters*, **93**, p. 111501, 2008.

[56] X. Lu, Z. Jiang, Q. Xiong, Z. Tang, Y. Pan. A single electrode room-temperature plasma jet device for biomedical applications. *Applied Physcis Letters*, **92**, p. 081502, 2008.

[57] M. Teschke, J. Kedzierski, E. G. Finantu-Dinu, D. Korzec, J. Engemann. High-speed photographs of a dielectric barrier atmospheric pressure plasma jet. *IEEE Transactions on Plasma Science*, **33**, p. 310, 2005.

[58] Q. Li, J.-T. Li, W.-C. Zhu, X.-M. Zhu, Y.-K. Pu. Effects of gas flow rate on the length of atmospheric pressure nonequilibrium plasma jets. *Applied Physics Letters*, **95**, p. 141502, 2009.

[59] J. Guo, K. Huang, J. Wang. Bactericidal effect of various non-thermal plasma agents and the influence of experimental conditions in microbial inactivation: A review. *Food control*, **50**, pp. 482–490, 2015.

[60] A. Shashurin, M. N. Shneider, A. Dogariu, R. B. Miles, M. Keidar. Temporal behavior of cold atmospheric plasma jet. *Applied Physics Letters*, **94**, p. 231504, 2009.

[61] V. Leveille, S. Coulombe. Design and preliminary characterization of a miniature pulsed RF APGD torch with downstream injection of the source of reactive species. *Plasma Sources Science and Technology*, **14**(3), p. 467, 2005.

[62] X. Lu, Y. Cao, P. Yang, Q. Xiong, Z. Xiong, Y. Xian, Y. Pan. An RC plasma device for sterilization of root canal of teeth. *IEEE Transactions on Plasma Science*, **37**, p. 668, 2009.

[63] E. Stoffels, I. E. Kieft, R. E. J. Sladek. Superficial treatment of mammalian cells using plasma needle. *Journal of Physics D: Applied Physics*, **36**, p. 2908, 2003.

[64] V. S. von der Gathen, L. Schaper, N. Knake, S. Reuter, K. Niemi, T. Gans, J. Winter. Spatially resolved diagnostics on a microscale atmospheric pressure plasma jet. *Journal of Physics D: Applied Physics*, **41**, p. 194004, 2008.

[65] J. Golda, J. Held, B. Redeker, M. Konkowski, P. Beijer, A. Sobota, G. Kroesen, N. S. J. Braithwaite, S. Reuter, M. M. Turner, T. Gans, D. O'Connell, V. S. von der Gathen. Concepts and characteristics of the 'COST Reference Microplasma Jet. *J. Phys. D: Appl. Phys.*, **49**, p. 084003, 2016.

[66] S. Schneider, M. Dünnbier, S. Hubner, S. Reuter, J. Benedikt. Atomic nitrogen: a parameter study of a micro-scale atmospheric pressure plasma jet by means of

molecular beam mass spectrometry. *Jurnal of Physics D: Applied Physics*, **47**, p. 505203, 2014.

[67] D. Maletic, N. Puac, S. Lazovic, G. Malovic, T. Gans, V. S. von der Gathen, Z. L. Petrovic. Detection of atomic oxygen and nitrogen created in a radio-frequency-driven micro-scale atmospheric pressure plasma jet using mass spectrometry. *Plasma Physcis and Control Fussion*, **54**, p. 124046, 2012.

[68] E. Wagenaars, T. Gans, D. O'Connell, K. Niemi. Two-photon absorption laser-induced fluorescence measurements of atomic nitrogen in a radio-frequency atmospheric pressure plasma jet. *Plasma Sources, Science and Technology*, **21**, p. 042002, 2012.

[69] T. Murakami, K. Niemi, T. Gans, D. O'Connell, W. G. Graham. Chemical kinetics and reactive species in atmospheric pressure helium-oxygen plasmas with humid-air impurities. *Plasma Sources. Science and Technology*, **22**, p. 015003, 2013.

[70] T. Murakami, K. Niemi, T. Gans, D. O'Connell, W. G. Graham. Interacting kinetics of neutral and ionic species in an atmospheric-pressure helium-oxygen plasma with humid air impurities. *Plasma Sources. Science and Technology*, **22**, p. 045010, 2013.

[71] A. Schmidt-Bleker, J. Winter, S. Iseni, M. Dunnbier, K. D. Weltmann, S. Reuter. Reactive species output of a plasma jet with a shielding gas device-combination of FTIR absorption spectroscopy and gas phase modelling. *J. Phys. D: Appl. Phys.*, **47**, p. 145201, 2014.

[72] B. Niermann, A. Kanitz, M. Boke, J. Winter. Impurity intrusion in radio-frequency micro-plasma jets operated in ambient air. *Journal of Physics D: Applied Physics*, **44**, p. 325201, 2011.

[73] M. M. Hefny, C. Pattyn, P. Lukes, J. Benedikt. Atmospheric plasma generates oxygen atoms as oxidizing species in aqueous solutions. *J. Phys. D: Appl. Phys.*, **49**, p. 404002, 2016.

[74] D. Schroder, S. Burhenn, D. Kirchheim, V. S. von der Gathen. Enhanced oxygen dissociation in a propagating constricted discharge formed in a self-pulsing atmospheric pressure microplasma jet. *Journal of Physics D: Applied Physics*, **46**, p. 464003, 2013.

[75] S. Spiekermeier, D. Schroder, V. S. von der Gathen, M. Boke, J. Winter. Helium metastable density evolution in a self-pulsing μAPPJ. *Journal of Physics D: Applied Physics*, **48**, p. 035203, 2015.

[76] S. Schneider, J. W. Lackmann, D. Ellerweg, B. Denis, F. Narberhaus, J. E. Bandow, J. Benedikt. The role of VUV radiation in the inactivation of bacteria with an atmospheric pressure plasma jet. *Plasma Process and Polymers*, **9**, pp. 561—568, 2012.

[77] J.-W. Lackmann, S. Schneider, E. Edengeiser, F. Jarzina, S. Brinckmann, E. Steinborn, M. Havenith, J. Benedikt, J. E. Bandow. Photons and particles emitted from cold atmospheric-pressure plasma inactivate bacteria and biomolecules independently and synergistically. *Journal of Royal Society Inteface*, **10**, p. 20130591, 2013.

[78] J. F. Kolb, A. A. H. Mohamed, R. O. Price, R. J. Swanson, A. Bowman, R. L. Chiavarini, M. Stacey, K. H. Schoenbach. Cold atmospheric pressure air plasma jet for medical applications. *Applied Physics Letters*, **92**, p. 241501, 2008.

[79] P. Sun, H. Wu, N. Bai, H. Zhou, R. Wang, H. Feng, W. Zhu, J. Zhang, J. Fang. Inactivation of Bacillus subtilis Spores in Water by a Direct-Current, Cold Atmospheric-Pressure Air Plasma Microjet. *Plasma Processes and Polymers*, **9**(2), pp. 157–164, 2012.

[80] W. D. Zhu, J. L. Lopez. A DC non-thermal atmospheric- pressure plasma microjet. *Plasma Sources, Science and Technology*, **21**, p. 034018, 2012.

[81] J. F. Kolb, A. M. Mattson, C. M. Edelblute, X. Hao, M. A. Malik, L. C. Heller. Cold DC-operated air plasma jet for the inactivation of infectious microorganisms. *IEEE Transactions on Plasma Science*, **40**, 2012.

[82] J. Li, N. Sakai, M. Watanabe, E. Hotta, M. Wachi. Study on plasma agent effect of a direct-current atmospheric pressure oxygen-plasma jet on Inactivation of *E. coli* using bacterial mutants. *IEEE Transactions in Plasma Sciecnce*, **41**, pp. 935–941, 2013.

[83] R. H. Stark, K. H. Schoenbach. Direct current high-pressure glow discharges. *Journal of Applied Physics*, **85**, 1999.

[84] J. S. Sousa, G. Bauville, V. Puech. Arrays of microplasmas for the controlled production of tunable high fluxes of reactive oxygen species at atmospheric pressure. *Plasma Sources, Science and Technology*, **22**, p. 035012, 2013.

[85] X. L. Deng, A. Y. Nikiforov, N. D. Geyter, R. Morent, C. Leys. Deposition of a TMDSO-based film by a non-equilibrium atmospheric pressure dc plasma jet. *Plasma Processes and Polymers*, **10**, pp. 641–648, 2013.

[86] Y. Xian, S. Wu, Z. Wang, Q. Huang, X. Lu, J. F. Kolb. Discharge Dynamics and Modes of an Atmospheric Pressure Non-Equilibrium Air Plasma Jet. *Plasma processes and polymers*, **10**, pp. 372–378, 2013.

[87] M. Jasinski, J. Mizeraczyk, Z. Zakrzewski, T. Ohkubo, J.-S. Chang. CFC-11 destruction by microwave torch generated atmospheric-pressure nitrogen discharge. *Journal of Physics D: Applied Physics*, **35**, 2002.

[88] T. Shimizu, B. Steffes, R. Pompl, F. Jamitzky, W. Bunk, K. Ramrath, M. Georgi, W. Stolz, H.-U. Schmidt, T. Urayama, S. Fujii, G. E. Morfill. Characterization of Microwave Plasma Torch for Decontamination. *Plasma Processes and Polymers*, **5**(6), pp. 577–582, 2008.

[89] A. V. Pipa, M. Andrasch, K. Rackow, J. E. J, K. D. Weltmann. Observation of microwave volume plasma ignition in ambient air. *Plasma Sources, Science and Technology*, **21**, p. 035009, 2012.

[90] M. Leins, M. Walker, A. Schulz, U. Schumacher, U. Stroth. Spectroscopic investigation of a microwave- generated atmospheric pressure plasma torch. *Contributions to Plasma Physics*, **52**, pp. 615–628, 2012.

[91] P. Bruggeman, R. Brandenburg. Atmospheric pressure discharge filaments and microplasmas: physics, chemistry and diagnostics. *Journal of Physics D: Applied Physics*, **46**, p. 464001, 2013.

[92] M. Baeva, A. Bosel, J. Ehlbeck, D. Loffhagen. Modeling of microwave-induced plasma in argon at atmospheric pressure. *Physics Review E*, **85**, p. 056404, 2012.

[93] W. S. Lai, H. R. Lai, S. P. Kuo, O. Taraenko, K. Levon. Decontamination of biological wafare agents by a microwave plasma torch. *Physis of plasmas*, **12**, 2005.

[94] T. Sato, T. Urayama, T. Nakatani, M. T. Inactivation of Escherichia coli by a coaxial microwave plasma flow. *IEEE Trans Plasma Sci.*, **43**, pp. 1159–1163, 2007.

[95] R. Brandenburg, U. Krohmann, M. Stieber, K. D. Weltmann, T. Woedtke, J. Ehlbeck. Antimicrobial treatment of heat sensitive products by atmospheric pressure plasma sources. In *Plasma Assisted Decontamination of Biological and Chemical Agents. In: Guceri S., Fridman A., Gibson K., Haas C. (eds) NATO Science for Peace and Security Series Series A: Chemistry and Biology. Springer, Dordrecht*, pp. 51–63. 2008.

[96] F. Judee, G. Wattieaux, N. Merbahi, M. Mansour, M. P. Castanie-Cornet. The antibacterial activity of a microwave argon plasma jet at atmospheric pressure relies mainly on UV-C radiations. *Journal of Physics D: Applied Physics*, **47**, p. 405201, 2014.

[97] G. Wattieaux, M. Yousfi, N. Merbahi. Optical emission spectroscopy for quantification of ultraviolet radiations and biocide active species in microwave argon plasma jet at atmospheric pressure. *Spectrochimica Acta B: Atomic Spectroscopy*, **89**, pp. 66–76, 2013.

[98] E. Sysolyatina, A. Mukhachev, M. Yurova, M. Grushin, V. Karalnik, A. Petryakov, N. Trushkin, S. Ermolaeva, Y. Akishev. Role of the Charged Particles in Bacteria Inactivation by Plasma of a Positive and Negative Corona in Ambient Air. *Plasma processes and polymers*, **11**, pp. 315–334, 2014.

[99] D. Dobrynin, G. Fridman, G. Friedman, A. Fridman. Physical and biological mechanisms of direct plasma interaction with living tissue. *New Journal of Physics*, **11**(11), p. 115020, 2009.

[100] G. Fridman, A. D. Brooks, M. Balasubramanian, A. Fridman, A. Gutsol, V. N. Vasilets, H. Ayan, G. Friedman. Comparison of direct and indirect effects of nonthermal atmospheric-pressure plasma on bacteria. *Plasma Processes and Polymers*, **4**, pp. 370–375, 2007.

[101] M. Laroussi, G. S. Sayler, B. B. Glascock, B. McCurdy, M. E. Pearce, N. G. Bright, C. M. Malott. Images of biological samples undergoing sterilization by a glow discharge at atmospheric pressure. *IEEE Transactions on Plasma Science*, **27**, pp. 34–35, 1999.

[102] D. A. Mendis, M. Rosenberg, F. Azam. A note on the possible electrostatic disruption of bacteria. *IEEE Transactions on Plasma Science*, **28**, pp. 1304–1306, 2000.

[103] I. Digel, A. T. Artmann, K. Nishikawa, M. Cook, E. Kurulgan, G. M. Artmann. Bactericidal effects of plasma-generated cluster ions. *Medical & Biological Engineering & Computing*, **43**, pp. 800–807, 2005.

[104] M. Laroussi, F. Leipold. Evaluation of the roles of reactive species, heat, and UV radiation in the inactivation of bacterial cells by air plasmas at atmospheric pressure. *International journal of mass spectrometry*, **233**, pp. 81–86, 2004.

[105] I. V. Timoshkin, M. Maclean, M. P. Wilson, M. J. Given, S. J. MacGregor, T. Wang, J. G. Anderson. Bactericidal effect of corona discharges in atmospheric air. *IEEE transactions on plasma science*, **40**, pp. 2322–2333, 2012.

[106] X. T. Deng, J. J. Shi, M. G. Kong. Physical mechanisms of inactivation of Baccilus subtilis spores using cold atmospheric plasmas. *IEEE transactions on plasma science*, **34**, pp. 1310–1316, 2006.

[107] S. J. Kim, T. H. Chung, S. H. Bae, S. H. Leem. Bacterial inactivation using atmospheric pressure single pin electrode microplasma jet with a ground ring. *Applied physics letters*, **94**, 2009.

[108] X. Lu, T. Ye, Y. Cao, Z. Sun, Q. Xiong, Z. Tang, Z. Xiong, J. Hu, Z. Jiang, Y. Pan. The roles of the various plasma agents in the inactivation of bacteria. *Journal of applied physics*, **104**, 2008.

[109] M. K. Boudam, M. Moisan, B. Saoudi, C. Popovici, N. Gherardi, F. Massines. Bacterial spore inactivation by atmospheric-pressure plasmas in the presence or absence of UV photons as obtained with the same gas mixture. *Journal of physics D – Applied physics*, **39**, pp. 3494–3507, 2006.

[110] H. Eto, Y. Ono, A. Ogino, M. Nagatsu. Low-temperature sterilization of wrapped materials using flexible sheet-type dielectric barrier discharge. *Applied physics letters*, **93**, 2008.

[111] M. Moisan, J. Barbeau, M.-C. Crevier, J. Pelletier, N. Philip, B. Saoudi. Plasma sterilization. Methods mechanisms. *Pure and applied chemistry*, **74**, pp. 349–358, 2002.

[112] N. Philip, B. Saoudi, M.-C. Crevier, M. Moisan, J. Barbeau, J. Pelletier. The respective roles of UV photons and oxygen atoms in plasma sterilization at reduced gas pressure: the case of N_2/O_2 mixtures. *IEEE Transactions on Plasma Science*, **30**, pp. 1429–1436, 2002.

[113] F. Rossi, O. Kylian, e. a. H Rauscher H. Low pressure plasma discharge for the sterilization and decontamination of surfaces. *New journal of physics*, **11**, 2009.

[114] H. S. Uhm, J. P. Lim, S. Z. Li. Sterilization of bacterial endospores by an atmospheric-pressure argon plasma jet. *Applied physics letters*, **90**, 2007.

[115] M. Laroussi. Low Temperature Plasma-Based Sterilization: Overview and State-of-the-Art. *Plasma Processes and Polymers*, **2**(5), pp. 391–400, 2005.

[116] R. M. B. (Gut). Seeded gas plasma sterilization method. *US Patent*, **4 207 286**, 1980.

[117] F. Bosshard, M. Bucheli, Y. Meur, T. Egli. The respiratory chain is the cell's Achilles' heel during UVA inactivation in *Escherichia coli*. *Microbiology-Sgm*, **156**, pp. 2006–2015, 2010.

[118] M. Moisan, J. Barbeau, S. Moreau, J. Pelletier, M. Tabrizian, L. Yahia. Low-temperature sterilization using gas plasmas: a review of the experiments and an analysis of the inactivation mechanisms. *International Journal of Pharmaceutics*, **226**, pp. 1–21, 2001.

[119] T. Sato, T. Miyahara, A. Doi, S. Ochiai, T. Urayama, T. Nakatani. Sterilization mechanism for *Escherichia coli* by plasma flow at atmospheric pressure. *Applied Physics Letters*, **89**(7), 2006.

[120] S. Moreau, M. Moisan, M. Tabrizian, J. Barbeau, J. Pelletier, A. Ricard, L. Yahia. Using the flowing afterglow of a plasma to inactivate *Bacillus subtilis* spores: Influence of the operating conditions. *Journal of Applied Physics*, **88**, pp. 1166–1174, 2000.

[121] N. D. Geyter, R. Morent. Nonthermal plasma sterilization of living and nonliving surfaces. *Annual Review of Biomedical Engineering*, **14**, pp. 255–274, 2012.

[122] H. W. Herrmann, I. Henins, J. Park, G. S. Selwyn. Decontamination of chemical and biological warfare (CBW) agents using an atmospheric pressure plasma jet (APPJ). *Physics of Plasmas*, **6**(5), pp. 2284–2289, 1999.

[123] D. Danil, F. Gregory, F. Gary, F. Alexander. Physical and biological mechanisms of direct plasma interaction with living tissue. *New journal of physics*, **11**, 2009.

[124] L. Jinasova. Comparison of effects on the inactivation of bacteria caused by UV radiation generated by corona discharge and gliding arc discharge. *Master thesis at FEE, CTU in Prague*, 2016.

[125] A. C. Rodriguez, J. W. Larkin, J. Dunn, E. Patazca, N. R. Reddy, M. Alvarez-Medina, R. Tetzloff, G. J. Fleischman. Model of the inactivation of bacterial spores by moist heat and high pressure. *Food science*, **69**, pp. 367–373, 2004.

[126] L. A. Herwaldt, W. A. Rutala. Disinfection and sterilization of patient-care items. *Infection Control & Hospital Epidemiology*, **17**, pp. 377–384, 1996.

[127] A. Bauermeister, R. Moeller, G. Reitz, S. Sommer, P. Rettberg. Effect of relative humidity on *Deinococcus radiodurans'* resistance to prolonged desiccation, heat, ionizing, germicidal, and environmentally relevant UV radiation. *Microbial Ecology*, **61**, pp. 715–722, 2011.

[128] J. Kaur, D. A. Ledward, R. W. A. Park, R. L. Robson. Factors affecting the heat resistance of *Escherichia coli* O157:H7. *Letters on Applied Microbiology*, **26**, pp. 325–330, 1998.

[129] K. L. Anderson, C. Roberts, T. Disz, V. Vonstein, K. Hwang, R. Overbeek, P. D. Olson, S. J. Projan, P. M. Dunman. Characterization of the *Staphylococcus aureus* heat shock, cold shock, stringent, and SOS responses and their effects on log-phase mRNA turnover. *Molecular Biology of Pathogens*, **188**, pp. 6739–6756, 2006.

[130] A. Mohamed, J. F. Kolb, K. H. Schoenbach. Low temperature, atmospheric pressure, direct current microplasma jet operated in air, nitrogen and oxygen. *The European Physical Journal D*, **60**(3), pp. 517–522, 2010.

[131] S. Q. Zhang, W. van Gaens, B. van Gessel, S. Hofmann, E. van Veldhuizen, e. a. A. Bogaerts. Spatially resolved ozone densities and gas tempera- tures in a time modulated RF driven atmospheric pressure plasma jet: an analysis of the production and destruction mechanisms. *Journal of Physics D — Applied Physics*, **46**, p. 12, 2013.

[132] J. J. Shi, M. G. Kong. Evolution of discharge structure in capacitive radio-frequency atmospheric microplasmas. *Physical Review Letters*, **96**, 2006.

[133] J. J. Shi, M. G. Kong. Mode characteristics of radio-frequency atmospheric glow discharges. *IEEE Transactions on Plasma Science*, **33**, pp. 624–630, 2005.

[134] J. J. Shi, M. G. Kong. Cathode fall characteristics in a dc atmospheric pressure glow discharge. *Journal of Applied Physics*, **94**, pp. 5504–5513, 2003.

[135] X. M. Zhu, M. G. Kong. Electron kinetic effects in atmospheric dielectric-barrier glow discharges. *Journal of Applied Physics*, **97**, 2005.

[136] S. Toepfl, V. Heinz, D. Knorr. Overview of pulsed electric field processing for food. *In Sun. D.V. ed 1, Emerging technologies of food processes*, pp. 65–69, 2005.

[137] D.-W. Sun. *Emerging technologies for food processing*. Elsevier Lrd., 2014.

[138] J. Julak, V. Scholtz, S. Kotucova, O. Janouskova. The persistent microbicidal effect in water exposed to the corona dischage. *European Journal of Medical Physics*, **28**, pp. 230–239, 2012.

[139] G. Kamgang-Youbi, J.-M. Herry, M.-N. Bellon-Fontaine, J.-L. Brisset, A. Doubla, M. Naitali. Evidence of temporal postdischarge decontamination of bacteria by

gliding electric discharges: application to *Hafnia alvei*. *Applied and environmental microbiology*, **73**, pp. 4791–4796, 2007.

[140] G. Friedman. Plasma pharmacology. In *in ICPM-3: 3rd International Conference on Plasma Medicine., Greifswald*. 2010.

[141] N. Shainsky, D. Dobrynin, U. Ercan, S. J. H. Joshi, A. Brooks, G. C. Y. Fridman, A. F. G. Griedman. Non-equilibrium plasma treatment of liquids, formation of plasma acid. In *in ISPC-20: 20th International Symposium on Plasma Chemistry, A. J. Drexel Plasma Institute, Philadelphia, PA.*. 2011.

[142] P. G. Rutberg, V. A. Kolikov, V. E. Kurochkin, L. K. Panina, A. P. Rutberg. Electric discharges and the prolonged microbial resistance of water. *IEEE Trans. Plasma Sci.*, **35**, pp. 1111–1118, 2007.

[143] M. Naitali, G. Kamgang-Youbi, J.-M. Herry, M.-N. Bellon-Fontaine, J.-L. Brisset. Combined effects of long-living chemical species during microbial inactivation using atmospheric plasma-treated water. *Applied and environmental microbiology*, **76**, pp. 7662–7664, 2010.

[144] M. J. Traylor, M. J. Pavlovich, S. Karim, P. Hait, Y. Sakiyama, D. S. Clark, D. B. Graves. Long-term antibacterial efficacy of air plasma-activated water. *Journal of Physics D: Applied Physics*, **44**, p. 472001, 2011.

[145] Z. Machala, B. Tarabova, K. Hensell, E. Spetlikova, L. Sikurova, P. Lukes. Formation of ROS and RNS in water electro-sprayed through transient spark discharge in air and their bactericidal effects. *Plasma Processes and Polymers*, **10**, pp. 649–659, 2013.

[146] C. A. J. van Gils, S. Hofmann, B. K. H. L. Boekema, R. Brandenburg, P. J. Bruggeman. Mechanisms of bacterial inactivation in the liquid phase induced by a remote RF cold atmospheric pressure plasma jet. *Journal of Physics D: Applied Physics*, **46**(17), p. 175203, 2013.

[147] F. Liu, P. Sun, N. Bai, Y. Tian, H. Zhou, S. Wei, Y. Zhou, J. Zhang, W. Zhu, K. Becker, J. Fang. Inactivation of Bacteria in an Aqueous Environment by a Direct-Current, Cold-Atmospheric-Pressure Air Plasma Microjet. *Plasma Processes and Polymers*, **7**(3-4), pp. 231–236, 2010.

[148] M. J. Pavlovich, H.-W. Chang, Y. Sakiyama, D. S. Clark, D. B. Graves. Ozone correlates with antibacterial effects from indirect air dielectric barrier discharge treatment of water. *Journal of Physics D: Applied Physics*, **46**(14), p. 145202, 2013.

[149] P. Lukes. Water treatment by pulsed streamer corona discharge in water. *PhD Dissertation. Institute of Plasma Physics AS CR, Prague, Czech Republic.*, 2002.

[150] J. L. Brisset, J. Lelievre, A. Doubla, J. Amouroux. Interactions with aqueous solutions of the air aqueous-phase chemistry of electrical discharge plasma corona products. *Rev. Phys. Appl.*, **25**, pp. 535–543, 1990.

[151] J. L. Brisset, B. Benstaali, D. Moussa, J. Fanmoe, E. Njoyim-Tamungang. Acidity control of plasma-chemical oxidation: Applications to dye removal, urban waste abatement and microbial inactivation. *Plasma Sources Sci. Technol.*, **20**, p. 034021, 2011.

[152] K. Oehmigen, M. Hahnel, R. Brandenburg, C. Wilke, K.-D. Weltmann, T. von Woedtke. The role of acidification for antimicrobial activity of atmospheric pressure plasma in liquids. *Plasma Processes Polymers*, **7**, pp. 250–257, 2010.

[153] J. Janca, S. Kuzmin, A. Maximov, J. Titova, A. Czernichowski. Investigation of the chemical action of the gliding and "point" arcs between the metallic electrode and aqueous solution. *Plasma Chem. Plasma Process.*, **19**, pp. 53–67, 1999.

[154] A. K. Sharma, D. M. Camaioni, G. B. Josephson, S. C. Goheen, G. M. Mong. Formation and measurement of ozone and nitric acid in a high voltage DC negative metallic point-to-aqueous-plane continuous corona reactor. *J. Adv. Oxid. Technol.*, **2**, 239–247.

[155] B. Benstaali, D. Moussa, A. Addou, J. L. Brisset. Plasma treatment of aqueous solutes: Some chemical properties of a gliding arc in humid air. *Eur. Phys. J.: Appl. Phys*, **4**, pp. 171–179, 1998.

[156] J.-L. Brisset, D. Moussa, A. Doubla, E. Hnatiuc, B. Hnatiuc, J.-M. H. Georges Kamgang-Youb and, M. Naitali, M.-N. Bellon-Fontaine. Chemical reactivity of discharges and temporal post-discharges in plasma treatment of aqueous media: examples of gliding discharge treated solutions. *Industial and Engineering Chemistry Research*, **47**, pp. 5761–5781, 2008.

[157] D. Moussa, A. Doubla, G. Kamgang-Youbi, J. L. Brisset. Postdischarge long life reactive intermediates involved in the plasma chemical degradation of an azoic dye. *IEEE Trans. Plasma Sci.*, **35**, pp. 444–453, 2007.

[158] R. Burlicaa, M. J. Kirkpatrick, W. C. Finney, R. J. Clark, B. R. Locke. Organic dye removal from aqueous solution by glidarc discharges. *Journal of Electrostatics*, **62**(4), pp. 309–321, 2004.

[159] D. Porter, M. D. Poplin, F. Holzer, W. C. Finney, B. R. Locke. Formation of hydrogen peroxide, hydrogen, and oxygen in gliding arc electrical discharge reactors with water spray. *IEEEn Trans. Ind. Appl.*, **45**, pp. 623–629, 2009.

[160] J. O. Lundberg, E. Weitzberg, M. T. Gladwin. The nitrate–nitrite–nitric oxide pathway in physiology and therapeutics. *Nature Reviewa – Drug Discovery*, **7**, pp. 156–167, 2008.

[161] D. X. Liu, Z. C. Liu, C. Chen, A. J. Yang, D. Li, M. Z. Rong, H. L. Chen, M. G. Kong. Aqueous reactive species induced by a surface air discharge: Heterogeneous mass transfer and liquid chemistry pathways. *Scientific Reports*, **6**, p. 23737, 2016.

[162] G. Kamgang-Youbi, J.-M. Herry, J.-L. Brisset, M.-N. Bellon-Fontaine, A. Doubla, M. Naitali. Impact on disinfection efficiency of cell load and of planktonic/adherent/detached state: case of Hafnia alvei inactivation by Plasma Activated Water. *Applied Microbiology and Biotechnology*, **81**, pp. 449–457, 2008.

[163] G. Kamgang-Youbi, J.-M. Herry, T. Meylheuc, J.-L. Brisset, M.-N. Bellon-Fontaine, A. Doubla, M. Naitali. Microbial inactivation using plasma-activated water obtained by gliding electric discharges. *Letters in applied microbiology*, **48**, pp. 13–18, 2009.

[164] J.-L. Brisset, E. Hnatiuc. Peroxynitrite: A re-examination of the chemical properties of non-thermal discharges burning in air over aqueous solutions. *Plasma Chemistry and Plasma Processing*, **32**, pp. 665–674, 2012.

[165] D. R. Merouani, F. Abdelmalek, M. R. Ghezzar, A. Semmoud, A. Addou, J. L. Brisset. Influence of peroxynitrite in gliding arc discharge treatment of alizarin red S and postdischarge effects. *Industrial and Engineering Chemistry Research*, **52**(4), pp. 1471–1480, 2013.

[166] J. Hibbs, R. Taintor, Z. Vavrin. Macrophage cytotoxicity: role for L-arginine deiminase and imino nitrogen oxidation to nitrite. *Science*, **235**(4787), pp. 473–476, 1987.

[167] P. C. Genest, B. Setlow, E. Melly, P. Setlow. Killing of spores of Bacillus subtilis by peroxynitrite appears to be caused by membrane damage. *Microbiology*, **148**, pp. 307–314, 2002.

[168] C. Szabo, H. Ohshima. DNA damage induced by peroxynitrite: subsequent biological effects. *Nitric Oxide*, **1**, pp. 373–385, 1997.

[169] B. Zingarelli, M. O'Connor, H. Wong, A. L. Salzman, C. Szaba. Peroxynitrite-mediated DNA strand breakage activates poly-adenosine diphosphate ribosyl synthetase and causes cellular energy depletion in macrophages stimulated with bacterial lipopolysaccharide. *Journal of Immunology*, **156**, pp. 350–358, 1996.

[170] P. Attri, Y. H. Y. H. Kim, J. H. P. D. H. Park, Y. J. Hong, A. F. H. S. Uhm KN. Kim, E. H. Choi. Generation mechanism of hydroxyl radical species and its lifetime prediction during the plasma-initiated ultraviolet (UV) photolysis. *Scientific Reports*, **5**, p. 9332, 2015.

[171] T. C. V. Penna, P. G. Mazzola, A. M. S. Martins. The efficacy of chemical agents in cleaning and disinfection programs. *BMC Infectious Deseases*, **1**, p. 16, 2001.

[172] S. Ikawa, K. Kitano, S. Hamaguchi. Effects of pH on Bacterial Inactivation in Aqueous Solutions due to Low-Temperature Atmospheric Pressure Plasma Application. *Plasma Processes and Polymers*, **7**(1), pp. 33–42, 2010.

[173] K. Satoh, S. J. MacGregor, J. G. Anderson, G. A. Woosley, R. A. Fouracre. Pulsed-plasma disinfection of water containing *E. coli*. *Japanese Journal of Applied Physics Part I — Regular Papers Brief Communications and Review Papers*, **46**, pp. 1137–1141, 2007.

[174] Y. Sakiyama, T. Tomai, M. Miyano, D. B. Graves. Disinfection of E. coli by nonthermal microplasma electrolysis in normal saline solution. *Applied Physics Letters*, **94**(16), p. 161501, 2009.

[175] R. Laurita, D. Barbieri, M. Gherardi, V. Colombo, P. Lukes. Chemical analysis of reactive species and antimicrobial activity of water treated by nanosecond pulsed DBD air plasma. *Clinical Plasma Medicine*, **3**, pp. 53–61, 2015.

[176] U. K. Ercan, H. Wang, H. Ji, G. Fridman, A. D. Brooks, S. G. Josh. Nonequilibrium plasma-activated antimicrobial solutions are broad-spectrum and retain their efficacies for extended period of time. *Plasma Processes and Polymers*, **10**(6), pp. 544–555, 2013.

[177] M. Wheelis. *Principles of modern microbiology*. Jones and Bartlett Publishers, 2008.

[178] R. A. Harvey, P. C. Campe, B. D. Fisher. *Lippincott's Illustrated Reviews: Microbiology, Second Edition*. Lippincott Williams & Wilkins, 2007.

[179] K. Rogers. *Bacteria and Viruses*. The Rosen Publishing Group, 2011.

[180] Prokaryotic Cell Structure – Online Textbook Chapters – Alyvea.com, 2016.

[181] A. Lee. *Biomembranes, Endocytosis and Exocytosis*. JAI PRESS inc., 1996.

[182] M. Sussman. *Escherichia Coli: Mechanisms of Virulence*. Cambridge University Press, 1997.

[183] L. Freeman-Cook, K. D. Freeman-Cook, I. E. Alcamo. *Staphylococcus Aureus Infections*. Infobase Publishing, 2006.

[184] J. R. Battist. Against All Odds: The Survival Strategies of Deinococcus radiodurans. *Annual Review of Microbiology*, **51**, pp. 203–224, 1997.

[185] R. Prasad. *Candida albicans: Cellular and Molecular Biology*. Springer, 2017.

[186] M. D. Rolfe, C. J. Rice, S. Lucchini, C. Pin, A. Thompson, A. D. S. Cameron, M. Alston, M. F. Stringer, R. P. Betts, J. Baranyi, M. W. Peck, J. C. D. Hinton. Lag Phase Is a Distinct Growth Phase That Prepares Bacteria for Exponential Growth and Involves Transient Metal Accumulation. *Journal of Bacteriology*, **194**, 2012.

[187] P. Pletnev, I. Osterman, P. Sergiev, A. Bogdanov, O. Dontsova. Survival guide: *Escherichia coli* in the stationary phase. *Acta Naturae*, **7**, pp. 22–33, 2015.

[188] M. T. Madigan, J. M. Martinko, J. Parker. *Brock biology of microorganisms*. Prentice-Hall, Upper Saddle River, NJ., 2000.

[189] D. J. Betteridge. What is oxidative stress? *Metabolism: clinical and experimental*, **49**, pp. 3–8, 2000.

[190] L. Moldovan, N. I. Moldovan. Oxygen free radicals and redox biology of organelles. *Histochemistry and Cell Biology*, **122**(4), pp. 395–412, 2004.

[191] P. Sharma, A. B. Jha, R. S. Dubey, M. Pessarakli. Reactive oxygen species, oxidative damage, and antioxidative defense mechanism in plants under stressful conditions. *Journal of Botany*, **2012**, p. 217037, 2012.

[192] B. Halliwell, J. M. C. Gutteridge. Oxygen toxicity, oxygen radicals, transition-metals anddisease. *Biochemical Journal*, **219**, pp. 1–14, 1984.

[193] M. Repetto, J. Semprine, A. Boveris. Lipid peroxidation: Chemical mechanism, biological implications and analytical determination. *Lipid Peroxidation*, pp. 3–30, 2012.

[194] H. Sies. Oxidative stress: from basic research to clinical application. *The American journal of medicine*, **91**, pp. 31–38, 1991.

[195] A. Ayala, M. F. Munoz, S. Arguelles. Lipid peroxidation: production, metabolism, and signaling mechanisms of malondialdehyde and 4-hydroxy-2-nonenal. *Oxidative Medicine and Cellular Longevity*, **2014**, pp. 1–31, 2014.

[196] H. Rubbo, A. Trostchansky, V. B. O'Donnell. Peroxynitrite-mediated lipid oxidation and nitration: Mechanisms and consequences. *Archives of Biochemistry and Biophysics*, **484**, pp. 167–172, 2009.

[197] H. Huang, I. D. Kozekov, A. Kozekova, H. Wang, R. S. Lloyd, C. J. Rizzo, M. P. Stone. DNA cross- link induced by trans-4-hydroxynonenal. *Environmental and Molecular Mutagenesis*, **51**, pp. 625–634, 2010.

[198] M. Jaganjac, O. Tirosh, G. Cohen, S. Sasson, N. Zarkovic. Reactive aldehydes — second messengers of free radicals in diabetes mellitus. *Free Radical Research*, **47**, pp. 39–48, 2013.

[199] S. J. Chapple, X. Cheng, G. E. Mann. Effects of 4- hydroxynonenal on vascular endothelial and smooth muscle cell redox signaling and function in health and disease. *Redox Biology*, **1**, pp. 319–331, 2013.

[200] P. V. Usatyuk, V. Natarajan. Hydroxyalkenals and oxidized phospholipids modulation of endothelial cytoskeleton, focal adhesion and adherens junction proteins in regulating endothelial barrier function. *Microvascular Research*, **83**(1), pp. 45–55, 2012.

[201] C. M. Spickett. The lipid peroxidation product 4-hydroxy-2-nonenal: advances in chemistry and analysis. *Redox Biology*, **1**(1), pp. 145–152, 2013.

[202] R. Sharma, A. Sharma, P. Chaudhary, M. Sahu, S. Jaiswal, S. Awasthi, T. C. Awasthi. Role of 4-hydroxynonenal in chemopreventive activities of sulforaphane. *Free Radical Biology and Medicine*, **52**, pp. 2177–2185, 2012.

[203] L. A. VanderVeen, M. F. Hashim, Y. Shyr, L. J. Marnett. Induction of frameshift and base pair substitution mutations by the major DNA adduct of the endogenous carcinogen mal- ondialdehyde. *Proceedings of the National Academy of Sciences of theUnited States of America*, **100**(24), pp. 14247–14252, 2003.

[204] C. Ji, C. A. Rouzer, L. J. Marnett, J. A. Pietenpol. Induction of cell cycle arrest by the endogenous product of lipid peroxidation, malondialdehyde. *Carcinogenesis*, **19**(7), pp. 1275–1283, 1998.

[205] M. S. Willis, L. W. Klassen, D. L. Carlson, C. F. Brouse, G. M. Thiele. Malondialdehyde-acetaldehyde haptenated protein bindsmacrophage scavenger receptor(s) and induces lysosomal damage. *International Immunopharmacology*, **4**(7), pp. 885–899, 2004.

[206] P. Lukes, M. Clupek, V. Babicky, I. Sisrova, V. Janda. The catalytic role of tungsten electrode material in the plasmachemical activity of a pulsed corona discharge in water. *Plasma Sources Sci. Technol.*, **20**, p. 034011, 2011.

[207] F. Iza, G. J. Kim, S. M. Lee, J. K. Lee, J. L. Walsh, Y. T. Zhang, M. G. Kong. Microplasmas: Sources, Particle Kinetics, and Biomedical Applications. *Plasma processes and polymers*, **5**, pp. 322–344, 2008.

[208] M. Valko, H. Morris, M. T. D. Cronin. Metals, toxicity and oxidative stress. *Current Topics in Medicinal Chemistry*, **12**, pp. 1161–1208, 2005.

[209] A. K. Sharma, B. R. Locke, P. Arce, W. C. Finney. A preliminary-study of pulsed streamer corona discharge for the degradation of phenol in aqueous-solutions. *Hazard. Waste Hazard. Mater.*, **10**, pp. 209–219, 1993.

[210] M. Repetto, A. Boveris. Bioactivity of sesquiterpenes: novel compounds that protect from alcohol-induced gastric mucosal lesions and oxidative damage. *Mini Reviews in Medicinal Chemistry*, **10**, pp. 615–623, 2010.

[211] N. C. Andrews. Mining copper transport genes. *Proceedings of the National Academy of Sciences of the United States of America*, **98**, pp. 6543–6545, 2001.

[212] J. A. Imlay, S. M. Chin, S. Linn. Toxic DNA damage by hydrogen peroxide through the Fenton reaction *in vivo* and *in vitro*. *Science*, **240**, pp. 640–642, 1988.

[213] D. H. Nies. Microbial heavy-metal resistance. *Applied Microbiology and Biotechnology*, **51**, pp. 730–750, 1999.

[214] L. I. Macomber, A. James. The iron-sulfur clusters of dehydratases are primary intracellular targets of copper toxicity. *Proceedings of the National Academy of Sciences of the United States of America*, **106**, pp. 8344–8349, 2009.

[215] I. Fridovich. Superoxide radical and superoxide dismutases. *Annual Review of Biochemistry*, **64**, pp. 97–112, 1995.

[216] P. J. Kiley, H. Beinert. Oxygen sensing by the global regulator, FNR: the role of the iron-sulfur cluster. *FEMS Microbiol Rev.*, **22**, pp. 341–352, 1998.

[217] E. C. Theil. Ferritin: structure, gene regulation and cellular function in animals, plants and microorganisms. *Annual Review in Biochemistry*, **56**, pp. 289–316, 1987.

[218] A. Leonhardt, G. Dahlen. Effect of titanium on selected oral bacterial species *in vitro*. *Eur J Oral Sci*, **103**, pp. 382–387, 1995.

[219] R. I. Joshi, A. Eley. The *in vitro* effect of a titanium implant on oral microflora: comparison with other metallic compounds. *J Med Microbiol*, **27**, pp. 105–107, 1988.

[220] K. Elagli, C. Neut, C. Romond, H. F. Hildebrand. *In vitro* effects of titanium powder on oral bacteria. *Biomaterials*, **13**, pp. 25–27, 1992.

[221] C. W. Berry, T. J. Moore, J. A. Safar, C. A. Henry, M. J. Wagner. Antibacterial activity of dental implant metals. *Impl Dent*, **1**, pp. 59–65, 1992.

[222] K. J. Bundy, M. F. B. abnd R. E. Hochman. An investigation of the bacteriostatic properties of pure metals. *Biomed Mater Res*, **14**, pp. 653–663, 1980.

[223] M. A. Malik. Synergistic effect of plasmacatalyst and ozone in a pulsed corona discharge reactor on the ecomposition of organic pollutants in water. *Plasma Sources Sci. Technol.*, **12**, pp. 26–32, 2003.

[224] P. Lukes, M. Clupek, V. Babicky, V. Janda, P. Sunka. Generation of ozone by pulsed corona discharge over water surface in hybrid gas–liquid electrical discharge reactor. *Journal of Physics D: Applied Physics*, **38**(3), p. 409, 2005.

[225] H. J. Wang, J. Li, X. Quan, Y. Wu. Enhanced generation of oxidative species and phenol degradation in a discharge plasma system coupled with TiO_2 photocatalysis. *Appl. Catal. B: Environ.*, **83**, pp. 72–77, 2008.

[226] J. A. Imlay, S. Linn. DNA damage and oxygen radical toxicity. *Science*, **240**, pp. 1302–1309, 1988.

[227] M. Dizdaroglu. *"Chemistry of free radical damage to DNA and nucleoproteins" in DNA and Free Radicals by B. Halliwell and O. I. Aruoma*. London, UK, 1993.

[228] N. L. Oleinick, S. mao Chiu, N. Ramakrishnan, L. yan Xue. The formation, identification, and significance of DNA-protein cross-links in mammalian cells. *British Journal of Cancer, supplement*, **8**, pp. 135–140, 1987.

[229] R. Meneghini. Iron homeostasis oxidative stress, and DNA damage. *Free Radical Biology and Medicine*, **23**, pp. 783–792, 1997.

[230] C. C. M. L. Michaels, A. P. Grollman, J. H. Miller. Evidence that MutY and MutM combine to prevent mutations by an oxidatively damaged form of guanine in DNA. *Proc. Natl. Acad. Sci. USA*, **89**, pp. 7022–7025, 1992.

[231] H.-S. Xu, N. Roberts, F. L. Singleton, R. W. Attwell, D. J. Grimes, R. R. Colwell. Survival and viability of nonculturableEscherichia coli andVibrio cholerae in the estuarine and marine environment. *Microbial Ecology*, **8**, pp. 313–323, 1982.

[232] B. Gret, T. R. Steck. Concentrations of copper thought to be toxic to *Escherichia coli* can induce the viable but nonculturable condition. *Applied and Environmental Microbiology*, pp. 5325–5327, 2001.

[233] J. D. Oliver. The viable but nonculturable state in bacteria (Short Survey). *Journal of Microbiology*, **43**, pp. 93–100, 2005.

[234] G. Bogosian, N. D. Aardema, E. V. Bourneuf, P. J. L. Morris, J. P. O'Neil. Recovery of hydrogen peroxidesSensitive culturable cells of vibrio vulnificus gives the appearance of resuscitation from a viable but nonculturable state. *J. Bacteriol.*, **182**, pp. 5070–5075, 2000.

[235] R. Tisserand, R. Young. *Essential oil safety: a guide for health care professionals*. Edinburgh: Elsevier Limited, 2014.

[236] R. L. Smith, S. M. Cohen, J. Doull, V. J. Feron, J. I. Goodman, L. J. Marnett, P. S. Portoghese, W. J. Waddell, B. M. Wagner, R. L. Hall, N. A. Higley, C. Lucas-Gavin, T. B. Adams. A procedure for the safety evaluation of natural flavor complexes used as ingredients in food: essential oils. *Food Chem. Toxicol.*, **43**, pp. 345–363, 2005.

[237] C. F. Carson, B. J. Mee, T. V.Riley. Mechanism of action of *Melaleuca alternifolia* (tea tree) oil on *Staphylococcus aureus* determined by time-kill, lysis, leakage and salt tolerance assays and electron microscopy. *Antimicrob. Agents Chemother*, **46**, pp. 1914–1920, 2002.

[238] K. Knobloch, A. Pauli, B. Iberl, H. Weigand, N. Weis. Antibacterial and antifungal properties of essential oil components. *J. Essen. Oil Res.*, **1**, pp. 119–128, 1989.

[239] I. M. Helander, H. L. Alakomi, K. Latva-Kala, T. Mattila-Sandholm, I. Pol, E. J. Smid, L. G. M. Gorris, A. V. Wright. Characterization of the action of selected essential oil components on gram negative bacteria. *J. Agric. Food Chem*, **46**, pp. 3590–3595, 1998.

[240] A. Ultee, M. H. Bennik, R. Moezelaar. The phenolic hydroxyl group of carvacrol is essential for action against the food-borne pathogen *Bacillus cereus*. *Appl. Environ. Microbiol.*, **68**, pp. 1561–1568, 2002.

[241] R. D. Pasqua, G. Betts, N. Hoskins, M. Edwards, D. Ercolini, G. Mauriello. Membrane toxicity of antimicrobial compounds from essential oils. *J. Agric. Food Chem.*, **55**, pp. 4863–4870, 2007.

[242] S. Burt. Essential oils: their antibacterial properties and potential applications in foods — a review. *Int. J. Food Microbiol.*, **94**, pp. 223–253, 2004.

[243] J. R. Calo, P. G. Crandall, C. A. O'Bryan, S. C. Ricke. Essential oils as antimicrobials in food systems — A review. *Food Control*, **54**, pp. 111–119, 2015.

[244] S. A. Novgorodov, T. I. Gudz. Permeability transition pore of the inner mitochondrial membrane can operate in two open states with different selectivities. *J. Bioenerg. Biomembr.*, **28**, pp. 139–146, 1996.

[245] N. Heatley. A method for the assay of penicillin. *Biochem. J.*, **38**, pp. 61–65, 1944.

[246] M. Balouiri, M. Sadiki, S. K. Ibnsouda. Methods for *in vitro* evaluating antimicrobial activity: A review. *Journal of Pharmaceutical Analysis*, **6**, pp. 71–79, 2016.

[247] V. Manohar, C. Ingram, J. Gray, N. A. Talpur, B. W. Echard, D. Bagchi, H. G. Preuss. Antifungal activities of origanum oil against *Candida albicans*. *Mol. Cell. Biochem.*, **228**, pp. 111–117, 2001.

[248] M. A. Botelho, N. A. Nogueira, G. M. Bastos, S. G. Fonseca, T. L. Lemos, F. J. Matos, D. Montenegro, J. Heukelbach, V. S. Rao, G. A. Brito. Antimicrobial activity of the essential oil from Lippia sidoides, carvacrol and thymol against oral pathogens. *Braz. J. Med. Biol. Res.*, **40**, pp. 349–356, 2007.

[249] B. Tepe, D. Daferera, M. Sokmen, M. Polissiou, A. Sokmen. The *in vitro* antioxidant and antimicrobial activities of the essential oil and various extracts of *Origanum syriacum L. var. bevanii*. *J. Sci. Food Agric*, **84**, pp. 1389–1396, 2004.

[250] A. Rosato, C. Vitali, N. D. Laurentis, D. Armenise, M. A. Milillo. Antibacterial effect of some essential oils administered alone or in combination with Norfloxacin. *Phytomedicine*, **14**, pp. 727–732, 2007.

[251] P. Kloucek, J. Smid, A. Frankova, L. Kokoska, I. Valterova, R. Pavela. Fast screening method for assessment of antimicrobial activity of essential oils in vapor phase. *Food Research International journal*, **47**, pp. 161–165, 2012.

[252] F. Bakkali, S. Averbeck, D. Averbeck, A. Zhiri, D. Baudoux, M. Idaomar. Antigenotoxic effects of three essential oils in diploid yeast (*Saccharomyces cerevisiae*) after treatments with UVC radiation, 8- MOP plus UVA and MMS. *Mutat. Res.*, **606**, pp. 27–38, 2005.

[253] S. A. F. Bakkali and, D. Averbeck, M. Idaomar. Biological effects of essential oils — A review. *Food and Chemical Toxicology*, **46**, pp. 446–475, 2008.

[254] J. S. Raut, S. M. Karuppayil. A status review on the medicinal properties of essential oils. *Industrial Crops and Products*, **62**, pp. 250–264, 2014.

[255] M. G. Miguel. Antioxidant and anti-inflammatory activities of essential oils: a short review. *Molecules*, **15**, pp. 9252–9287, 2010.

[256] A. Tyagi, A. Malik. Antimicrobial action of essential oil vapours and negative air ions against *Pseudomonas fluorescens*. *International Journal of Food Microbiology*, **143**, pp. 205–210, 2010.

[257] M. M. Obaidat, J. F. Frank. Inactivation of *Salmonella* and *Escherichia coli* O157:H7 on sliced and whole tomatoes by allyl isothiocyanate, carvacrol, and cinnamaldehyde in vapor phase. *J Food Prot.*, **72**, pp. 315–324, 2009.

[258] L. B. van Alphen, S. A. Burt, A. K. Veenendaal, N. M. Bleumink-Pluym, J. P. van Putten. The natural antimicrobial carvacrol inhibits *Campylobacter jejuni* motility and infection of epithelial cells. *PLoS One*, **7**, p. 45343, 2012.

[259] C. Marcos-Arias, E. Eraso, L. Madariaga, G. Quindos. *In vitro* activities of natural products against oral *Candida* isolates from denture wearers. *BMC Complement Altern Med.*, **26**, p. 119, 2011.

[260] K. M. Arunasree. Anti-proliferative effects of carvacrol on a human metastatic breast cancer cell line, MDA-MB 231. *Phytomedicine*, **17**, pp. 581–588, 2010.

[261] W. Z. Liang, C. H. Lu. Carvacrol-induced [Ca^{2+}]i rise and apoptosis in human glioblastoma cells. *Life Sci.*, **15**, pp. 703–711, 2012.

[262] W. Z. Liang, C. T. Chou, T. Lu, C. C. Chi, L. L. Tseng, C. C. Pan, K. L. Lin, C. C. Kuo, C. R. Jan. The mechanism of carvacrol-evoked [Ca2+]i rises and non-Ca^{2+}-triggered cell death in OC2 human oral cancer cells. *Toxicology*, **7**, pp. 152–161, 2013.

[263] T. Kulisi, A. Krisko, V. Dragovi-Uzelac, M. Milos, G. Pifat. The effects of essential oils and aqueous tea infusions of oregano (*Origanum vulgare L. spp. hirtum*), thyme (*Thymus vulgaris L.*) and wild thyme (*Thymus serpyllum L.*) on the copper-induced oxidation of human low-density lipoproteins. *Int J Food Sci Nutr.*, **58**, pp. 87–93, 2007.

[264] Y. Lu, C. Wu. Reduction of *Salmonella enterica* contamination on grape tomatoes by washing with thyme oil, thymol, and carvacrol as compared with chlorine treatment. *J Food Prot.*, **73**, pp. 2270–2275, 2010.

[265] H. J. D. Dorman, S. G. Deans. Antimicrobial agents from plants: antibacterial activity of plant volatile oils. *J. Appl. Microbiol.*, **88**, pp. 308–316, 2000.

[266] S. K. Filoche, K. Soma, C. H. Sissons. Antimicrobial effects of essential oils in combination with chlorhexidine digluconate. *Oral Microbiol Immunol.*, **20**, pp. 221–225, 2005.

[267] N. Moszner, U. Salz, V. Rheinberger. Synthesis and polymerization of unsaturated derivatives of thymol. *Polymer Bulletin.*, **33**, pp. 7–12, 1994.

[268] K. Palaniappan, R. A. Holley. Use of natural antimicrobials to increase antibiotic susceptibility of drug resistant bacteria. *International Journal of Food Microbiology*, **140**, pp. 164–168, 2010.

[269] P. Griess. Bemerkungen zu der Abhandlung der HH. Weselsky und Benedikt „Ueber einige Azoverbindungen". *Berichte der deutschen chemischen Gesellschaft*, **12**, pp. 426–428, 1879.

[270] P. corporation. Technical bulletin - Griess reagent system, 2009.

[271] G. M. Eisenberg. Colorimetric determination of hydrogen peroxide. *Ind. Eng. Chem. Anal. Ed.*, **15**(5), pp. 327–328, 1943.

[272] C. N. Satterfield, A. H. Bonnell. Interferences in titanium sulfate method for hydrogen peroxide. *Analytical chemistry*, **27**(7), pp. 1174 – 1175, 1955.

[273] J. R. Norris, D. W. Ribbons. *Methods in Microbiology, Volume 3, Part 2*. Academic press Inc. London, LTD, 1969.

[274] C.-Y. Chen, G. W. Nace, P. L. Irwin. A 6 × 6 drop plate method for simultaneous colony counting and MPN enumeration of Campylobacter jejuni, Listeria monocytogenes, and Escherichia coli. *Journal of Microbiological Methods*, **55**, pp. 475–479, 2003.

[275] J. O'Brein, I. Wilson, T. Orton, F. Pognan. Investigation of the Almar Blue (resazurin) fluorescent dye for the assessment of mammalian cell cytotoxocity. *European journal of biochemistry*, **267**, pp. 5421–5426, 2000.

[276] R. D. Fields, M. V. Lancaster. Dual-attribute continuous monitoring of cell poliferation/cytotoxicity. *Am. Biotechnol. Lab*, **11**, pp. 48–50, 1993.

[277] T. F. Guerin, M. Mondido, B. McClenn, B. Peasley. Application of resazurin for estimating abundance of contaminant-degrading microorganisms. *Letters on Applied Microbiology*, **32**, pp. 340–345, 2001.

[278] i. d. t. Molecular Probes. *LIVE/DEAD BacLight Bacterial Viability Kits*, 2004.

[279] G. N. von Carona, P. J. Stephensb, C. J. Hewittc, J. R. Powella, R. A. Badleya. Analysis of bacterial function by multi-color fluorescence flow cytometry and single cell sorting. *Journal of microbiological methods*, **42**, pp. 97–114, 2000.

[280] F. Joux, P. Lebaron. Use of fluorescent probes to assess physiological functions of bacteria at single-cell level. *Microbes and infection*, **2**, pp. 1523–1535, 2000.

[281] D. Hoefel, W. L. Grooby, P. T. Monis, S. Andrews, C. P. Saint. Enumeration of water-borne bacteria using viability assays and flow cytometry: a comparison to culture-based techniques. *Journal of microbiological methods*, **55**, pp. 585–597, 2003.

[282] M. Virta, S. Lineri, P. Kankaanpaa, M. Karp, K. Peltonen, J. Nuutila, , E.-M. Lilius. Determination of complement-mediated killing of bacteria by viability staining and bioluminescence. *Applied and environmental microbiology*, **64**, pp. 515–519, 1998.

[283] H. F. Moselhy, R. G. Reid, S. Yousef, S. Boyle. A specific, accurate, and sensitive measure of total plasma malondialdehyde by HPLC. *Journal of Lipid Research*, pp. 852–858, 2013.

[284] C. C. Company. *TBARS Assay Kit*, 2017.

[285] T. F. Slater, B. C. Sawyer. The stimulatory effects of carbon tetrachloride and other halogenoalkanes on peroxidative reactions in rat liver fractions in vitro. General features of the systems used. *Biochemical Journal*, pp. 805—-814, 1971.

[286] P. Kostka, C. Y. Kwan. Instability ofmalondialdehyde in the presence of H_2O_2: impli- cations for the thiobarbituric acid test. *Lipids*, **24**, pp. 545–549, 1989.

[287] K. Kleppe, E. Ohtsuka, R. Kleppe, I. Molineux, H. G. Khorana. Studies on polynocleotides XCVI, Repair replications of short synthetic DNA's as catalyzed by DNA polymerases. *J. Mol. Biol*, **56**, pp. 341–361, 1971.

[288] R. K. Saiki, S. Scharf, F. Faloona, K. B. Mullis, G. T. Horn, H. A. Erlich, N. Arnheim. Enzymatic amplification of beta-globin fwnomic sequences and restriction side analysis for diagnosis of sickle cell anemia. *Science*, **230**, pp. 1350–1354, 1985.

[289] D. H. Best, J. J. Swensen. *Molecular genetics and personalized medicine*. New York : Humana Press, 2012.

[290] Polymerase Chain Reaction (PCR) – An Introduction — ABM Inc., 2017.

[291] K. M. Ririe, R. P. Rasmussen, , C. T. Wittwer. Product differentiation by analysis of DNA melting curves during the polymerase chain reaction. *Analytical biochemistry*, **245**, pp. 154–160, 1997.

[292] B.-R. Laboratories. *Precision Melt Supermix*, 2017.

[293] A. A. H. Mohamed, J. F. Kolb, K. H. Schoenbach. Low temperature, atmospheric pressure, direct current microplasma jet operated in air, nitrogen and oxygen. *The European Physical Journal D*, **60**, pp. 517–522, 2010.

[294] X. Hao, A. M. Mattson, C. M. Edelblute, M. A. Malik, L. C. Heller, J. F. Kolb. Nitric Oxide Generation with an Air Operated Non-Thermal Plasma Jet and Associated Microbial Inactivation Mechanisms. *Plasma Processes and Polymers*, **11**(11), pp. 1044–1056, 2014.

[295] L. Heller, C. Edelblute, A. Mattson, X. Hao, J. Kolb. Inactivation of bacterial opportunistic skin pathogens by nonthermal DC-operated afterglow atmospheric plasma. *Letters in Applied Microbiology*, **54**(2), pp. 126–132, 2012.

[296] P. Small, D. Blankenhorn, D. Welty, E. Zinser, J. L. Slonczewski. Acid and base resistance in *Escherichia coli* and *Shigella flexneri*: Role of *rpoS* and growth pH. *Journal of Bacteriology*, **176**, pp. 1729–1737, 1994.

[297] G. Borkow, J. Gabbay. Copper as a biocidal tool. *Current Medicinal Chemistry*, **12**, pp. 2163–2175, 2005.

[298] C. Cervantes, F. Gutierrez-Corona. Copper resistance mechanisms in bacteria and fungi. *FEMS Microbiology Reviews*, **14**(2), pp. 121–137, 1994.

[299] R. K. Sani, B. M. Peyton, L. T. Brown. Copper-Induced Inhibition of Growth of Desulfovibrio desulfuricans G20: Assessment of Its Toxicity and Correlation with Those of Zinc and Lead. *Applied and Environmental Microbiology*, **67**, pp. 4765—-4772, 2001.

[300] S. Silver. Bacterial resistances to toxic metal ions - A Review. *Gene*, **179**, pp. 9–19, 1996.

[301] M. Nawaz, C. Manzl, V. Lacher, G. Krumschnabel. Copper-Induced Stimulation of Extracellular Signal-Regulated Kinase in Trout Hepatocytes: The Role of Reactive Oxygen Species, Ca2+, and Cell Energetics and the Impact of Extracellular Signal-Regulated Kinase Signaling on Apoptosis and Necrosis. *Toxicological Sciences*, **92**(2), p. 464, 2006.

[302] S. results on the performance of a selective set of atmospheric plasma jets for separation of photons, reactive particles. Simon Schneider and Fabian Jarzina and Jan-Wilm Lackmann and Judith Golda and Vincent Layes and Volker Schulz-von der Gathen and Julia Elisabeth Bandow and Jan Benedikt. *Journal of Physics D: Applied Physics*, **48**, 2015.

[303] E. Codorniu-Hernandez, K. W. Hall, A. D. Boese, D. Ziemianowicz, S. Carpendale, P. G. Kusalik. Mechanism of O(3P) formation from a hydroxyl radical pair in aqueous solution. *J. Chem. Theory Comput.*, **11**, pp. 4740–4748, 2015.

[304] E. Codorniu-Hernandez, K. W. Hall, D. Ziemianowicz, S. Carpendale, P. G. Kusalik. Aqueous production of oxygen atoms from hydroxyl radicals. *Phys. Chem. Chem. Phys.*, **16**, pp. 26094–26102, 2014.

[305] E. Dolezalova, P. Lukes. Membrane damage and active but nonculturable state in liquid cultures of Escherichia coli treated with an atmospheric pressure plasma jet. *Bioelectrochemistry*, **103**, pp. 7–14, 2015.

[306] S. G. Joshi, M. Cooper, A. Yost, M. Paff, U. K. Ercan, G. Fridman, G. Friedman, A. Fridman, A. D. Brooks. Nonthermal dielectric-barrier discharge plasma-induced inactivation involves oxidative DNA damage and membrane lipid peroxidation in *Escherichia coli*. *Antimicrobial Agents and Chemotherapy*, **55**, pp. 1053–1062, 2011.

[307] B. F. Spencer, K. Tokio. Oxidative stress responses in *Escherichia coli* and *Salmonella typhimurium*. *Micribiological Reviews*, **55**, pp. 561–585, 1991.

[308] R. Sachidanandham, K. Y. Gin, C. L. Poh. Monitoring of active but non-culturable bacterial cells by flow cytometry. *Biotechnol Bioeng.*, **89**, pp. 24–31, 2005.

[309] A. E. Yousef, V. K. Juneja. *Microbial Stress Adaptation and Food Safety*. CRC Press, Taylor & Francis group, 2002.

[310] P. S. Hair, K. H. Schoenbach, E. S. Buescher. Sub-microsecond, intense pulsed electric field applications to cells show specificity of effects. *Bioelectrochemistry*, **61**, pp. 65–72, 2003.

[311] A. Silve, I. Leray, L. M. Mir. Demonstration of cell membrane permeabilization to medium-sizedmolecules causedby a single 10 ns electric pulse. *Bioelectrochemistry*, **87**, pp. 260–264, 2012.

[312] P. T. Vernier, Y. H. Sun, M. T. Chen, M. A. Gundersen, G. L. Craviso. Nanosecond electric pulse-induced calcium entry into chromaffin cells. *Bioelectrochemistry*, **73**, pp. 1–4, 2008.

[313] B. L. Ibey, D. G. Mixon, J. A. Payne, A. Bowman, K. Sickendick, G. J. Wilmink, W. P. Roach, A. G. Pakhomov. Plasma membrane permeabilization by trains of ultrashort electric pulses. *Bioelectrochemistry*, **79**, pp. 114–121, 2010.

[314] J. Marmur, P. Doty. Determination of the base composition of dioxyribonucleic acid from its thermal melting temperature. *J. Mol. Biol.*, **5**, pp. 109–118, 1962.

[315] P. Yakovchuk, E. Protozanova, M. D. Frank-Kamenetskii. Base-stacking and base-pairing contributions into thermal stability of the DNA double helix. *Nucleic Acids Research*, **34**, pp. 564–574, 2006.

[316] E. Linley, S. P. Denyer, G. McDonnell, C. Simons, J. Maillard. Use of hydrogen peroxide as a biocide: new consideration of its mechanisms of biocidal action. *J Antimicrob Chemother*, **67**, pp. 1589–1596, 2012.

[317] J. Goncalves, M. T. Cruz, C. Cavaleiro, M. C. Lopes, L. Salgueiro. Chemical, antifungal and cytotoxic evaluation of the essential oil of T*Thymus zygis* subsp. *sylvestris*. *Industrial Crops and Products*, **32**, pp. 70–75, 2010.

[318] P. Lopez, C. Sanchez, R. Batlle, C. Nerin. Solid and vapor-phase antimicrobial activities of six essential oils: Susceptibility of selected foodborne bacterial and fungal strains. *Journal of Agriculture and Food Chemistry*, **53**, pp. 6939–6946, 2005.

[319] A. K. Tyagi, A. Malik. Bactericidal action of lemon grass oil vapors and negative air ions. *Innovative Food Science & Emerging Technologies*, **13**, pp. 169–177, 2012.

[320] A. I. Nazer, A. Kobilinsky, J. L. Tholozan, F. Dubois-Brissonnet. Combinations of food antimicrobials at low levels to inhibit the growth of *Salmonella sv Typhimurium*: a synergistic effect. *Food Microbiology*, **22**, pp. 391–398, 2005.

[321] K. Bazaka, M. V. Jacob, W. Chrzanowski, K. Ostrikov. Anti-bacterial surfaces: natural agents, mechanisms of action, and plasma surface modification. *RSC Advances*, **5**, pp. 48739–48759, 2015.

[322] L. T. Gaunt, S. C. Higgins, J. F. Hughes. Interaction of air ions and bactericidal vapours to control microorganisms. *Journal of Applied Microbiology*, **99**, pp. 1324–1329, 2005.

[323] N. Matan, M. Nisoa, N. Matan, T. Aewsiri. Effect of cold atmospheric plasma on antifungal activities of clove oil and eugenol against molds on areca palm (*Areca catechu*) leaf sheath. *International Biodeterioration & Biodegradation*, **86**, 2014.

[324] K. Bazaka, M. V. Jacob, R. J. Crawford, E. E. P. Ivanova. Plasma-assisted surface modification of organic biopolymers to prevent bacterial attachment. *Acta Biomaterialia*, **7**, pp. 2015–2028, 2011.

[325] K. Bazaka, M. V. Jacob, V. K. Truong, R. J. Crawford, E. P. Ivanova. The effect of polyterpenol thin film surfaces on bacterial viability and adhesion. *Polymers*, **3**, pp. 388–404, 2011.

[326] K. Bazaka, M. V. Jacob, V. K. Truong, F. Wang, W. A. A. Pushpamali, J. Y. Wang, A. V. Ellis, C. C. Berndt, R. J. Crawford, E. P. Ivanova. Plasma-enhanced synthesis of bioactive polymeric coatings from monoterpene alcohols: A combined experimental and theoretical study. *Biomacromolecules*, **11**, pp. 2016–2026, 2010.

[327] K. Nishikawa, H. Nojima. Air purification effect of positively and negatively charged ions generated by plasma at atmospheric pressure. *Japanese Journal of Applied Physics*, **40**, pp. 835–837, 2001.

[328] A. K. Tyagi, B. K. Nirala, A. Malik, K. Singh. The effect of negative air ion exposure on *Escherichia coli* and *Pseudomonas fluorescens*. *Journal of Environmental Science and Health Part A.*, **43**, pp. 694–699, 2008.

[329] Y. Han, S. O. Manolach, F. Denes, R. M. Rowell. Cold plasma treatment on starch foam reinforced with wood fiber for its surface hydrophobicity. *Carbohydr. Polym.*, **86**, pp. 1031–1037, 2011.

[330] Y. Cheng, L. Lu, W. Zhang, J. Shi, Y. Cao. Reinforced low density alginate based aerogels: preparation, hydrophobic modification and characterization. *Carbohydr. Polym.*, **88**, pp. 1093–1099, 2012.

[331] L. Nedorostova, P. Kloucek, L. Kokoska, M. Stolcova, J. Pulkrabek. Antimicrobial properties of selected essential oils in vapour phase against foodborne bacteria. *Food Control*, **20**, pp. 157–160, 2009.

[332] E. L. Souza, T. L. M. Stamford, E. O. Lima, V. N. Trajano. Effectiveness of *Origanum vulgare L.* essential oil to inhibit the growth of food spoiling yeasts. *Food Control*, **18**, pp. 409 – 413, 2007.

[333] Y. Luo, Z. Han, S. Chin, S. Linn. Three chemically distinct types of oxidants formed by iron-mediated Fenton reactions in the presence of DNA. *Proceedings of the National Academy of Sciences of the United States of America*, **91**, pp. 12438–42, 1994.

[334] J. Sikkema, J. A. M. de Bont, B. Poolman. Interactions of cyclic hydrocarbons with biological membranes. *The Journal of biological chemistry*, **11**, pp. 8022—-8028, 1994.

Appendix A
List of publications, grants and other academic activities

A.1 Publications

Papers in impact journals

- P. Stenclova, V. Celedova, A. Artemenko, V. Jirasek, J. Jira, B. Rezek, A. Kromka, Surface chemistry of water dispersed detonation nanodiamonds modified by atmospheric DC plasma afterglow. *RSC Advances* 62(7), 38973–38980, 2017.
- I. Malikova, L. Janousek, V. Fantova (now Celedova), J. Jira, V. Kriha, Impact of low frequency electromagnetic field exposure on selected microorganisms. *Journal of electrical engineering* 66(2), 108–112, 2015.
- K. Bujacek, V. Fantova (now Celedova), V. Kriha, Decontamination effects of the corona discharge with plane to bent needle configuration.*Problems of Atomic Science and Technology*, 2, 187–189, 2012 (contribution of V. Celedova 50 %).
- J. Slama, V. Kriha, J. Julak, V. Fantova (now Celedova), Comparison of dielectric barrier discharge modes fungicidal effect on *Candida albicans* grows. *Problems of Atomic Science and Technology*, 1. 237–239, 2013.

Papers in other journals and conference proceedings

- P. Bakovsky, V. Fantova (now Celedova), K. Chumachenko, Bacterial Inactivation by Physiologically Relevant Liquids Activated by Atmospheric Pressure Non-thermal Plasma. *Proceedings of* 19$^{\text{th}}$ *international student conference Poster*, 2016. (Presented by V. Celedova, winner of the best poster awards).
- L. Jonasova, V. Fantova (now Celedova), Bactericidal Effects of the UV Radiation Generated by a Negative Corona Discharge. *Proceedings of* 19$^{\text{th}}$ *international student conference Poster*, (presented by V. Celedova), 2016.
- V. Fantova (now Celedova), J. Jira, V. Kriha, Dependence of bacteria and yeast inactivation on charge transported to the contaminated surface. Accepted paper for 32$^{\text{nd}}$ *International Conference on Phenomena in Ionized Gases (ICPIG)*, 2015.
- V. Fantova (now Celedova), Bactericidal Effects of the Negative Corona Discharge. *Proceedings of* 17$^{\text{th}}$ *international student conference Poster*, 2015.
- V. Fantova (now Celedova), Infrared spectroscopy – attenuated total reflection. *Proceedings of* 17$^{\text{th}}$ *international student conference Poster*, 2013.
- V. Fantova, K. Bujacek, V. Kriha, J. Julak, Inactivation of *Candida albicans* by corona discharge: The increase of inhibition zones area after subsequent exposition. *Acta Polytechnica*, 53(2), 2013.

Oral or poster presentations without papers in proceedings

- V. Fantova (now Celedova), J. Jira, K. Vlkova, V. Kriha, P. Kloucek, Synergistic Effects of Essential Oregano Oil and Positive Streamer on Bacteria and Yeasts. 6th International Conference on Plasma Medicine (ICPM-6), September 4-9, Bratislava, Slovakia, 2016.
- V. Fantova (now Celedova), V. Kriha. Inactivation of *Candida albicans* by corona discharge: growth inhibition by near and far discharge exposition. International school on low temperature plasma physics: basics and applications, Bad Honnef, Germany, 2014.
- V. Fantova (now Celedova), J. Jira, V. Kriha, *Candida albicans* Inactivation by the Pin-to-Rotating Plane Corona Discharge. 3rd Young Professionals Workshop on Plasma Medicine, Greifswald, Gemrany, 2014.
- V. Fantova, M. Lavalhegas, J. Jira, V. Kriha, Inactivation of *Candida albicans* by Corona Discharge in System with Rotating Electrode, 26th Symposium on Plasma Physics and Technology, Prague, Czech Republic, 2014.
- V. Fantova, J. Jira, K. Vlkova, V. Kriha, P. Kloucek, P. Stenclova, Synergistic effects of essential oil and positive streamer discharge on bacteria and yeasts. 27th Symposium on Plasma Physics and Technology, Prague, Czech Republic, 2016 (oral presentation).
- V. Fantova, J. Jira, K. Vlkova, V. Kriha, P. Kloucek, Bacteria inactivation by synergistic effects of non-thermal plasma and oregano essential oil, 27th Symposium on Plasma Physics and Technology, Prague, Czech Republic, 2016.

A.2 Activities in academic life

Supervising of master theses

- V. Dvořaková, Changes in nanodiamond suspense biocidal properties after plasma treatment. Defended in 2017 (in Czech language).
- K. Vlková, Synergistic effects of essential oil and non-thermal plasma on microorganisms on the surface on defined cultivation media. Defended in 2016 (in Czech language).
- L. Jonašová, Comparison of the influence of UV radiation generated by the corona discharge and gliding arc on bacteria inactivation. Defended in 2016 (in Czech language).
- L. Koudela, Usage of laser schlieren deflectometry in detection of plasma filaments rotation frequency. Defended in 2014 (in Czech language).

Supervising of visiting students

- M. Lavalhegas Hallack first year master student of physics in University Campinas - UNICAMP, Sao Paolo, Brazil; Voluntary research on topic "Effects of low temperature plasma on biological organisms in suspensions and on surfaces". Term: 2. 01 – 31. 03. 2016.
- I. Malḱová, Ph.D. student of the Faculty of Electrical Engineering, University of Žilina, Slovakia; ERASMUS scholarship on topic "Impact of low frequency electromagnetic field exposure on the *Candida albicans* in combination with plasma treatment". Term: 01. 03. – 30. 04. 2015.

- M. Warga, master student of Biomedical Engineering, AGH University of Science and Technology in Krakow, Poland. Internship on topic "Effects of essential oils combined with non-thermal plasma treatment on bacteria and yeasts". 1. 09 – 28. 10. 2015.
- M. Lavalhegas Hallack from University Campinas - UNICAMP, third year bachelor student. Voluntary research on topic "Effects of low temperature plasma on biological organisms". 2. 01 – 31. 03. 2014.

Supervising of undergraduate students

- J. Říha, High school of electrical engineering in Prague, Long term experimental work at biocidal effects of non-thermal plasma. Defended in 2016 (in Czech language).

Lectures and courses

- Establishing of regular lecture and complementary laboratory exercise on topic "Non-thermal plasma in medicine" within the regular course of Physics for Therapy (main course for Biomedical Engineering Master program at FEE, CTU in Prague) - started at 2014/2015 summer semester.
- Popular laboratory exercises for high school students on topic of biocidal properties of non-thermal plasma established. 2014, 2015, 2016 (in Czech language).
- Holding popular lectures on plasma medicine for high school physics teachers withing the Summer school at FEE, CTU in Prague, 2015, 2016 (in Czech language).

Appendix B
Used symbols and abbreviations

B.1 Symbols

d	Distance (!zmenit u warburga na l).
d	Thickness of the cell membrane.
f, (f_g, f_r)	Fluorescence (at 530 and 630 nm).
F_t	Force.
h	Planck constant.
j	Current density.
m	Mass.
r	Radius.
T, (T_i, T_e, T_n)	Termodynamic temperature (of ions, electrons or neutrals).
t	Time.
V	Voltage.
V_{cr}	Critical voltage.
V_t	Volume treated.
ϕ	Charge potential.
ν	Photon frequency.
$\oslash$	Diameter.

B.2 Abbreviations

AC	Alternating current.
APPJ	Atmospheric pressure plasma jet.
AT	Adenine-thymine Watson-Crick base pair (in DNA).
ATP	Adenosine triphosphate.
CFU	Colony forming units.
CL	Carrier liquid.
COST	European cooperation in science and technology.
DBD	Dielectric barrier discharge.
DC	Direct current.
DFE	Dielectric free electrode (jet).
DI water or DIW	Deionized water.
DNA	Deoxyribonucleic acid.
dNTP	Deoxynucleotide.
dsDNA	Double stranded deoxyribonucleic acid.
EHDA	ElectroHydroDynamic atomization.
EO	Essential oil.
FE-DBD	Floating electrode dielectric barrier discharge.

FTIR-ATR	Fourier transform infrared spectroscopy - attenuated total reflection.
FTIR-GAR	Fourier transform infrared spectroscopy - grazing angle reflection.
GC	Guanine-cytosine Watson-Crick base pair (in DNA).
GC-MS	Gas chromatography - mass spectrometry.
HNE	4-hydroxynonenal.
HTP	High temperature plasma.
HV	High voltage.
L/D	Live/dead fluorescence signal ration.
LB	Luria-Bertani (agar or broth).
LPO	Lipid peroxidation.
LTP	Low temperature plasma.
µAPPJ	Micro atmospheric pressure plasma jet.
MCSD	Microcathode sustained discharges.
MDA	Malondialdehyde.
m-FC	Fecal coliform (agar base).
M-H	Muller-Hinton (agar or broth).
MIC	Minimal inhibitory concentration.
mRNA	Messenger ribonucleic acid.
MT	Mass transfer.
MW	Microwave.
NAI	Negative air ions.
NED	N-1-napthylethylenediamine dihydrochloride.
NTP	Non-thermal plasma.
OEO	Oregano essential oil.
PAW	Plasma activated water.
PB	Phosphate buffer.
PBS	Phosphate buffered saline.
PCR	Polymerase chain reaction.
PET	Polyethylene terephthalate.
pH	Potential of hydrogen (scale to specify acidity).
PI	Propidium iodide.
POM	Polyoxymethylene.
PUFA	Polyunsaturated fatty acid.
qPCR	Qualitative polymerase chain reaction.
RF	Radio frequency.
RFU	Relative fluorescence units.
RNS	Reactive nitrogen species.
RONS	Reactive oxygen and nitrogen species.
ROS	Reactive oxygen species.
RVA	Resazurin viability assay.
S agar	Sabouraud dextrose agar.
SA	Sulfanilamide or Suldanil acid.
SE jet	Single electrode jet.
SS	Stainless steel.
ssDNA	Single stranded deoxyribonucleic acid.
SYTO9	Green fluorescent nucleic acid stain.
TBA	Thiobarbituric acid.
UV	Ultraviolet radiation.
UV-A	UV with wavelength 315 – 400 nm.

VUV	Vacuum UV with wavelength 10 – 200 nm.
VBNC	Viable but nonculturable (state of bacteria).

B.3 A note considering terminology

Sterilization	Probability of live organisms in volume or on surface. Sterility should be proved by a suitable and validated production process. Sterility assurance level (SAL) is described as a probability of one not sterile item in a group. Widely accepted pharmaceutical sterilization is SAL=10^{-6}, that stands for maximum 1 not sterile item in a million. The term is usually used in plasma treatment technology to describe its efficiency. The reported efficiency of plasma treatment is far from SAL=10^{-6}; therefore, the term decontamination or inactivation is more suitable [??].
Decontamination	Freeing a volume or surface from some contaminating substances such as bacteria, yeasts, etc.
Inactivation	The process of destroying or removing an activity or effects of an agent, substance or microorganism.
Viability	Capability of living. Viable cells are those with functional metabolism and/or respiration; however, it does not mean that such cells will create visible colonies.
Culturability	Ability of microorganisms to form visible colonies on defined growth medium.
Plasma jet	Gas discharge, which is operated in a non-sealed electrode arrangement and projected outside the electrode arrangement into the environment [50].
APPJ	Abbreviation for Atmospheric Pressure Plasma Jet, which was originally introduced for RF-generated plasma jets in helium and argon with bare electrodes but mean- while also used for other plasma jet configuration [71].